BMP SIGNALING IN THE MORPHOGENESIS OF THE ESOPHAGUS AND TRACHEA

By

Yina Li

Dissertation

Submitted to the Faculty of the

Graduate School of Vanderbilt University

in partial fulfillment of the requirements for

the degree of

DOCTOR OF PHILOSOPHY

in

Cell and Developmental Biology

May, 2007

Nashville, Tennessee

Approved:

Professor Chin Chiang

Professor David M. Miller

Professor Robert J. Coffey

Professor David B. Polk

Professor Roy Zent

To my mother,

my husband and our baby boy

ACKNOWLEDGEMENTS

There is a Chinese saying: only 50 percent of a 100-mile journey is accomplished when you pass the 90-mile landmark, implying that it is often the last small remaining portion that is the most difficult to fulfill. It is very true when I think about how my Ph.D work proceeded during the past years: the more it progressed, the more new questions appeared. It also always reminds me of how limited we are in the world of science, no matter how much has been achieved.

None of this work would have been possible without the guidance of my mentor, Dr. Chin Chiang. His enthusiasm, preciseness, perceptive, and intuitive curiosity toward biological research have had a huge impact on my scientific training, which I would always feel grateful for. I would also like to thank past and present members of the Chiang lab, especially Dr. Ying Litingtung, who played indispensable roles in my projects and in fostering lab harmony.

I would especially like to thank my Thesis Committee, Drs. David Miller, Robert Coffey, Brent Polk, and Roy Zent for keeping me on track and providing me with invaluable suggestions on my projects.

A special thank goes to our collaborators and people who provided reagents and advice on this work, especially Dr. Julie Gordon, Dr. Nancy Manley, Dr. Peter ten Dijke and Dr. Guoqiang Gu.

I would also like to thank the Department of Cell and Developmental Biology for

providing such a diverse and welcoming scientific environment during the years of my study. In addition, none of this work would be possible without funding from the National Institutes of Health and the March of Dimes.

Finally, I am full of gratitude to my family and friends for their support. Thanks to my friends, Xiaoyan Yin, Nan Gao, Zheng Zhou, Zheyong Yu, Lei Zhu, Yuki Ohi and Dan Boyer. I thank my mother, a devoted and determined lady who has overcome many difficulties to raise her two children when our father passed away long time ago. I would not have gone this far without her. I am very grateful to my husband, Wei Ding, who is also my best friend, for his steadfast support, both in science and in our everyday life. He made my journey in pursuing the Ph.D degree more joyful.

TABLE OF CONTENTS

LIST OF TABLES

LIST OF FIGURES

LIST OF ABBREVIATIONS

ActR	Activin receptor
ADE	anterior definitive endoderm
a.k.a	also known as
Alk	Activin receptor-like kinase
AP	alkaline phosphatase
APS	anterior primitive streak
BAMBI	Bmp and Activin membrane-bound inhibitor
BHT	butylated hydroxytoluene
Bmp	bone morphogenic protein
BmpR	bone morphogenetic protein receptor
bp	base pair
BrdU	bromodeoxyuridine
BSA	bovine serum albumin
BSM	bronchial smooth muscle
CHAPS	3-[(3-Cholamidopropyl)dimethylammonio]-1-propanesulfonate
cDNA	complementary DNA
CHARGE	coloboma, heart defect, atresia choanae, retarded growth, genital, and ear anomalies

Ci	cubitus interruptis
Co-Smad	common Smad
DAB	3’3-diaminobenzidine tetrahydrochloride
DEPC	diethyl pyrocarbonate
DIG	digoxygenin
DMSO	dimethyl sulfoxide
DNA	deoxyribonucleic acid
Dpp	decapentaplegic
DV	dorsoventral
E	embryonic day
EA	esophageal atresia
ECM	extracellular matrix
EDTA	disodium ethylenediamine tetra-acetate
Fgf	fibroblast growth factor
Flk-1	fetal liver kinase-1
Foxf1	forkhead box f1
GSK3	glycogen synthase kinase 3
GST	Glutathionine-S-Transferase
HCl	hydrochloric acid
H&E	hematoxylin and eosin

Hh	Hedgehog
HRP	horseradish peroxidase
HSPG	heparin sulfate proteoglycan
IPTG	Isopropyl-b-D-thiogalactoside
I-Smad	inhibitory Smad
M	molar
MAPK	Mitogen-Activated Protein Kinase
μg	microgram
μl	microliter
ml	milliliter
μm	micrometer
mM	millimolar
$MgCl_2$	magnesium chloride
NaCl	sodium chloride
N-myc	neuroblastoma myc-related oncogene
Nog	Noggin (mouse)
NOG	NOGGIN (human)
PAGE	Polyacrylamide Gel Electrophoresis
PBS	phosphate buffered saline
PCP	prechordal plate
PCR	Polymerase Chain Reaction

PECAM-1	platelet endothelial cell adhesion molecule-1
PFA	paraformaldehyde
PS	primitive streak
Ptch	Patched
RAR	retinoic acid receptor
RNA	ribonucleic acid
R-Smad	receptor-regulated Smad
RT	room temperature
SDS	sodium dodecyl sulfate
SEM	standard error of the mean
sFRP	secreted frizzled-related protein
Shh	Sonic Hedgehog
SMA	smooth muscle alpha-actin
SMM	smooth muscle myosin
Smurf	Smad ubiquitination regulatory factor
SNP	single nucleotide polymorphism
Sp-C	surfactant protein C
SSC	standard saline citrate
TA	tracheal agenesis
TAB	TAK binding protein
TAK1	Tgfβ activated kinase 1

Tbx	T-box gene
TEF	tracheoesophageal
TGCE	temperature gradient capillary electrophoresis
Tgfβ	transforming growth factor β
Tris	tris(hydroxymethyl)aminomethane
TUNEL	terminal dUTP nick-end labeling
VATER	vertebral or vascular, anal, TEF, EA, and radial limb or renal
VACTERL	vertebral, anal, cardia, tracheal, esophageal, renal and limb
VCAM-1	vascular cell adhesion molecule-1
VE	visceral endoderm
VEGF	vascular endothelial growth factor
WT	wildtype
X-gal	5-bromo-4-chloro-3-indolyl-β-D-galactopyranoside
Xtj	extra toe
ZO-1	zona occludens 1

CHAPTER I

GENERAL INTRODUCTION

The esophagus and trachea are, respectively, digestive and respiratory organs that originate from a common progenitor, the anterior foregut endoderm, during embryogenesis. Perturbed foregut patterning in development can result in a spectrum of congenital malformations, such as esophageal atresia (EA), tracheoesophageal fistula (TEF), and tracheal agenesis (TA). Despite a common occurrence of foregut defects in humans, in particular EA with TEF, the molecular and cellular etiologies remain poorly understood, in part, due to lack of genetic mouse models that recapitulate the different types of abnormalities. Bmp signaling has been recognized as a critical player in many aspects during development, including lung morphogenesis; however, its role during normal and abnormal patterning of the esophagus and trachea has not been studied. The focus of my thesis work is to elucidate the role of Bmp signaling in anterior foregut patterning, specifically, the development of the esophagus and trachea.

Part I: Anterior Foregut Development

Overview of foregut morphogenesis

The esophagus and trachea are derived from a common anterior foregut endodermal tube which is surrounded by splanchnic mesoderm. Clonal lineage analyses have indicated that the anterior foregut endoderm emerges from the anterior definitive endoderm (ADE), which is contributed by cells at the most anterior end of the early and mid primitive streak (PS) during gastrulation (Figure 1.1) (Kinder, Tsang et al. 2001; Lawson and Schoenwolf 2003). These anterior primitive streak (APS) cells possess organizer properties (Levak-Svajger and Svajger 1974; Beddington 1994; Kinder, Tsang et al. 2001) and also contribute to the prechordal plate (PCP) mesoderm, the most rostral population of midline axial mesoderm (Sulik, Dehart et al. 1994). During gastrulation, the ADE moves rostrally and displaces the visceral endoderm (VE) into the extraembryonic yolk sac (Figure 1.1) (Thomas and Beddington 1996). The APS cells at late streak stage (E7.5), identifiable as the mouse node, give rise to precursor cells of the floor plate and notochord (Beddington 1994; Sulik, Dehart et al. 1994), with minimal contribution to the foregut endoderm (Kinder, Tsang et al. 2001). At this time, the future notochord forms as a plate and is embedded in the dorsal gut endoderm, hence transiently participating in the formation of the roof of the primitive gut tube in rodent and human (Jurand 1974; Lamers, Spliet et al. 1987; Sulik, Dehart et al. 1994; Cleaver and Krieg 2001; Muller and O'Rahilly 2003). At the early headfold stage (E8.0), the lateral edges of the flat endoderm

Figure 1.1 Foregut endoderm formation.
The region located immediately anterior to the primitive streak (anterior PS, dark green, E7.0) contains progenitor cells for the axial mesendoderm (orange), which is laid down as the anterior PS elongates rostrally. The axial mesendoderm gives rise to both the prechordal plate (PCP) and anterior definitive endoderm (ADE). During gastrulation, the ADE (orange) moves rostrally and displaces the visceral endoderm (VE, yellow) into the extraembryonic yolk sac. Identifiable at late streak (E7.5), the mouse node (red), is the source of precursor cells for the floor plate and notochord (pink) (Beddington 1994; Sulik, Dehart et al. 1994) with minimal contribution to the foregut endoderm (Kinder, Tsang et al. 2001). At the early headfold stage (E8.0), the lateral edges of the flat endoderm (orange) begin to converge (foregut cross-section, curved arrows) medio-ventrally beginning at the cephalic and lateral regions and progressing caudally. Dotted line across E8.0 headfold stage embryo represents the foregut cross-section. By E8.5, the foregut tube is closed.

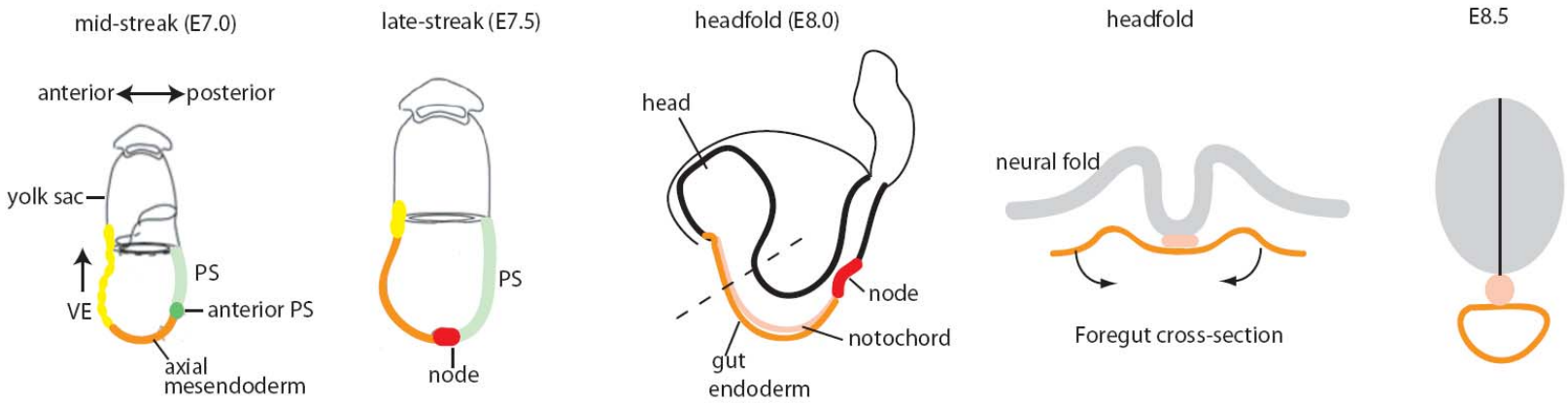
mid-streak (E7.0)
anterior
posterior
yolk sac
PS
VE
anterior PS
axial
mesendoderm
late-streak (E7.5)
PS
node
headfold (E8.0)
head
node
notochord
gut
endoderm
headfold
neural fold
Foregut cross-section
E8.5

begin to converge medio-ventrally through a complex process of differential growth and embryonic folding that starts at the cephalic and lateral regions and progresses caudally. The movements by which the future ventrally-positioned foregut is brought to the midline also serve to bring the associated splanchnic mesoderm into the prospective medial position. During this period, cells of the notochordal plate coalesce and fold off into a rod-shaped structure (Jurand 1974; Lamers, Spliet et al. 1987; Sulik, Dehart et al. 1994; Cleaver and Krieg 2001; Muller and O'Rahilly 2003). The notochord moves dorsally, eventually separating from the endoderm and lying underneath the neural tube where it functions as a signaling center to pattern the adjacent embryonic structures and subsequently becomes the axis of the developing vertebral column (Stemple 2005). The molecular mechanism regulating the detachment of notochordal plate from the dorsal gut endoderm in a timely manner is unknown (Jurand 1974; Sausedo and Schoenwolf 1994). By E8.5, the foregut tube is closed (Figure 1.1), and its most anterior portion gives rise to the thyroid, thymus, trachea, lung and esophagus (Wells and Melton 1999).

Morphogenesis of the murine respiratory and digestive systems begins at around E9.5, when the respiratory primordium appears as a result of an endodermal outgrowth from the ventral wall of the foregut at the border with the pharyngeal endoderm (Kauffman 1992). Concomitant with the primary lung bud formation, the primitive trachea arises ventrally from a relatively more anterior portion of the foregut compared to the lung rudiments, and separates from the dorsal foregut, the primitive esophagus. By E11.5, division of the foregut is complete, yielding the trachea on the ventral side and the

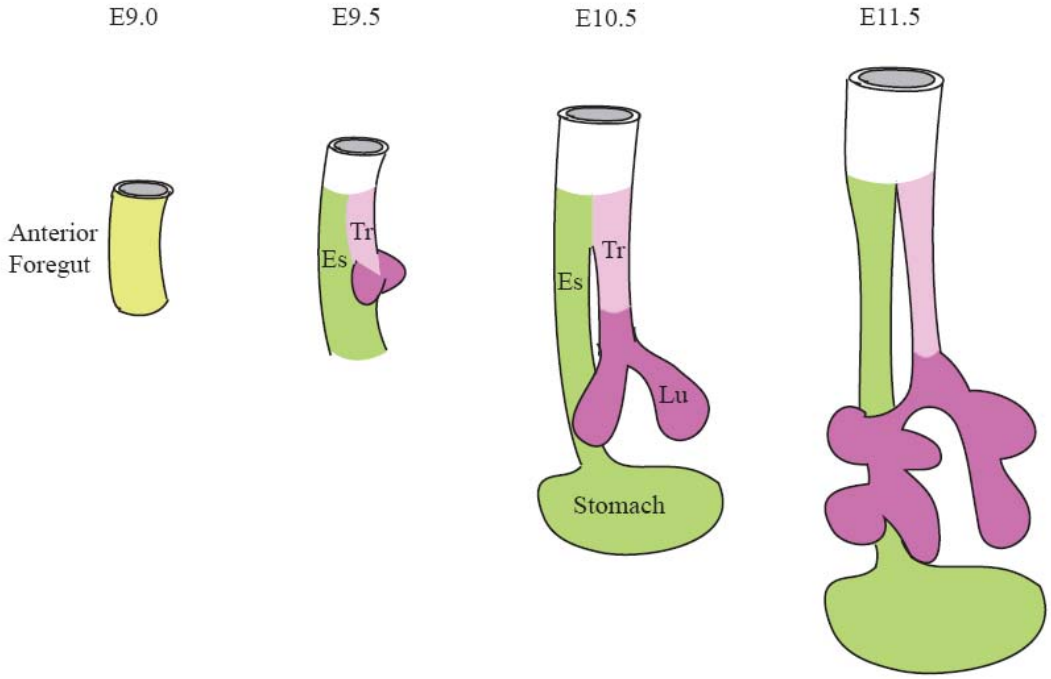

Figure 1.2 Morphogenesis the esophagus and trachea.
In mouse, at E9.5, shortly after formation of a closed foregut tube, separation of the esophagus and trachea begins, with two primitive lung buds appear as a result of an endodermal outgrowth from the ventral wall of the foregut at the border with the pharyngeal endoderm. Concomitant with the primary lung bud formation, the primitive trachea arises ventrally from a relatively more anterior portion of the foregut compared to the lung rudiments, and separates from the dorsal foregut, the primitive esophagus. By E11.5, division of the foregut is complete, yielding the trachea on the ventral side and the esophagus on the dorsal side (Kauffman 1992; Cardoso and Lu 2006). Es-esophagus; Tr-trachea; Lu-lung.

esophagus on the dorsal side (Figure 1.2) (Kauffman 1992; Cardoso and Lu 2006). How the trachea and esophagus are specified and divided is not clear. Many models have been proposed to explain this morphogenetic process (Zaw-Tun 1982; Kluth, Steding et al. 1987; Merei, Farmer et al. 1997; Possogel, Diez-Pardo et al. 1998). One theory suggests that the division results from fusion of the lateral ridges/folds that appear in the lateral wall of the foregut, which advances in a caudal to cranial direction (Skandalakis 1994). It is supported by histological examinations of the foregut (Qi and Beasley 2000; Orford, Manglick et al. 2001; Sasaki, Kusafuka et al. 2001; Williams, Qi et al. 2001); however, since the lateral ridges/folds do not appear to exist all the time, this once widely accepted concept has now been challenged (Zaw-Tun 1982; Kluth, Steding et al. 1987; Kluth and Fiegel 2003). Another more recent model proposes that the tracheo-esophageal separation is driven by the outgrowth and elongation of the respiratory primordium. The mesenchymal tissue that lies between the respiratory and digestive tubes constitutes the tracheo-esophageal septum which necessarily accompanies the separation of the esophagus and trachea (Zaw-Tun 1982; Sanudo and Domenech-Mateu 1990). This theory is supported by several studies which showed that the separation point of the respiratory and digestive systems remained at a constant somitic-vertebral level during downgrowth of the tracheal diverticulum (O'Rahilly and Muller 1984; Sutliff and Hutchins 1994; Williams, Quan et al. 2003). However, other investigators argue that the septum may actively move cranially along the foregut tube while the esophageal and tracheal tubes elongate posteriorly (Qi and Beasley 2000; Kluth and Fiegel 2003; Felix, Keijzer et al.

2004). Other theories also have been suggested, such as differential proliferation (Kluth and Fiegel 2003) and/or cell death that may play important roles in the separation process (Sutliff and Hutchins 1994; Zhou, Hutson et al. 1999; Qi and Beasley 2000; Williams, Qi et al. 2000).

Foregut morphogenesis is a complex process of inductive interactions between the endoderm and its surrounding splanchnic mesoderm. Secreted signaling molecules produced by the mesenchyme such as Bmps, Wnts, and Fgfs may dynamically regulate the proliferation and/or differentiation of the endoderm in a paracrine fashion. Bmp signaling has been shown to play important roles during lung morphogenesis (Weaver, Yingling et al. 1999; Weaver, Dunn et al. 2000; Weaver, Batts et al. 2003); however, whether and how Bmp signaling is involved in patterning of the esophagus and trachea, physiologically or pathologically, still remains to be determined.

Congenital foregut malformations

Separation of the trachea and esophagus, a major developmental maneuver, presents enormous opportunities for malformations to occur. The occurrence of foregut anomalies is common in humans, approximately 1 in 3,000 live births (Skandalakis 1994). Based on their clinical manifestations, foregut defects have been divided into the following groups (Figure 1.3):

(1) complete (agenesis) or partial (atresia) absence of the esophagus;

(2) complete (agenesis) or partial (atresia) absence of the trachea;

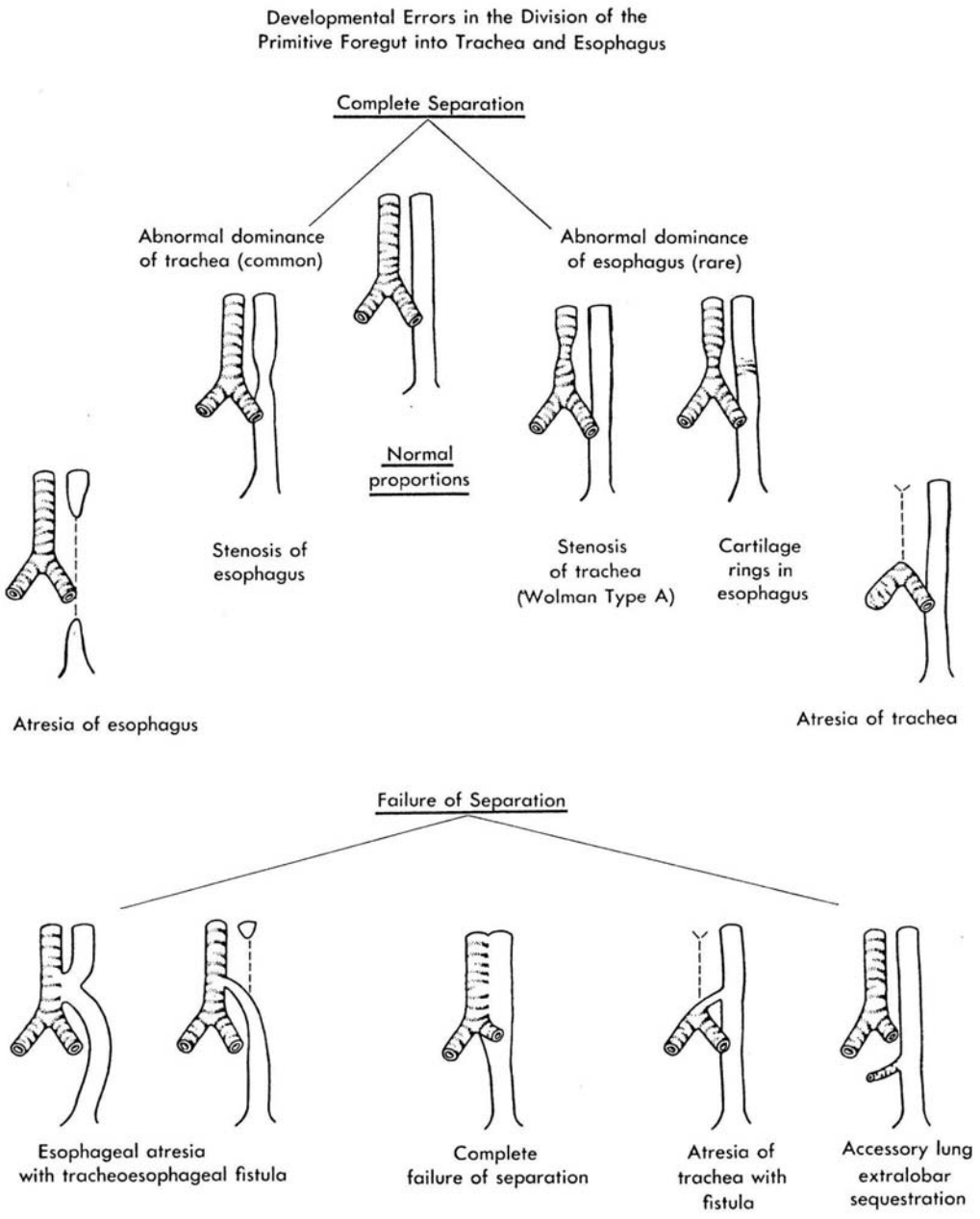

Figure 1.3 Different forms of foregut malformations.
Reprinted from Skandalakis 1994.

(3) stenosis of the esophagus;

(4) stenosis of the trachea;

(5) complete or partial failure of separation of the trachea and esophagus, which is often referred to as persistent foregut, or tracheoesophageal fistula (TEF, fistula refers to the abnormal connection). Normally, failure of separation does not affect differentiation. TEF is often accompanied with other defects in the esophagus and/or trachea, such as tracheal agenesis (TA) with tracheaoesophageal fistula (TA/TEF) and esophageal atresia (EA) with tracheaoesophageal fistula (EA/TEF).

Approximately 1 in 4,000 babies are born with EA/TEF (Shapiro, Eddy et al. 1958; Myers 1974; de Lorimier and Harrison 1985; Skandalakis 1994). About 50% of infants with EA/TEF have non-hereditary concurrence of three or more defects of various systems including the constellations known as VATER (vertebral or vascular, anal, TEF, EA, and radial limb or renal, a.k.a VACTERL [vertebral, anal, cardia, tracheal, esophageal, renal and limb]) and CHARGE (coloboma, heart defect, atresia choanae, retarded growth, genital, and ear anomalies) (Cano Garci-Nuno, Solis Sanchez et al. 1992; Kutiyanawala, Wyse et al. 1992; Torfs, Curry et al. 1995; Blake, Davenport et al. 1998; Tellier, Cormier-Daire et al. 1998; Shaw-Smith 2006). The cause of EA/TEF remains unknown but there are some associations with diabetic mothers (David and O'Callaghan 1975; Aberg, Westbom et al. 2001), sex hormone exposure (Nora, Nora et al. 1978; Lammer and Cordero 1986), increase in maternal age (Torfs, Curry et al. 1995),

chromosomal abnormalities such as trisomies 13, 18 and 21 (Ein, Shandling et al. 1989; Kallen, Mastroiacovo et al. 1996; Beasley, Allen et al. 1997; Sparey, Jawaheer et al. 2000) and twinning (Orford, Glasson et al. 2000). EA/TEF has been further classified according to the type of esophageal defect and location of the fistula (Table 1.1). The most prevalent is Type C, occurring in about 86.5% of infants born with EA/TEF (Hicks and Mansfield 1981; Engum, Grosfeld et al. 1995; Sparey, Jawaheer et al. 2000). In Type C EA/TEF, the esophagus, usually narrower than normal, fails to form a continuous tube connecting the oral cavity to the stomach; instead the upper esophagus simply ends in a blind pouch (EA), with the distal segment of the esophagus abnormally connected to the trachea via a fistula (TEF). While the survival rate after surgery to repair the abnormal fistula and reconnect the upper and lower esophagus has been tremendously improved for afflicted infants without other severe anomalies or associated problems (Sharma, Shekhawat et al. 2000), nevertheless, the relatively high frequency of EA/TEF incidence does pose great clinical and familial burden.

Tracheal atresia/agenesis are relatively rare congenital foregut anomalies (less than 1:50,000) that produce respiratory distress and are incompatible with life (Manschot, van den Anker et al. 1994). Though tracheal agenesis (TA) and tracheal atresia are different entities anatomically, which are characterized by partial and complete absence of trachea respectively, both fall into a spectrum of foregut defects, often referred to as tracheal atresia, whereby the trachea is underdeveloped/deformed to various degrees, resulting in disrupted communication between the larynx proximally and the lungs

Table 1.1 Different forms of esophageal atresia with tracheoesophageal fistula

Type	Description	Diagram
Type A Esophageal Atresia (7.7%)	Both segments of the esophagus end in blind pouches. Neither segment of the esophagus is attached to the trachea	
Type B Esophageal Atresia with Tracheoesophageal fistula (0.8%)	The upper segment of the esophagus forms a fistula to the trachea. The lower segment ends in a blind pouch.	
Type C Esophageal Atresia with Tracheoesophageal fistula (86.5%)	The upper segment of the esophagus ends in a blind pouch. The lower segment forms a fistula to the trachea.	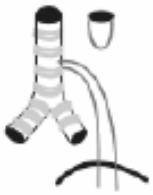
Type D Esophageal Atresia with Tracheoesophageal fistula (0.7%)	Both segments of the esophagus are attached to the trachea.	
Type H Tracheoesophageal Fistula (4.2%)	There is no esophageal atresia. However, fistula is present between the esophagus and the trachea.	

distally (Kerschner and Klotch 1997; Evans, Greenberg et al. 1999; Saleeby, Vustar et al. 2003; Lander, Schauer et al. 2004). According to the anatomy, TA has been classified into three types (Figure 1.4) (Floyd, Campbell et al. 1962): type 1 refers to absence of the proximal (upper segment) trachea with a short segment of the distal trachea, which connects to the esophagus via a fistula; in type 2, the most common form, the entire trachea is absent with the main bronchi fused in the midline at the carina; in type 3, the entire trachea is also missing, but the main bronchi do not fuse in the middle. Instead, they arise separately from the esophagus. Like EA/TEF, babies born with TA are also often found to have defects in other organs. It has been suggested that TA could be part of the VA(C)TER(L) and TACRD (tracheal agenesis or laryngotracheal atresia, complex congenital cardiac abnormalities or ventricular septal defect, radial ray defects, and duodenal atresia) associations (Evans, Reggin et al. 1985; Diaz, Adams et al. 1989).

While different in manifestation, foregut malformations were believed to have a common embryonic origin (Skandalakis 1994). It is thought that misregulation of signaling pathway(s) during a critical period of embryogenesis by environmental influences, such as exposure to certain teratogenic drugs or disease condition, could lead to those abnormalities, since familial occurrence of the congenital defect with associated anomalies is not common (Auchterlonie and White 1982; McMullen, Karnes et al. 1996; Nezarati and McLeod 1999). Although several theories have been proposed, such as intraembryonic pressure and abnormal development of the tracheoesophageal septum (Fluss and Poppen 1951; Moyson 1970; Merei and Hutson 2002), the etiology and

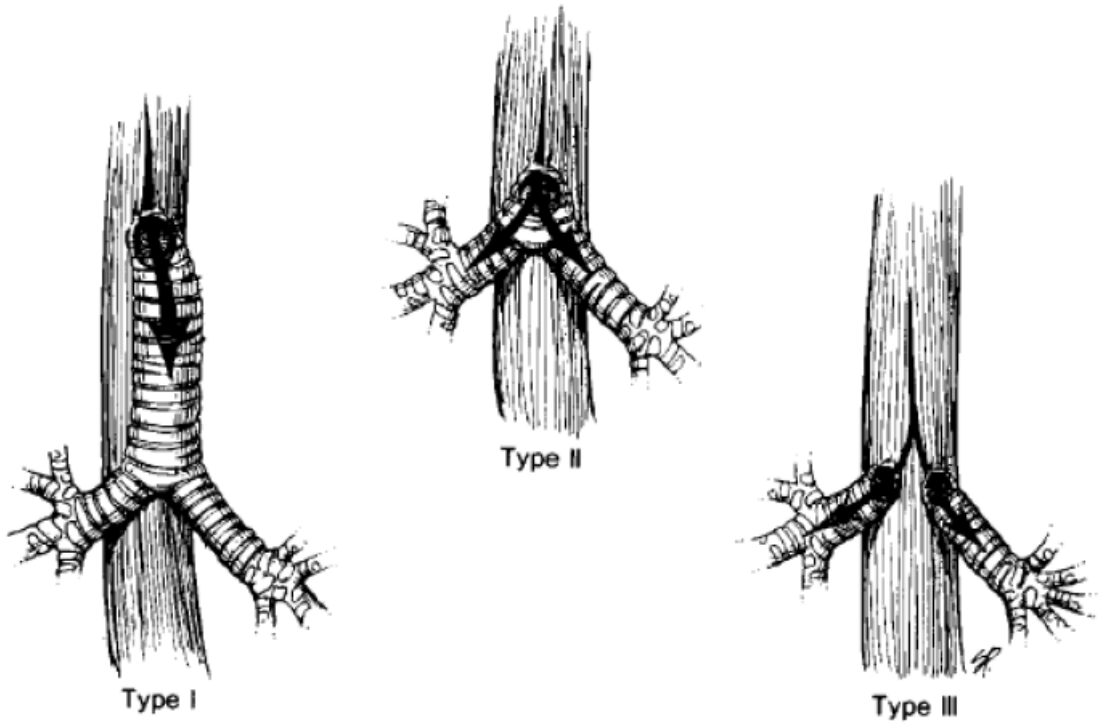

Figure 1.4 Floyd's classification of tracheal agenesis/atresia. Reprinted from Diaz et al. 1989.

molecular mechanism of foregut abnormalities remain obscure, in part due to short of embryos demonstrating different types of malformations (Evans, Greenberg et al. 1999; van Veenendaal, Liem et al. 2000; Merei and Hutson 2002; Saleeby, Vustar et al. 2003; Lander, Schauer et al. 2004).

Animal models with foregut anomalies

A few mutant mouse lines have been generated that exhibit, among other abnormalities, defects in tracheal and esophageal morphogenesis, such as *Shh*$^{-/-}$ lacking Sonic hedgehog (Shh) function (Litingtung, Lei et al. 1998; Pepicelli, Lewis et al. 1998); *Gli2*$^{-/-}$*;Gli3*$^{+/-}$, deficient in Shh signaling (Motoyama, Liu et al. 1998); *Nkx2.1*$^{-/-}$, deficient in respiratory endoderm expression (Minoo, Su et al. 1999) and *RARα*$^{-/-}$*;β2*$^{-/-}$ or *RARα1*$^{-/-}$*;β*$^{-/-}$, deficient in retinoic acid receptors α and β2 function (Mendelsohn, Lohnes et al. 1994). As shown in Table 1.2, in the *Shh*$^{-/-}$ and *Gli2*$^{-/-}$*; Gli3*$^{+/-}$ foregut, the upper segment of the esophagus ends in a blind pouch and the lower segment appears to completely fail to separate from the trachea. The single foregut tubes observed in *Nkx2.1*$^{-/-}$ and *RARα*$^{-/-}$*; β2*$^{-/-}$ or *RARα1*$^{-/-}$*;β*$^{-/-}$ exhibit esophagotracheal characteristics. Haploinsufficiency of *Foxf1*, a member of forkhead family of transcription factors, displays a foregut phenotype highly reminiscent of *Shh*$^{-/-}$ foregut, and it has been suggested that *Foxf1* is involved in Shh pathway, downstream of Shh (Mahlapuu, Enerback et al. 2001). *Hoxc4* is a homeobox gene that encodes a highly conserved transcription factor. *Hoxc4* null foregut

Table 1.2 Summary of mutant mouse embryos exhibiting foregut malformations

Gene	Mutant phenotype	Human locus
RARα$^{-/-}$;*β2*$^{-/-}$ or *RARα1*$^{-/-}$;*β*$^{-/-}$	TEF; lung hypoplasia or agenesis	*RARα*: 17q21.1; *RARβ*: 3p24
Shh$^{-/-}$	EA/TEF; lungs form rudimentary sacs	7q36
Gli2$^{-/-}$;*Gli3*$^{+/-}$	EA/TEF; severe lung phenotype	*Gli2*$^{-/-}$: 2q14; *Gli3*$^{-/-}$: 7p13
Gli2$^{-/-}$;*Gli3*$^{-/-}$	no formation of esophagus, trachea and lung	
Foxf1$^{-/-}$	lethal before E10, extra embryonic defects	16q24
Foxf1$^{+/-}$	EA/TEF; lung hypoplasia; lobulation defects	
Nkx2.1$^{-/-}$ (*TTF-1*$^{-/-}$)	TEF; rudimentary peripheral lung primordia	14q13
Hoxc4$^{-/-}$	partial or completely blocked esophageal lumen; Disruption of esophageal musculature	12q13.3
Tbx4 misexpression	TEF	17q21-q22

EA: esophageal atresia; TEF: tracheoesophageal fistula. (Adapted from Felix et al. 2004)

exhibits a partially or completely blocked esophageal lumen and a disruption of esophageal musculature (Boulet and Capecchi 1996). *Tbx4* belongs to the T-box family of transcription factors. An early study in the chick reported that it was expressed in the lung bud and trachea, where it was postulated to be involved in the separation of the trachea and esophagus (Gibson-Brown, S et al. 1998). Transient misexpression of *Tbx4* in the prospective esophageal-respiratory region results in formation of tracheoesophageal fistula (Sakiyama, Yamagishi et al. 2003). The occurrence of grossly similar foregut defects by altering the functions of different genes suggests that multiple signaling pathways are likely to be involved in normal foregut tube morphogenesis. Notably, the foregut defects revealed in these mutant embryos are not highly reminiscent the Type C EA/TEF (Table 1.1), the most common form observed in humans. Additionally, no one so far has reported genetically altered mutant mouse models that exhibit tracheal atresia/agenesis.

In addition to mutant mouse lines, an adriamycin rat/mouse model has also been used by investigators to study different types of foregut malformations, including Type C EA/TEF and TA. Adriamycin, an anthracycline antibiotic and chemotherapeutic drug (Young, Ozols et al. 1981; Tewey, Rowe et al. 1984; Muller, Jenner et al. 1997) with teratogenic potential, has been widely used to produce a spectrum of anomalies in developing rat and mouse fetuses, depending on the dose, duration and time of administration(Thompson, Molello et al. 1978). Intraperitoneal injection of pregnant females with adriamycin at E6.0-9.0 in rat or at E7.5-8.5 in mouse results in more than

50% of the embryos developing EA/TEF, some of which display Type C EA/TEF. Adriamycin-treated embryos can also display TA, although at a much lower frequency (about 3%) (Diez-Pardo, Baoquan et al. 1996; Possogel, Diez-Pardo et al. 1998; Qi and Beasley 1999; Ioannides, Chaudhry et al. 2002; Dawrant, Giles et al. 2007). A prominent abnormality in adriamycin-treated rat embryos is hypertrophy of the notochord with ventrally displaced branches making prolonged contacts with or in very close proximity to the dorsal foregut endoderm, raising the possibility that the abnormal notochord branches may contribute to the pathogenesis of EA/TEF (Possoegel, Diez-Pardo et al. 1999; Qi and Beasley 1999; Orford, Manglick et al. 2001; Qi, Beasley et al. 2001; Williams, Qi et al. 2001; Mortell, O'Donnell et al. 2004). Efforts have been made to study possible alteration in Shh signaling in this context, based on the fact that Shh is expressed in the notochord and Shh signaling may function to pattern the adjacent tissues. In addition, adriamycin treatment can generate other defects similar to the VA(C)TER(L) association in humans, and defects in Shh signaling have been shown to exhibit a VA(C)TER(L) phenotype. However, molecular expression analysis of Shh target genes such as *Patched1* (*Ptch*), which encodes a putative Shh transmembrane receptor, failed to provide evidence for ectopic Shh signaling in the adriamycin-treated foregut (Orford, Manglick et al. 2001).Taken together, although the adriamycin-treated embryo serves as a useful model to characterize the phenotypes of foregut abnormalities, the precise cellular and molecular mechanism of adriamycin action remains largely unknown.

Part II: Bmp Signaling and Embryonic Development

The Bmp signaling pathways

The bone morphogenetic proteins (Bmps) were originally discovered and hence named based on their bone and cartilage-inducing activities (Urist 1965; Urist, Mikulski et al. 1975; Urist, Nogami et al. 1976; Wozney, Rosen et al. 1988). Subsequent purification, cDNA cloning and functional studies revealed a large family of these secreted proteins, which play remarkable roles in many aspects of development, by regulating cell proliferation, survival, differentiation, migration and cell fate determination (Hogan 1996; Wozney 1998). To date, over 20 members of the Bmp family have been identified, in organisms ranging from *Caenorhabditis elegans* to humans (Balemans and Van Hul 2002; de Caestecker 2004). Based on their amino acid sequence homology and functional similarity, they can be grouped into subsets, such as Bmp2/4/Dpp and 60A subgroups (boxes in Figure 1.5).

Bmps belong to the structurally related transforming growth factor β (Tgfβ) superfamily. Like all members of the Tgfβ superfamily, Bmps are initially synthesized as large precursors that contain a signal sequence and a pro-domain. These proteins are subsequently proteolytically cleaved to release the carboxy-terminal mature domains, which homo- or hetero-dimerize via a disulfide link to generate the active signaling molecules (Wozney 1992; Hogan 1996; Canalis, Economides et al. 2003). Bmps are distinguished from other Tgfβ superfamily members in that they have seven, rather than

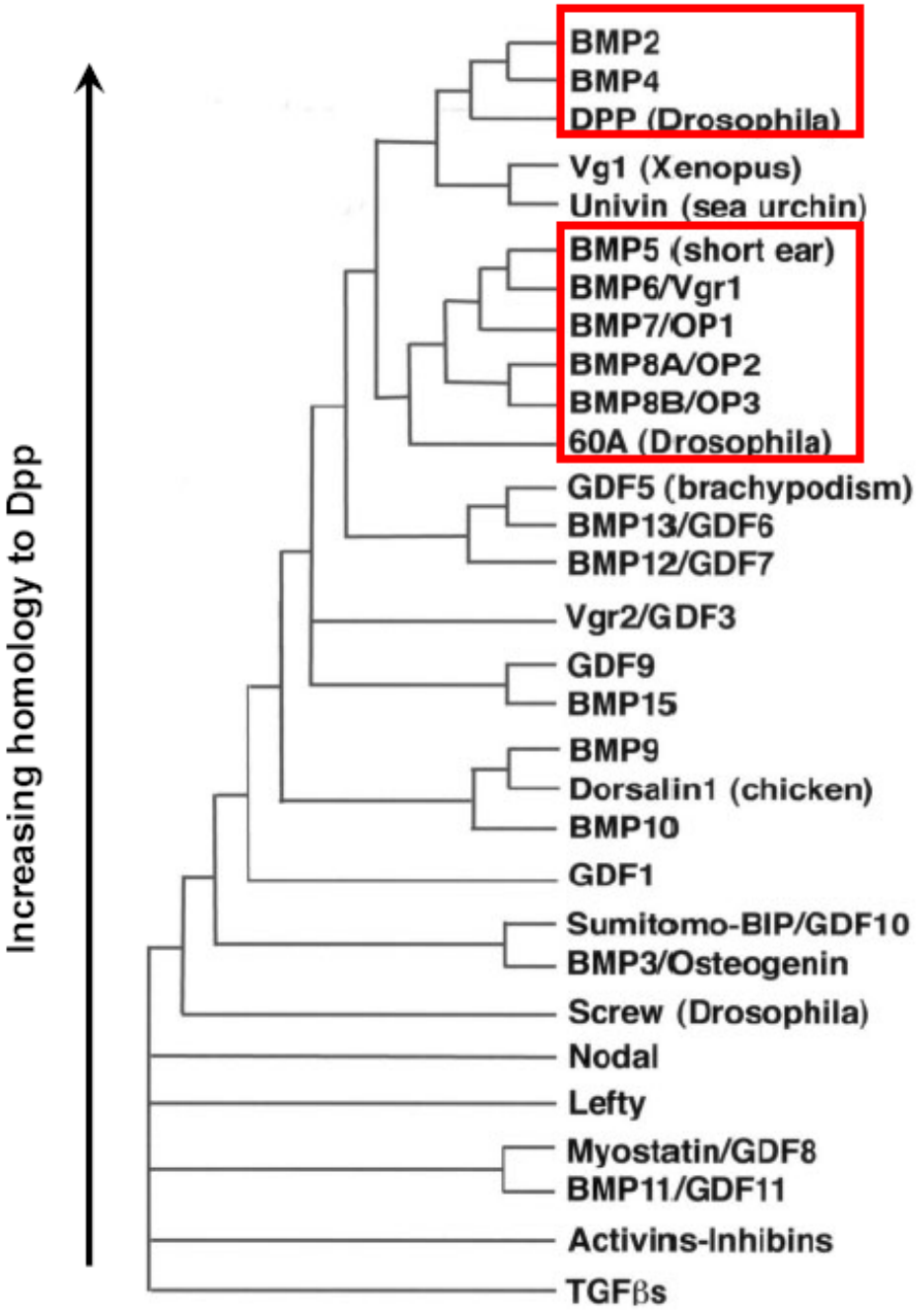

Figure 1.5 Classes of Bmp members and relationships of Bmps with other Tgfβs. Within the Bmp family, members can be grouped into subsets based on the amino acid sequence homology, such as subgroups Bmp2/4/Dpp and 60A, as highlighted by boxes. Vertical arrow indicates increasing homology to Dpp. Adapted from Zhao et al., 2003.

nine, conserved cysteine residues in the mature domain (Griffith, Keck et al. 1996; Wozney 1998; Scheufler, Sebald et al. 1999). In addition, they signal through a structurally related set of receptors to activate a set of downstream effectors that are different from those activated by Tgfβ/Activin/Nodal (Massague and Chen 2000).

Signaling by Bmps is mediated by a receptor complex consisting of type I and type II serine-threonine kinases, two distinct but related transmembrane proteins, both of which contain an extracellular ligand-binding domain composed of 10-12 cysteine residues capable of forming a three-finger toxin fold, a single transmembrane domain, and an intracellular serine-threonine kinase domain. The type I and type II receptors have different conserved sequences in their kinase domain. In addition, the type I receptors share a glycine/serine residue-rich domain (GS-box) in the juxtamembrane region, which is essential for type I receptor activation (ten Dijke, Korchynskyi et al. 2003). So far, three type I receptors are found to bind to Bmps, including Alk3 (Activin receptor-like kinase-3, a.k.a BmpR-IA), Alk6 (BmpR-IB) and Alk2 (ActR-IA) (Massague and Chen 2000). Three type II receptors for Bmps have also been identified which are BmpR-II, ActR-IIA and ActR-IIB (Kawabata, Chytil et al. 1995; Rosenzweig, Imamura et al. 1995). While Alk3, Alk6 and BmpR-II are specific for Bmps, Alk2, ActR-IIA and ActR-IIB are also receptors for activins (Chen, Zhao et al. 2004).

Upon ligand binding to the receptor complex, the constitutively active type II receptor transphosphorylates the associated type I receptor at serine residues in the GS box, resulting in conformational changes which allow the type I receptor to bind ATP and

subsequently phosphorylate its substrates, receptor-regulated Smads (R-Smads) (Huse, Muir et al. 2001). Bmps activate R-Smad1/5/8, not R-Smad 2/3, in that a cluster of residues within the L45 loop in the kinase domain of the Bmp-activated type I receptor (Alk2, 3, 6) tend to interact well with the L3 loop in the carboxy-terminus of R-Smad1/5/8, whereas the Tgfβ/Activin/Nodal-activated type I receptors pair well with R-Smad2/3 (Massague and Chen 2000). Following dissociation from the type I receptor, phosphorylated R-Smads heterodimerize with the common Smads (Co-Smads), Smad4, which itself cannot be phosphorylated by type I receptors, but its association with R-Smads is necessary for intracellular transduction. The resulting heterdimeric Smad complex then translocates into the nucleus to activate or repress transcription depending on the recruited transcriptional co-modulators (Figure 1.6) (Massague and Wotton 2000; Shi and Massague 2003; Miyazono, Maeda et al. 2005). The specificity of Bmp signaling is controlled primarily by type I receptor. For instance, Bmp2 and Bmp4 primarily bind to Alk3 and Alk6, whereas Bmp7 binds to Alk2 with high affinity compared to Alk3 and Alk6 (Hsu, Rovinsky et al. 2005).

In addition to the canonical Smad pathway, accumulating evidence suggests that Smad-independent pathways also exist to relay Bmp signals. In particular, an alternative Bmp-mitogen-activated protein kinase (MAPK) signaling pathway has been described (Figure 1.6), in which activation of Bmp-induced receptor complexes results in the activation of $p38^{MAPK}$ pathway, likely via TAK1 (Tgfβ Activated Kinase 1)-TAB1 (TAK binding protein). It appears that binding of Bmps to the preformed receptor complex

Figure 1.6 Bmp signaling pathways.
Binding of Bmps to the preformed receptor complexes results in the activation of the canonical Smad signaling pathway (middle), whereas formation of Bmp binding-induced receptor complexes leads to the activation of the alternative $p38^{MAPK}$ pathway (left). It appears that Bmp can also activate Ras and ERK (right), via an unknown mechanism. Modulation of Bmp signaling occurs at different levels (Massague and Chen 2000). Extracellularly, antagonists such as Noggin interact with Bmps, thus preventing ligand binding to its receptor. On the cell surface, BAMB1, a transmembrane protein that has similar sequence to type I receptors but lacks the intracellular kinase domain, blocks Bmp signaling by interfering with functional receptor complex formation. Intracellularly, I-Smads compete with R-Smads, for association either with the type I receptor or with Co-Smad, i.e. Smad4. I-Smad (Smad6) can also inhibit Bmp-$p38^{MAPK}$ pathway by directly binding to and inhibiting TAK1(Kimura, Matsuo et al. 2000; Massague and Chen 2000). In addition to the I-Smads, Smurfs have also been found to interact with R-Smads, thus targeting R-Smads for ubiquitin-mediated degradation by the proteasome. EC-extracellular; IC-intracellular.

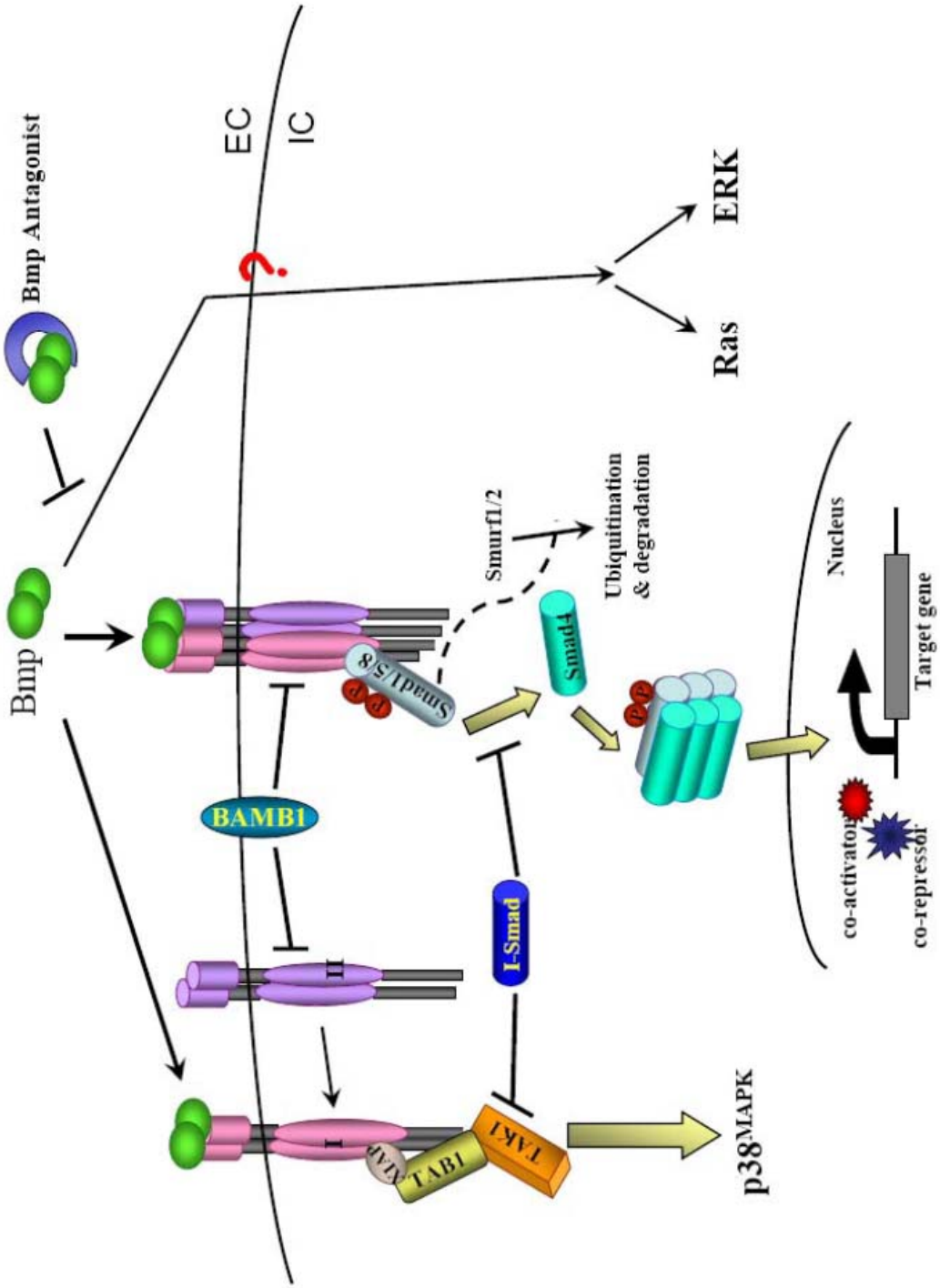
Bmp Antagonist
Bmp
EC
IC
?
ERK
Ras
BAMB1
Smad1/5/8
P
P
Smurf1/2
Ubiquitination
& degradation
Smad4
P
P
I-Smad
II
I
XIAP
TAB1
TAK1
p38MAPK
Nucleus
Target gene
co-activator
co-repressor

leads to activation of the Smad signaling pathway, whereas ligand binding to the homo-oligomeric type I receptors and recruitment of the type II receptors results in activation of the alternative MAPK pathway. Studies have shown Ras and ERK can also be activated by Bmps, but not much is known about the mechanism (Kawabata, Chytil et al. 1995; Moustakas and Heldin 2005).

Modulation of Bmp signaling

Transduction of Bmp signaling is rather complex when one thinks about how Bmps mediate such diverse biological functions, with over 20 ligands, three type I and three type II receptors, and three Bmp-activated R-Smads and alternative intracellular effectors. Inside the nucleus, tissue/cell-specific expression of a combination of signaling components and recruitment of different co-factors (co-activators or co-repressors) can provide specificity toBmp signaling in that particular tissue or cell. In addition, Bmp signaling can be exquisitely regulated at the levels of extracellular space, cell surface or cytoplasm (Massague and Chen 2000; Nohe, Keating et al. 2004).

Extracellularly, secreted polypeptide antagonists bind Bmp ligands and sequester them from their cognate receptors (Figure 1.6). Numerous Bmp antagonists have been identified, including *Noggin*, *Chordin*, and the DAN family (which includes Cerberus and Gremlin) (Smith and Harland 1992; Piccolo, Sasai et al. 1996; Hsu, Economides et al. 1998; Pearce, Penny et al. 1999; Piccolo, Agius et al. 1999). Noggin, which was originally isolated and characterized as a component of the Spemann organizer in

Xenopus (Smith and Harland 1992), binds and inactivates Bmps by blocking the molecular interfaces of the binding epitopes for both type I and type II receptors (Groppe, Greenwald et al. 2002). Noggin binds Bmp-2, -4, -7, -5, -6, GDF-5, -6, and Vg1 with various degrees of affinity, but not other Tgfβ members (Zimmerman, De Jesus-Escobar et al. 1996; Canalis, Economides et al. 2003). Compared to Noggin, the cysteine-rich repeat protein Chordin plays a subtler role in modulating Bmp signaling. It acts as a sink for the ligands, thus preventing their binding to the receptors. Degradation of Chordin by specific proteases then releases the ligands and promotes receptor activation (Larrain, Bachiller et al. 2000; Larrain, Oelgeschlager et al. 2001). In additions to antagonists, heparin sulfate proteoglycans (HSPGs) in the extracellular matrix (ECM) may also sequester Bmps, thereby limiting their diffusion and/or availability to the receptors (Fisher, Li et al. 2006).

On the cell surface, a transmembrane protein termed BAMBI (Bmp and Activin membrane-bound inhibitor) can block Bmp signaling by interfering with functional receptor complex formation. *BAMBI* is the *Xenopus* and *Zebrafish* orthologue of the mammalian *Nma* (Degen, Weterman et al. 1996; Onichtchouk, Chen et al. 1999) (Figure 1.6). The extracellular domain of BAMBI has a sequence similar to type I receptors and its short intracellular domain lacks kinase activity. BAMBI binds to type I receptors, thus precluding their association with cognate type II receptors and phosphorylation of R-Smads (de Caestecker 2004). During *Xenopus* embryogenesis, expression of BAMBI resembles that of *Bmp4*, and maintenance of BAMBI expression requires sustained Bmp

signaling, suggesting BAMBI functions as a negative feedback loop in Bmp signaling (Onichtchouk, Chen et al. 1999).

Intracellularly, Bmp signaling can be modulated by actions of inhibitory Smads (I-Smads) 6 and 7, and Smad ubiquitination regulatory factors (Smurfs) 1 and 2. I-Smads compete with R-Smads for the association either with the activated type I receptor (Smad6 and 7) or with Co-Smads, i.e. Smad4 (Smad6) (Figure 1.6) (Miyazono 1999; Massague and Chen 2000; ten Dijke, Korchynskyi et al. 2003). As Smad7 constitutively interacts with HECT-domain ubiquitin ligases Smurfs1 and 2, Smad7 can also inhibit Smad signaling via receptor degradation. Upon recruitment of the Smad7/Smurf complex to the activated type I receptor, Smurf1 or 2 induces receptor degradation via proteasomal and lysosomal pathways (Kavsak, Rasmussen et al. 2000; Ebisawa, Fukuchi et al. 2001; ten Dijke, Korchynskyi et al. 2003). Smad6 has also been shown to inhibit Bmp-MAPK pathway by directly binding to and inhibiting TAK1 (Kimura, Matsuo et al. 2000; Massague and Chen 2000). In addition to the I-Smads, Smurfs have also been found to interact with R-Smads, thus targeting R-Smads for ubiquitin-mediated degradation by the proteasome (Figure 1.6) (Zhu, Kavsak et al. 1999; Zhang, Chang et al. 2001).

Bmp signaling in foregut development

Bmp signaling has always been a focus of biologists, since the time it was discovered (Urist 1965). It has proven to be an important pathway with roles in almost

every aspect of embryogenesis (Hogan 1996; Zhao 2003; Chen, Zhao et al. 2004; Pogue and Lyons 2006).

As to the patterning of the anterior foregut, studies of Bmp signaling have focused on lung morphogenesis and, in particular, the role of Bmp4 during lung development. Two additional Bmps are expressed in the lung, i.e. Bmp5 and Bmp7; however, they are not essential for lung development based on their mutant phenotypes (King, Marker et al. 1994; Dudley, Lyons et al. 1995). In the mouse lung, two prominent domains of *Bmp4* expression have been reported. *Bmp4* is expressed dynamically in epithelial cells at the distal tips of growing lung buds (Bellusci, Henderson et al. 1996), where it antagonizes fibroblast growth factor 10 (Fgf10) initiated outgrowth of lung bud which is critical for further branching of the distal endoderm (Weaver, Dunn et al. 2000). Overexpression of *Xnoggin* or a dominant negative Bmp receptor-*dnAlk6* in the distal epithelium using the surfactant protein C (Sp-C) promoter/enhancer resulted in increased proximal cell types at the expense of distal cell types, indicating another critical role of Bmp4 in controlling proximal-distal patterning of the lung epithelium (Weaver, Yingling et al. 1999). Besides epithelial expression, Bmp4 is also expressed in the lung mesenchyme. Unlike the endodermally expressed Bmp4 at the distal tips, which is controlled by localized Fgf signals (including Fgf10), evidence indicates that this mesenchymal Bmp4 expression is induced by Shh expressed in the endoderm, suggesting that *Bmp4* can be regulated by different signals in adjacent cell populations (Weaver, Batts et al. 2003).

In addition to its expression in the developing lung, Bmp4 has also been reported to be highly expressed throughout the ventral mesenchyme encompassing the future lungs and trachea at about E9.75 (27 somites) (Weaver, Yingling et al. 1999), thus raising the possibility that Bmp signaling may play a pivotal role in the morphogenesis of the trachea. However, assessing this potential biological function awaits generation of a mouse line that specifically deletes Bmp4 function in the ventral foregut domain, since *Bmp4* null mutants exhibit early lethality and rarely survive past the egg cylinder stage (E6.5).

Novel roles of Bmp signaling in patterning the esophagus and trachea

To elucidate new roles of Bmp signaling in anterior foregut patterning, we took advantage of two genetic mouse models, i.e. *Noggin* (*Nog*) null embryos and *Bmp4* conditional mutants generated by *Foxg1Cre*.

We have found that mouse embryos with complete loss of *Noggin* function display Type C EA/TEF, and notochordal abnormalities that are strikingly similar to those reported in adriamycin-treated rat embryos. In accord with esophageal atresia, *Nog*$^{-/-}$ embryos displayed reduction in the dorsal foregut endoderm which was associated with reduced adhesion and disrupted basement membrane. However, no significant apoptosis in the *Nog*$^{-/-}$ dorsal foregut was observed. Instead, non-notochordal, likely endodermal, cells were found in *Nog*$^{-/-}$ notochord suggesting that *Noggin* function is required in the notochordal plate for its proper delamination from the dorsal foregut. Notably, ablating

Bmp7 function in *Nog*$^{-/-}$ embryos rescued EA/TEF and notochord branching defects, suggesting a critical role of Noggin mediated Bmp7 antagonism in EA/TEF pathogenesis.

Conditional ablation of *Bmp4* in the ventral foregut region by a *Foxg1Cre* transgene resulted in loss of trachea. Further analysis indicated that the initial tracheal specification was unaffected; however subsequent outgrowth of the trachea was severely impaired. Consistent with the reduced growth capacity, the anterior foregut domain displayed significantly reduced epithelial and mesenchymal proliferation without apparent alterations in apoptotic cell death. While we did not observe alteration of Wnt/β-catenin signaling in the *Bmp4*-deficient foregut, we detected consistent reduced expression of Shh, a signaling molecule known to promote cell proliferation, in the ventral foregut of *Bmp4*-deficient embryos. Therefore, these findings elucidate a critical role of Bmp signaling and cell proliferation in tracheal morphogenesis and implicate potential Bmp-Shh crosstalk in anterior foregut morphogenesis.

CHAPTER II

ABERRANT BMP SIGNALING AND NOTOCHORD DELAMINATION IN THE PATHOGENESIS OF ESOPHAGEAL ATRESIA

Introduction

The esophagus and trachea are respectively dorsal and ventral derivatives of a common foregut tube. Abnormal development of these organs can lead to profound functional defects in humans. The most prevalent foregut malformation is known as Type C EA/TEF, which is characterized by an upper esophageal pouch and lower often severely stenosed esophagus that makes an abnormal connection with the trachea via a fistula (Hicks and Mansfield 1981; Engum, Grosfeld et al. 1995; del Rosario and Orenstein 1998; Clark 1999; Sparey, Jawaheer et al. 2000; Brunner and van Bokhoven 2005). Despite the common occurrence of EA/TEF, the etiology and molecular pathogenesis of this developmental abnormality remain unknown. Feingold syndrome which is manifested by defects including intestinal atresia is one of a few such conditions that have been linked to a molecular defect (van Bokhoven, Celli et al. 2005). Several genetically-modified mouse mutants have been shown to display an array of foregut malformations indicating that foregut development is regulated by a complex genetic network (Mendelsohn, Lohnes et al. 1994; Litingtung, Lei et al. 1998; Motoyama, Liu et al. 1998; Pepicelli, Lewis et al. 1998; Minoo, Su et al. 1999).

Adriamycin is an antineoplastic antibiotic with teratogenic potential and has been widely used to induce EA/TEF and the VACTERL association in rat and mouse embryos (Thompson, Molello et al. 1978; Diez-Pardo, Baoquan et al. 1996; Beasley, Diez Pardo et al. 2000; Ioannides, Chaudhry et al. 2002). A prominent abnormality in adriamycin-treated rat embryos is hypertrophy of the notochord with ventrally displaced branches making prolonged contacts with or in very close proximity to the dorsal foregut endoderm (Possoegel, Diez-Pardo et al. 1999; Qi and Beasley 1999; Orford, Manglick et al. 2001; Qi, Beasley et al. 2001; Williams, Qi et al. 2001; Mortell, O'Donnell et al. 2004). However, the cellular and molecular mechanisms regulating notochord and endoderm interaction remain poorly understood.

The notochord, a signaling tissue, functions as an organizer for adjacent embryonic structures and subsequently becomes the axis of the developing vertebral column (Stemple 2005). The notochord is initially formed as a plate with precursor cells embedded in the dorsal gut endoderm, hence transiently participating in the formation of the roof of the primitive gut tube in rodents and humans (Jurand 1974; Lamers, Spliet et al. 1987; Sulik, Dehart et al. 1994; Cleaver and Krieg 2001; Muller and O'Rahilly 2003). As development proceeds, cells of the notochordal plate coalesce and fold off into a rod-shaped structure which eventually separates from the endoderm (Jurand 1974; Lamers, Spliet et al. 1987; Sulik, Dehart et al. 1994; Cleaver and Krieg 2001; Muller and O'Rahilly 2003). The molecular mechanism controling notochordal plate detachment from the dorsal gut endoderm in a timely manner is not known (Jurand 1974; Sausedo

and Schoenwolf 1994).

We have found that mouse embryos with complete loss of *Noggin* (*Nog*) function display Type C EA/TEF with prominent narrowing of the esophagus. These embryos also display notochord abnormalities that are strikingly similar to those reported in adriamycin-treated rat embryos. The *Noggin* gene (*Nog*) contains a single exon and encodes a secreted polypeptide initially identified through its ability to antagonize Bmps to induce dorsal development in *Xenopus* embryos (Smith and Harland 1992). It was subsequently found that Noggin directly binds Bmps and inhibits their signaling during vertebrate development (Zimmerman, De Jesus-Escobar et al. 1996; Groppe, Greenwald et al. 2002; Canalis, Economides et al. 2003). In humans, *NOGGIN (NOG)* mutations have been linked to disorders affecting skeletal development (Krakow, Reinker et al. 1998; Gong, Krakow et al. 1999); however, their association with visceral malformations has not been reported. In reviewing the literature, we have identified three EA/TEF patients having interstitial deletions in chromosome 22 that span the *NOG* locus (Park, Moeschler et al. 1992; Dallapiccola, Mingarelli et al. 1993; Marsh, Wellesley et al. 2000). In collaboration with Dr. Harold Lovvorn, here at Vanderbilt, we have obtained blood samples from patients with EA/TEF, and carried out a screen to look for point mutations within the *NOG* coding sequence.

Materials and Methods

Generation and genotyping of *Nog* and *Bmp7* mutant embryos and mice

Nog hemizygotes were kindly provided by Dr. Richard Harland and *Bmp7* mice (Luo, Hofmann et al. 1995) were obtained from the Jackson Laboratory. Both $Nog^{+/-}$ and $Bmp7^{+/-};Nog^{+/-}$ compound hemizygotes were maintained in either CD1 (ICR) or C57BL6 background backcrossed for at least six generations, as a less penetrant phenotype was observed when mice were maintained in a mixed background. Since the foregut phenotypes were identical in either background, embryos maintained in the CD1/ICR background were used for the following studies.

Genotyping of wildtype (WT) and *Nog* mutant alleles were performed as described (McMahon, Takada et al. 1998), using the following primers:

Nog1, 5'-GCATGGAGCGCTGCCCCAGC-3';

Nog2, 5'-GAGCAGCGAGCGCAGCAGCG-3';

Gal1, 5'-AAGG-GCGATCGGTGCGGGCC-3'.

PCR conditions for both *Nog* WT and mutant alleles were: 94°C for 4 minutes; 40 cycles of (94°C for 30 seconds, 68.5°C for 40 seconds, 72°C for 45 seconds); 72°C for 10 minutes. Amplifications of WT and mutant alleles generate a 211-bp product (primers Nog1 and Nog2) and a 160-bp product (primers Nog1 and Gal1), respectively.

Genotyping for WT and targeted *Bmp7* mutant (MT) alleles were determined by PCR using the following primers:

Bmp7 WT (forward), 5'-CTCAACGCCATCTCTGTCCTCTAC-3';

Bmp7 WT (reverse), 5'-CTGCTTGGTTTCCCTTCAACAC-3';

Bmp7 MT (forward), 5'-GGCAAAGGATGTGATACGTGGAAG-3';

Bmp7 MT (reverse), 5'-CCAGTTTCACTAATGACACAAACATG-3'.

PCR conditions for *Bmp7* WT and mutant alleles were: 94°C for 4minutes; 35 cycles of (94°C for 30 seconds, WT-58.8°C/MT 55°C for 40 seconds, 72°C for 45 seconds); 72°C for 10 minutes. Amplifications of WT and mutant alleles yield a 503-bp product and a 850-bp product, respectively.

Antibody production

Anti-Foxa2 antibody was generated in rabbits against a purified bacterially-expressed GST fusion protein containing 127 N-terminal amino acids of mouse Foxa2 (DNA construct kindly provided by Dr. H. Sasaki). GST-Foxa2N127 fusion protein was produced and purified according to standard protocol. Briefly, BL21 (deficient in *omp*T and *lon* proteases) harboring the expression construct GST-Foxa2N127 was pre-cultured in 50 ml LBA (LB+100μg/ml ampicillin) medium overnight at 37°C and at 230rpm, and then cultured in large scale (20ml of overnight culture in 500ml LBA) at 37°C for 3-4 hours until the OD_{600} reached 0.5-0.6. Expression of the GST fusion protein was induced with 0.2mM IPTG, followed by culturing at 37°C for 3 hours. The bacterial pellet was obtained by centrifugation of cultured medium at 4000rpm for 15 minutes at 4°C. GST fusion protein was purified with B-PER™ GST Fusion Protein Purification Kit (Pierce),

according to the manufacturer's protocol. The eluted protein was assayed by SDS-PAGE and concentrated by Centricon30 (Millipore), then shipped to Cocalico Biological Inc. for injection. After evaluating the affinity of sample serum by Western blotting, a terminal bleed was collected and affinity-purified using a column of Affigel-10 beads (Bio-Rad) conjugated with GST-Foxa2 fusion proteins according to manufacturer's instruction.

Immunohistochemistry

For whole-mount immunohistochemistry, embryos were fixed in 4% paraformaldehyde (PFA) for 2-4 hours at 4°C and washed with PBS three times, followed by overnight incubation in 100% methanol:DMSO (4V:1V) solution at 4°C with shaking on a nutator. Samples were then stored in 100% methanol at -20°C until use. To quench endogenous peroxidase activity, embryos were bleached with 100% methanol:DMSO:30%H_2O_2 (4V:1V:1V) solution for 5 hours at room temperature (RT), and then rehydrated into PBS through a series of methanol dilutions in PBS (75%, 50%, 25%). Samples were permeabilized in PBS containing 2% TritonX-100 for 1 hour at RT, then blocked in PBTM (PBT+5% non-fat dry milk, PBT: PBS containing 0.2%Triton and 0.1%BSA) for 2 hours at RT, prior to overnight incubation with primary antibody diluted in PBTM at RT. To remove unbound primary antibody, embryos were thoroughly washed in PBT for 5-6 hours with several changes (1 hour per wash), and then re-blocked in PBTM prior to overnight incubation with secondary antibody diluted in PBTM at RT. Specimens were washed in PBT with several changes for a whole day before being

transferred to DAB solution (one 10mg DAB tablet from Sigma, dissolved in 33ml PBS plus 0.1% Tween20 and filtered through 0.45μm filter to remove particles) and incubated for 30 minutes. Then 0.1% H_2O_2 was added into the DAB solution to initiate the enzymatic color reaction. Samples were kept in the dark during color development and checked periodically until signals were detected (normally 2 hours). Following several PBS washes, embryos were dehydrated in 100% methanol, and cleared in a solution composed of benzylbenzoate and benzyl alcohol (2V:1V) and subsequently photographed.

For section immunostaining, staged embryos were fixed in 4% PFA for 1 hour at 4°C and dehydrated in a series of methanol washes (25%, 50%, 75% methanol/PBS+0.1%Tween, and 2X 100% methanol), except for those used for immunostainings of Brachyury and p-Smad1 which were fixed in EFA solution (100% ethanol:37% formaldehyde:100% acetic acid 6V:3V:1V) for 3 hours at 4°C, as described (Li, Zhang et al. 2006). For paraffin embedding, samples were treated with the following solutions, for 30 minutes at each step: 100% methanol (RT); 1:1 methanol/xylenes (RT); xylenes (RT); 1:1 xylenes/paraffin (60°C); three changes of paraffin (60°C). Sections of 6 μm thickness were collected on Superfrost Plus slides (Fisher). The procedure for section immunostaining was described previously (Li, Zhang et al. 2004). Briefly, slides were dewaxed in xylene (3X, 5 minutes each) and rehydrated through a series of ethanol/PBS washes (2X 100% ethanol, 2X 95% ethanol, 1X 70% ethanol, 3X PBS, 3 minutes each). Endogenous peroxidase activity was blocked in methanol with 3% H_2O_2 for 10 min at RT. After washing in PBS 3 times, sections were antigen-retrieved in Tris-EDTA buffer

(10mM Tris Base, 1mM EDTA Solution, 0.05% Tween 20, pH 9.0) for 20 minutes, using a Black and Decker Handy Steamer. Slides were slowly cooled down in retrieval solution on the lab bench for 20 minutes, and rinsed in PBS prior to 1-hour blocking in PBS containing 10% goat or donkey serum depending on the host of the secondary antibody. For detection of p-Smad1, the Tyramide Signal Amplification kit (Perkin Elmer) was used as described (Li, Zhang et al. 2006). Primary antibodies were added onto the slides and incubated overnight at 4°C, at the following dilutions: mouse anti-Nkx2.1 (Lab Vision, 1:200); rat anti-E-cadherin (Zymed, 1:200); rabbit anti-ZO-1 (Zymed, 1:200); rabbit anti-laminin (Sigma-Aldrich, 1:50); goat anti-Brachyury (Santa Cruz, 1:500), rabbit anti-Foxa2 (1:10); rabbit anti-Sox9 (gift of Dr. Michael Wegner, 1:2,000); rabbit anti-Foxp4 (gift of Dr. Edward Morrisey, 1:400) and anti-phospho-Smad1/5/8 (gift of Dr. Peter ten Dijke, 1:1,500). After three 10 minutes washes in PBS, Alexa 488 (green)- or Alexa 568 (red)-conjugated secondary antibodies (Invitrogen) were applied at 1:500 dilutions for 1.5 hours at RT in the dark. For counterstaining, Hoechst dye was used and shown in red or blue in appropriate figures. Some images were analyzed using FluoView 1000 confocal microscope (Olympus).

LacZ staining

To detect *Noggin-lacz* expression, E7.5 to E9.5 embryos were dissected in cold PBS and fixed in 4% PFA on ice for 30 minutes. Embryos were then rinsed 3 times in cold PBS, and incubated in X-gal solution for 6 hours to overnight at 37°C. The reaction

was stopped by rinsing samples in PBS and post-fixing in 4% PFA for 20 minutes at RT. Embryos were then embedded in paraffin and sectioned as described above.

Plastic thin section and cell death analysis

E8.5 WT and *Nog*$^{-/-}$ embryos were fixed in 4% PFA at 4°C for 4 hours, dehydrated and embedded in JB-4 polymer according to manufacturer's protocol (Polysciences Inc.). Embryos were then sectioned at 2 um, followed by staining with 1% toluidine blue solution.

TUNEL assay was used for detection of apoptotic cells in embryo sections according to manufacturer's instruction (ApopTag Apoptosis Detect Kit, Chemicon).

***In situ* hybridization**

The synthesis of digoxigenin (DIG)-labeled probes was performed according to manufacturer's protocols (Roche). Briefly, one *in vitro* transcription reaction (20µl) contains: 1µg of linearized DNA template (normally 2-4µl); 1X DIG RNA labeling mix (1mM ATP; CTP and GTP; 0.65mM UTP; 0.35mM DIG-11-UTP pH7.5); 1X transcription buffer; 40U RNasin (RNase inhibitor, Promega) and 50U of the appropriate RNA polymerase (T7,T3 or SP6). Transcription reaction was performed at 37°C for 2 hours, and stopped by adding RNase-free DNaseI (20U) for 15 minutes at 37°C which destroys the template DNA. The labeled probes were precipitated with 3M sodium acetate (pH 5.2) and 100% ethanol, washed in 70% ethanol, resuspended in diethyl

pyrocarbonate (DEPC)-treated water and stored at -80°C. The following cDNAs were used as templates for synthesizing digoxygenin- labeled riboprobes: *Pax9* (R. Balling); *Bmp7* (E. Robertson); *Foxa2* (H. Sasaki and B. L. Hogan); *Hex* (R.S.P. Beddington); *Goosecoid* (E.M. De Robertis); *Mixl1*(L. Robb); *Bmp4* (S-J. Lee); *Gli1* (C-c, Hui); *Ptch1* (M. Scott).

Whole-mount *in situ* hybridization was performed according to a protocol from the De Robertis laboratory, with minor modifications. Embryos were fixed in 4% PFA (RNase-free) overnight at 4°C, rinsed in DEPC-PBS containing 0.1%Tween20 (PBTw), dehydrated through a series of methanol washes in DEPC-PBTw (25%, 50%, 75%, and 2X 100% methanol), and stored at -20°C until use. Embryos were rehydrated into DEPC-PBTw and treated with 15µg/ml proteinase K in DEPC-PBTw for various lengths of time (normally 3-12 minutes), depending on the location of tissue of interest, sample size and embryonic stage. After post-fixation in 4% PFA(RNase-free) containing 0.2% glutaraldehyde for 15 minutes at RT, embryos were rinsed in DEPC-PBTw, equilibrated with hybridization buffer (RNase-free, 50%formamide, 5X SSC, 1% Boehringer Block, 1mg/ml torula RNA, 0.1mg/ml heparin, 0.1% Tween20, 0.1% CHAPS, 5mM EDTA) and prehybridized in hybridization buffer for at least 2 hours at 70°C. Hybridization solution containing about 0.2µg/ml probe was then added for overnight incubation at 70°C. On the following day, several washing steps were performed at 70°C: the hybridization solution was replaced by 800µl of hybridization buffer and washed for 5 minutes; 400µl 2XSSC (pH 4.5) was added twice into the vials and washed for 5 minutes each time; the washing

buffer was replaced and washed twice with 2XSSC containing 0.1%CHAPS (pH 7.0) for 30 minutes each time. RNase treatment was then performed at RT, with 0.1%CHAPS containing 2XSSC plus 200μg/ml RNaseA, followed two 10 minute washes in MABT (0.1M maleic acid, 0.15M NaCl pH 7.5, and 0.1% Tween20) for 10 minutes each time. Embryos were washed in MABT twice at 70°C for 30 minutes each wash. RT wash in MABT was repeated once again for 10 minutes followed by two 10 minute washes in PBTw. Embryos were incubated in filtered blocking buffer (PBTw containing 10% goat serum plus 1% Boehringer blocking reagent) for at least 2 hours at 4°C. Anti-DIG antibody conjugated to alkaline phosphatase (AP) (Roche) was added into the blocking buffer at 1:2,000 dilution for overnight incubation at 4°C. Samples were extensively washed 8-10 times in MABT for 1 hour each wash at RT, followed by overnight wash in MABT prior to the color reaction. For color development, embryos were first equilibrated by two 20 minute washes in NTM (0.1M Tris-pH9.5, 0.05M $MgCl_2$, 0.1M NaCl) containing 0.1% Tween20 at RT. Chromogenic substrate BM purple (Roche) was then added into vials and incubation was carried at either 37°C or RT until specific signals were detected. The color reaction was stopped by rinsing in PBS, and post-fixed in 4%PFA for 20 minutes.

Section *in situ* hybridization was carried out as described (Hogan, Beddington et al. 1994), with some modifications. After dissection, embryos were directly embedded in Tissue-Tek® OCT compound in cold ethanol-dry ice bath and stored at -80°C. Cryosections at 15μm thickness containing desired embryonic regions were collected on

Superfrost Plus slides and dried in a 37°C incubator for 40 minutes, before being fixed in 4% PFA for 20 minutes at RT. Slides were then washed twice in DEPC-PBS for 5 minutes each time, followed by proteinase K treatment (2μg/ml in 50mM Tris pH7.5 and 5mM EDTA) at RT for various lengths of time depending on the embryonic stage. After a brief rinse in DEPC-PBS, samples were post-fixed in 4% PFA for 15 minutes at RT. To enhance signaling, sections were treated for acetylation with 250ml 0.1M triethanolamine-HCl (pH 8.0) containing 0.625ml acetic anhydride. After two 5 minute washes in DEPC-PBS at RT, slides were incubated with hybridization buffer (same as in whole-mount hybridization) for at least 2 hours at 60°C until DIG-labeled probes were added onto slide at 1-2μg/ml and incubated overnight at 60°C. Unbound probes were removed by a series of washes in 1XSSC (60°C, 10 minutes), 1.5XSSC (60°C, 10 minutes), 2XSSC (37°C, 20 minutes, twice), 2XSSC containing 0.2μg/ml RNaseA (37°C, 30 minutes), 2XSSC (RT, 10 minutes), 0.2XSSC (60°C, 30 minutes, twice), PBTw (60°C, 10 minutes, twice; RT, 10 minutes), and PBT (PBS containing 0.1% TritonX-100 and 0.2% BSA) (RT, 15 minutes). Slides were incubated in blocking buffer (PBT containing 20% goat serum) for at least 2 hours at RT, before anti-DIG antibody conjugated to AP was added into the blocking buffer at 1:,2000 dilution for overnight incubation at 4°C. After three 30 minute washes in PBT at RT, sections were equilibrated in NTM without or with 5mM levamisole for 5 minutes each time and incubated in BM Purple at 37°C until specific signals were detected. The color reaction was stopped by rinsing slides in PBS.

Genetic screening of point mutations within the *NOG* locus

Blood samples were collected by our collaborator, Dr. Harold Lovvorn, from patients with EA/TEF (3ml for each patient), and stored at -80°C. Genomic DNA was extracted from blood samples using QIAamp spin column (Qiagen, CA). The *NOG* coding region was amplified by PCR with proofreading polymerase (9 units AmpliTaq Gold + 1 unit Pfu Turbo), using the following primers:

NOG (Forward): 5'-GGACGCGGGACGAAGCAGCAG-3';

NOG (Reverse): 5'-GAGGATCAAGTGTCCGGGTGC-3'.

The PCR condition was as follows: 94°C for 4minutes; 35 cycles of (94°C for 30 seconds, 64°C for 60 seconds, 72°C for 60 seconds); 72°C for 10 minutes. The 765-bp PCR product was evaluated by electrophoresis. To prepare for TGCE (temperature gradient capillary electrophoresis) analysis, PCR fragments were denatured for 3 min at 95°C and annealed in a thermal cycler via a stepwise reduction in temperature as follows: decrease from 95°C to 80°C at 3°C/min; decrease from 80°C to 55°C at 1°C/min; hold at 55°C for 20 min; decrease from 55°C to 45°C at 1°C/min; and decrease from 45°C to 25°C at 2°C/min(Li, Liu et al. 2002). Samples were sent for TGCE /Reveal analysis performed at the Vanderbilt Neuroscience Core. Samples that came out positive for SNP (single nucleotide polymorphism) were further evaluated by direct sequencing.

Results

Nog$^{-/-}$ embryos displayed foregut reduction and Type C EA/TEF

The respiratory bud is discernible as an outpocketing of the ventral foregut tube at E9.5 (Figure 2.2A) to give rise to the trachea and lung while the dorsal foregut develops into an esophagus which is clearly seen at E10.5 by immunolabeling Foxa2, an endoderm marker (Figure 2.1C). We found that *Nog*$^{-/-}$ embryos displayed Type C EA/TEF (Figure 2.1D, B), consisting of an upper esophageal pouch (red arrowheads in B, D) while the lower stenosed esophagus as highlighted by an esophageal marker *Pax9* (Neubuser, Koseki et al. 1995) (Figure 2.1E, F), makes an abnormal connection with the trachea (Figure 1.1B, D**,** black arrowheads); this phenotype is highly reminiscent of the most common form of EA/TEF in humans (Hicks and Mansfield 1981; Engum, Grosfeld et al. 1995; Clark 1999). While most *Nog*$^{-/-}$ embryos displayed Type C EA/TEF (27/33 or 82%), a few embryos showed a milder phenotype indicative of esophageal stenosis (6/33 or 18%; Figure 2.1B, inset).

We observed dorsoventral reduction in the *Nog*$^{-/-}$ foregut at E9.5 (Figure 2.2B, arrowheads, n=6) compared with WT (Figure 2.2A). We next investigated whether there was specific reduction of dorsal foregut endoderm since we observed narrowing of the esophagus relative to the trachea. Interestingly, by immunolabeling with Nkx2.1 to demarcate the respiratory (ventral) from the dorsal foregut at E9.5 (Minoo, Su et al. 1999), we observed specific reduction of the dorsal foregut in *Nog*$^{-/-}$ compared with WT

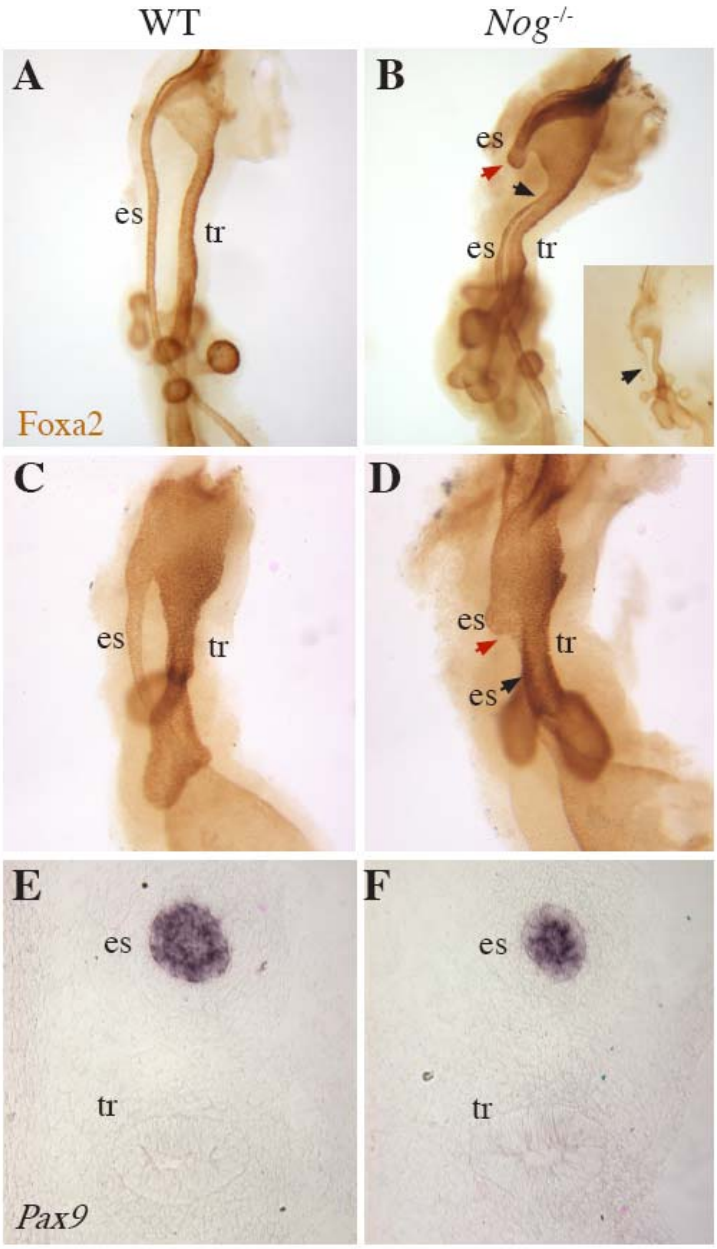

Figure 2.1 *Nog*$^{-/-}$ foregut displays Type C EA/TEF.
Whole-mount Foxa2 immunostaining of WT (A, C) and *Nog*$^{-/-}$ embryos (B, D) at E11.5 (A, B) and E10.5 (C, D). In *Nog*$^{-/-}$ foregut, the upper esophagus ends in a blind pouch (red arrowheads in B, D); the lower esophagus, which expresses an esophageal marker *Pax9* (F), connects to the trachea via a fistula (black arrowheads in B, D). While most *Nog*$^{-/-}$ embryos display Type C EA/TEF (27/33 or 82%), a few embryos show a milder phenotype indicative of esophageal stenosis (6/33 or 18%; B, inset).es, esophagus; tr, trachea. Magnification: A, B, 500X; C, D 900X; E, F, 200X.

Figure 2.2 *Nog*$^{-/-}$ foregut displays selective reduction of dorsal foregut endoderm and notochord defects.
Whole-mount Foxa2 immunostaining of WT (A) and *Nog*$^{-/-}$ (B) foreguts at E9.5 demonstrates a clear reduction in the dorsoventral diameter of *Nog*$^{-/-}$ foregut (arrowheads in B). Immunostaining with Nkx2.1, a respiratory marker, at the level of the respiratory bud in E9.5 WT and *Nog*$^{-/-}$ (C, D), reveals reduction of the dorsal foregut endoderm in *Nog*$^{-/-}$ embryos (region highlighted by white dots). Hematoxylin and eosin (H&E) staining of WT and *Nog*$^{-/-}$ cross-sections at E8.5-E9.0 (E-H) reveals the morphologically aberrant notochord in *Nog*$^{-/-}$ which remains close to the dorsal foregut (H, arrowhead and F). Immunostaining of T and Laminin at E8.5 shows delayed detachment of notochord in *Nog*$^{-/-}$ embryos (J, L) compared to WT embryos (I, K). Notochord defect persists at later stages in *Nog*$^{-/-}$ embryos with lateral branches in close proximity or tethered to the dorsal foregut at E9.5 (B, arrows). es, esophagus; tr, trachea; n, notochord; lb, lung bud and fg, foregut. Magnification: A, B, 630X; C-F, 200X; G-L, 400X.

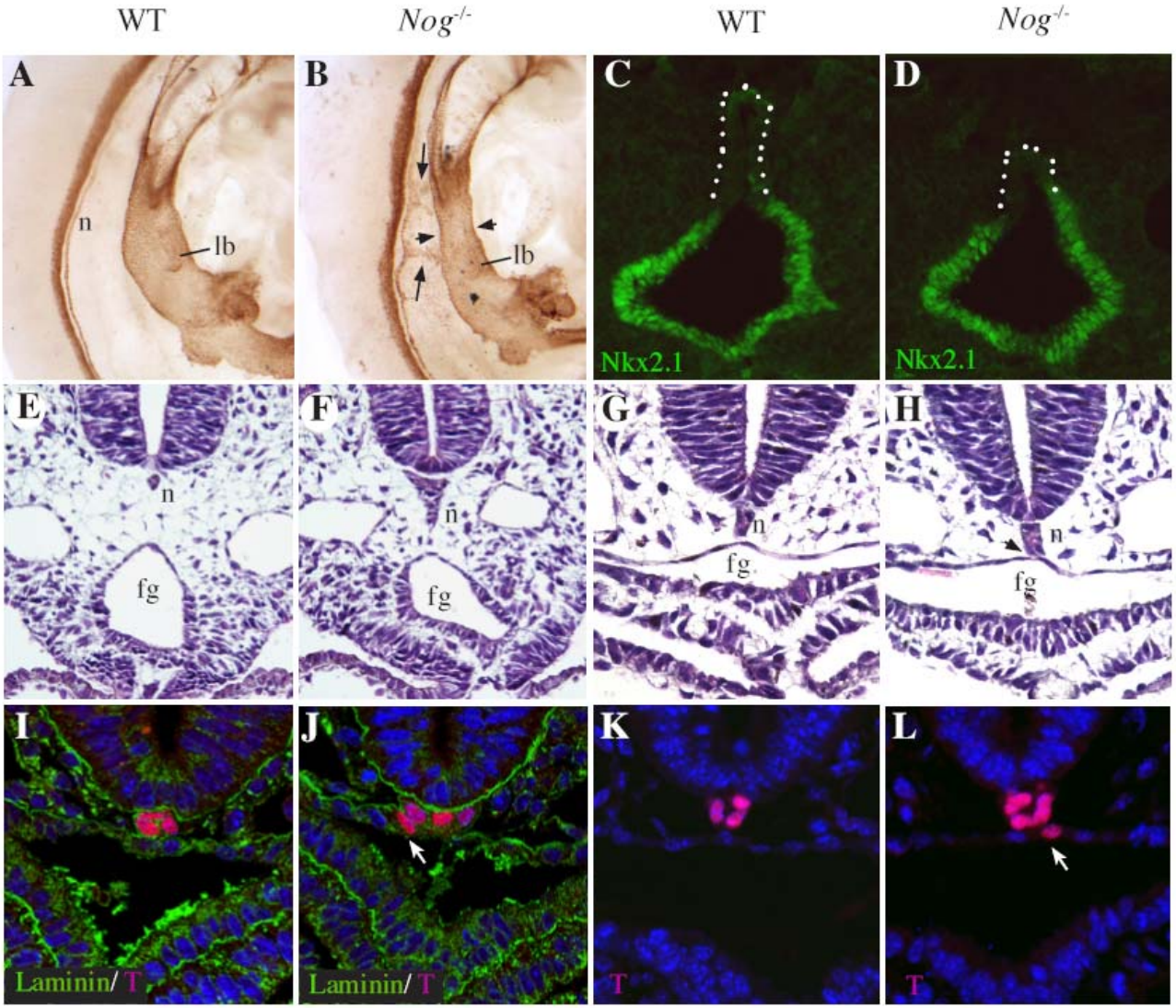
WT
Nog-/-
WT
Nog-/-
A
B
C
D
n
lb
lb
Nkx2.1
Nkx2.1
E
F
G
H
n
fg
n
fg
n
fg
n
fg
I
J
K
L
Laminin/ T
Laminin/ T
T
T

(Figure 2.2C, D, dotted outline), consistent with esophageal defects in *Nog*$^{-/-}$ embryos. By contrast, the respiratory domain in *Nog*$^{-/-}$ embryos appeared comparable with WT embryos (Figure 2.2C, D), which is consistent with the observation that *Nog*$^{-/-}$ foregut developed ventral structures, the trachea and lung (Figure 2.1B).

We also examined earlier embryos to determine if foregut endoderm defects observed in *Nog*$^{-/-}$ embryos could be due to abnormal endoderm tube formation. The foregut endoderm originates from the anterior definitive endoderm, contributed by cells at the most anterior end of the early and mid primitive streak during gastrulation (Kinder, Tsang et al. 2001). As morphogenesis progresses, the lateral edges of the flat endodermal sheet begin to converge medio-ventrally by a complex process of differential growth and embryonic folding. By E8.5, the foregut tube is closed followed by further growth and patterning (Wells and Melton 1999). We did not observe significant differences in the expression levels of several early mesendodermal markers (Figure 2.3); consistent with this observation, we did not detect differences in the size, cellular content (Figure 2.4 A,B) or apoptotic cell death (Figure 2.4 C, D) of *Nog*$^{-/-}$ foregut tube at E8.5 (at somite stages 11-13s) compared with WT suggesting that foregut size reduction likely occurred after foregut tube formation.

Nog$^{-/-}$ dorsal foregut endoderm failed to reveal significant apoptosis

We reasoned that induction of apoptotic cell death within the dorsal foregut domain could be a mechanism by which dorsal foregut cells are lost resulting in

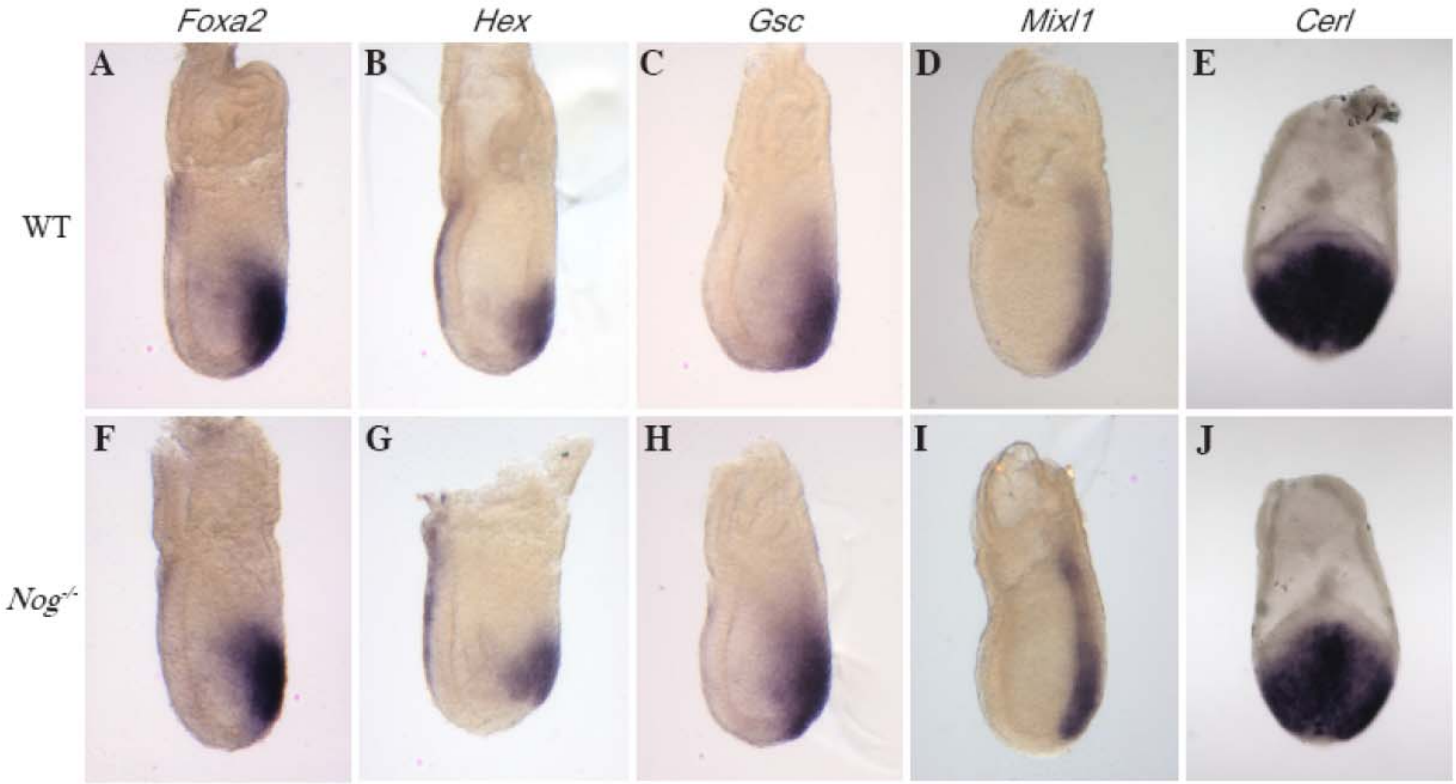

Figure 2.3. Foregut endoderm specification in *Nog*$^{-/-}$ embryos appears normal compared with WT embryos.
Nog$^{-/-}$ embryos at E7.0-7.5 does not display statistically significant alterations in their levels of expressions of anterior definitive endoderm ADE markers (f-i) compared with WT embryos (a-d), except slightly decreased expression of *Cerl* (J, *Nog*$^{-/-}$, e, WT), implicating functional compensation by another Bmp antagonist such as Chordin. Ablation of both Noggin and Chordin results in ADE defects (Bachiller, Klingensmith et al. 2000).

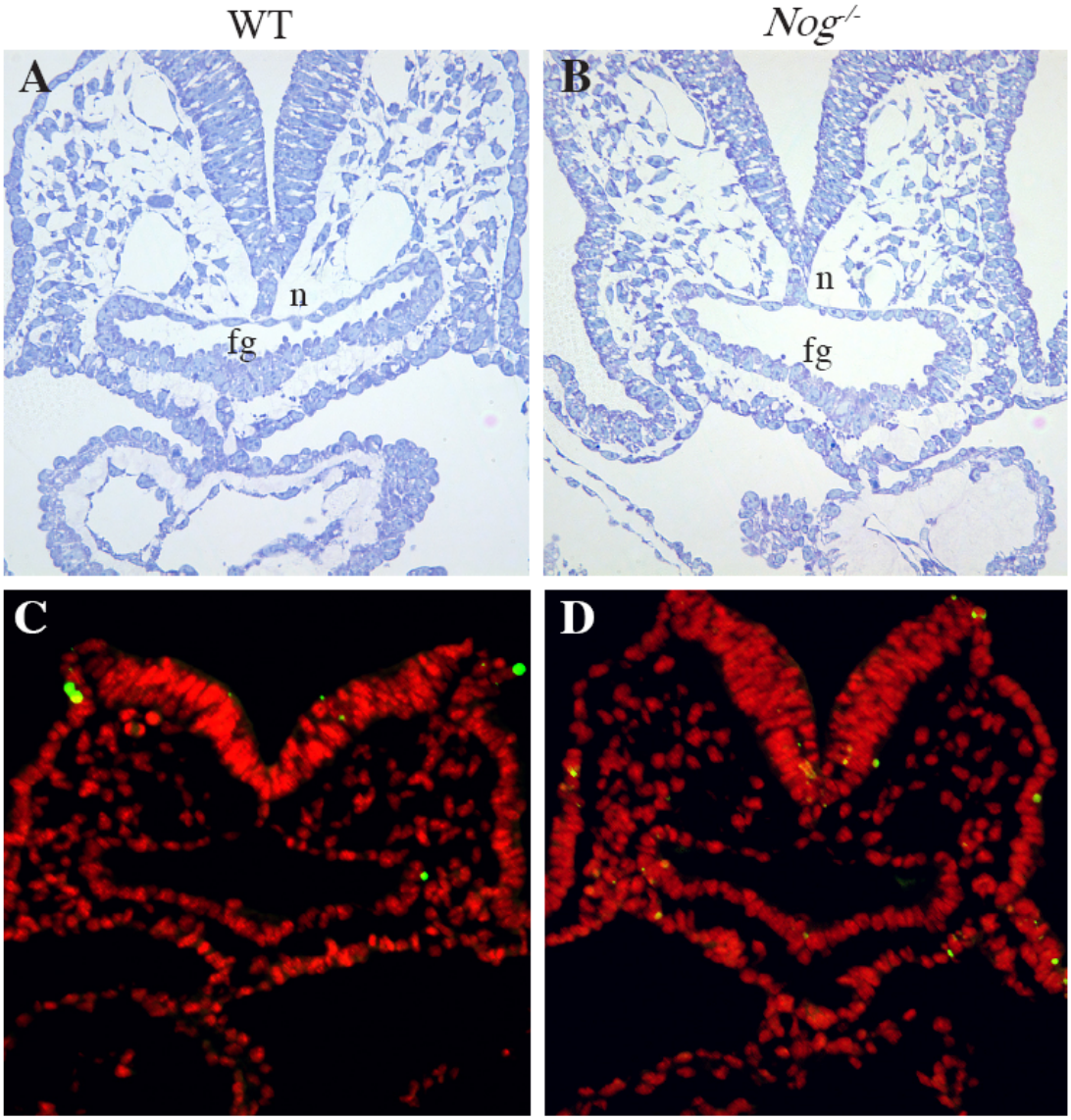

Figure 2.4 Plastic thin sections and TUNEL analysis of E8.5 embryos.
(A, B) A toluidine blue-stained section shows no obvious differences in cellular morphology in the foregut endoderm of *Nog*$^{-/-}$ embryo compared to WT embryo. WT and *Nog*$^{-/-}$ foregut tubes are comparable in size and cellular content suggesting that gut size reduction likely occurs after foregut tube closure. (C, D) TUNEL assay shows no appreciable cell death in the *Nog*$^{-/-}$ dorsal endoderm as compared to WT endoderm. n, notochord; fg, foregut. Magnification, 200X.

esophageal atresia/stenosis. However, we did not observe significant apoptotic cells within the dorsal foregut domain of *Nog*$^{-/-}$ embryos between E9.0-9.75 (18-25s), a developmental window in which we observed dorsal foregut reduction (Figure 2.5).

Nog$^{-/-}$ embryos displayed notochord detachment defects

In addition to foregut defects, we observed morphologically abnormal notochord in *Nog*$^{-/-}$ embryos at E8.5 (Figure 2.2H) and E9.0 (Figure 2.2F), indicating delayed detachment from the dorsal foregut endoderm. *Nog*$^{-/-}$ notochord also appeared hypertrophic compared with WT notochord at E9.0 (Figure 2.2F). By contrast, WT notochord cells appeared more tightly packed in a rod-like structure and showed clear delamination from the dorsal foregut endoderm (Figure 2.2E, G). We observed cells positive for the notochord marker Brachyury (T^+) still embedded within the dorsal foregut at E8.5 in *Nog*$^{-/-}$ embryos (Figure 2.2 J, L, arrows). Laminin immunostaining in these sections also revealed a clear basement membrane abutting the WT notochord and gut endoderm; by contrast, the boundary between notochord and endoderm was not clearly demarcated in *Nog*$^{-/-}$ embryos. Notochord defects persisted at later stages in *Nog*$^{-/-}$ embryos with lateral branches in close proximity or tethered to the dorsal foregut at E9.5 (Figure 2.2B**,** arrows) in contrast with WT notochord (Figure 2.2A).

As mentioned earlier, although no significant apoptosis was detected in the *Nog*$^{-/-}$ dorsal foregut, we did observe increased apoptotic cells in the notochord branches compared with WT foregut by TUNEL labeling (Figure 2.5). Even though notochord

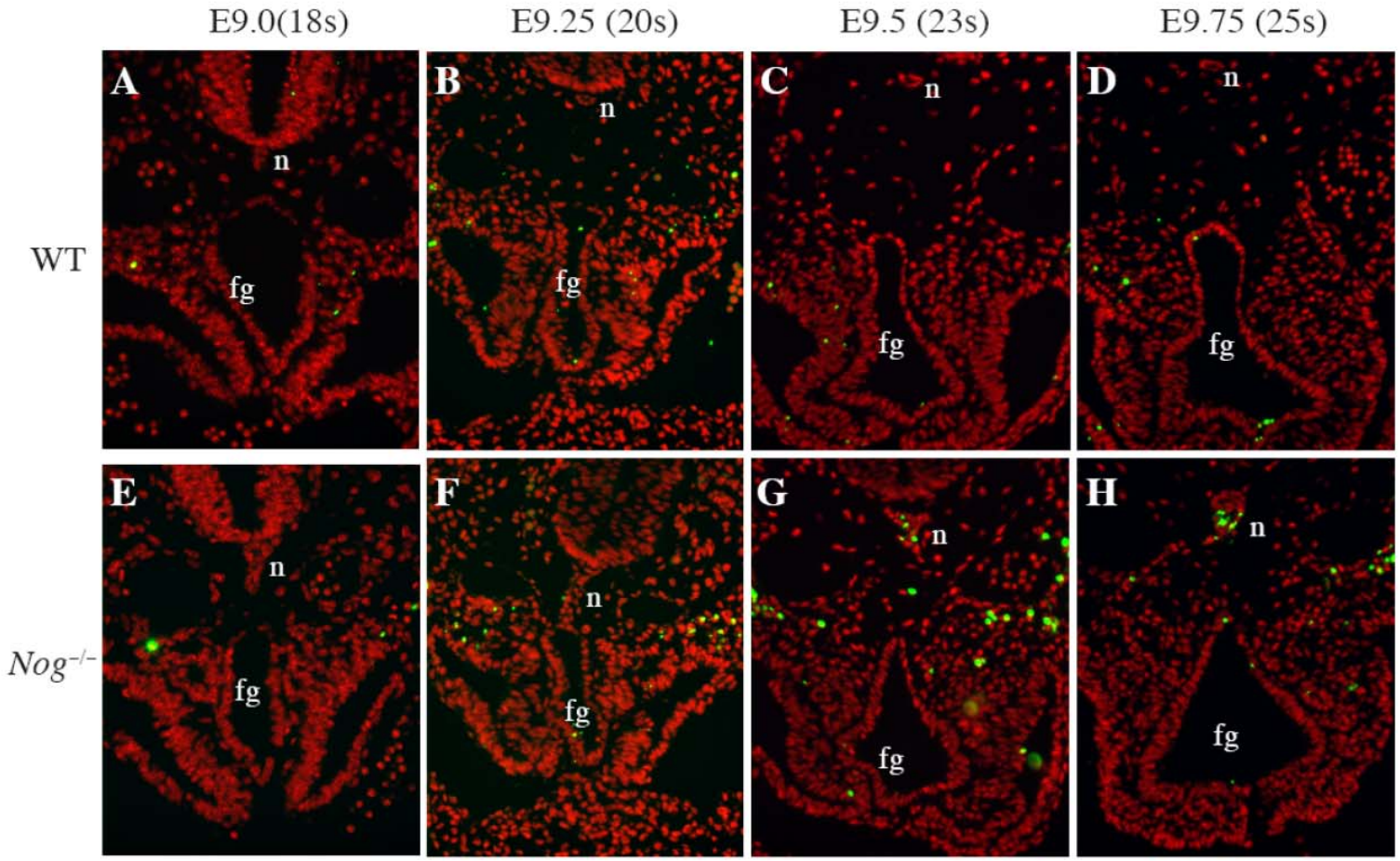

Figure 2.5 Cell death occurs in the notochord branches but not in the dorsal foregut endoderm of *Nog*$^{-/-}$ embryos.
TUNEL labeling of WT and *Nog*$^{-/-}$ embryos reveals increased apoptotic cells (green) in the notochord branches of *Nog*$^{-/-}$ embryos between the 23-somite and 25-somite stages (E9.5-9.75) compared to WT embryos. s, somite; n, notochord; fg, foregut. Magnification: 200X.

branches in *Nog*$^{-/-}$ embryos were clearly apparent by E9.25 (20s, Figure 2.5F), we detected increased number of apoptotic cells in these branches at a slightly later stage when the lung buds have clearly emerged between E9.5-E9.75 (23-25s, Figure 2.5 G, H).

Presence of non-notochordal cells in *Nog*$^{-/-}$ notochord

The notochord is initially formed as a plate with cells embedded in the dorsal gut endoderm, and as development proceeds, cells of the notochordal plate coalesce, fold off and precisely detach from the dorsal gut endoderm (Jurand 1974; Sulik, Dehart et al. 1994). It is possible that imprecise detachment of the notochord due to its prolonged contact with the dorsal endoderm may account for the loss of dorsal foregut endodermal cells in *Nog*$^{-/-}$ embryos. In support of this model, we detected cells in the *Nog*$^{-/-}$ notochord that were negative for notochord marker expression at E9.0 (17-18s). While notochord cells are normally positive for both T and Foxa2 (T^{+}/Foxa2^{+}), gut endoderm cells are T^{-} but Foxa2^{+} and surrounding mesodermal cells are T^{-}/Foxa2^{-} (Figure 2.6A, C). We consistently found T^{-}/Foxa2^{+} cells amongst T^{+}/Foxa2^{+} cells in the *Nog*$^{-/-}$ notochord while WT notochord contained only T^{+}/Foxa2^{+} cells (Figure 2.6B, D, arrowheads) (n=5 embryos for each genotype). This finding is indicative of the presence of non-notochordal cells, likely Foxa2^{+} endodermal cells, within the *Nog*$^{-/-}$ notochord. We did not observe T^{-}/Foxa2^{+} cells in the surrounding mesenchyme suggesting that endodermal cells are unlikely becoming lost in the mesenchyme. Sox9, a SRY-related transcription factor, is expressed in the notochord and surrounding mesoderm but not in the dorsal foregut

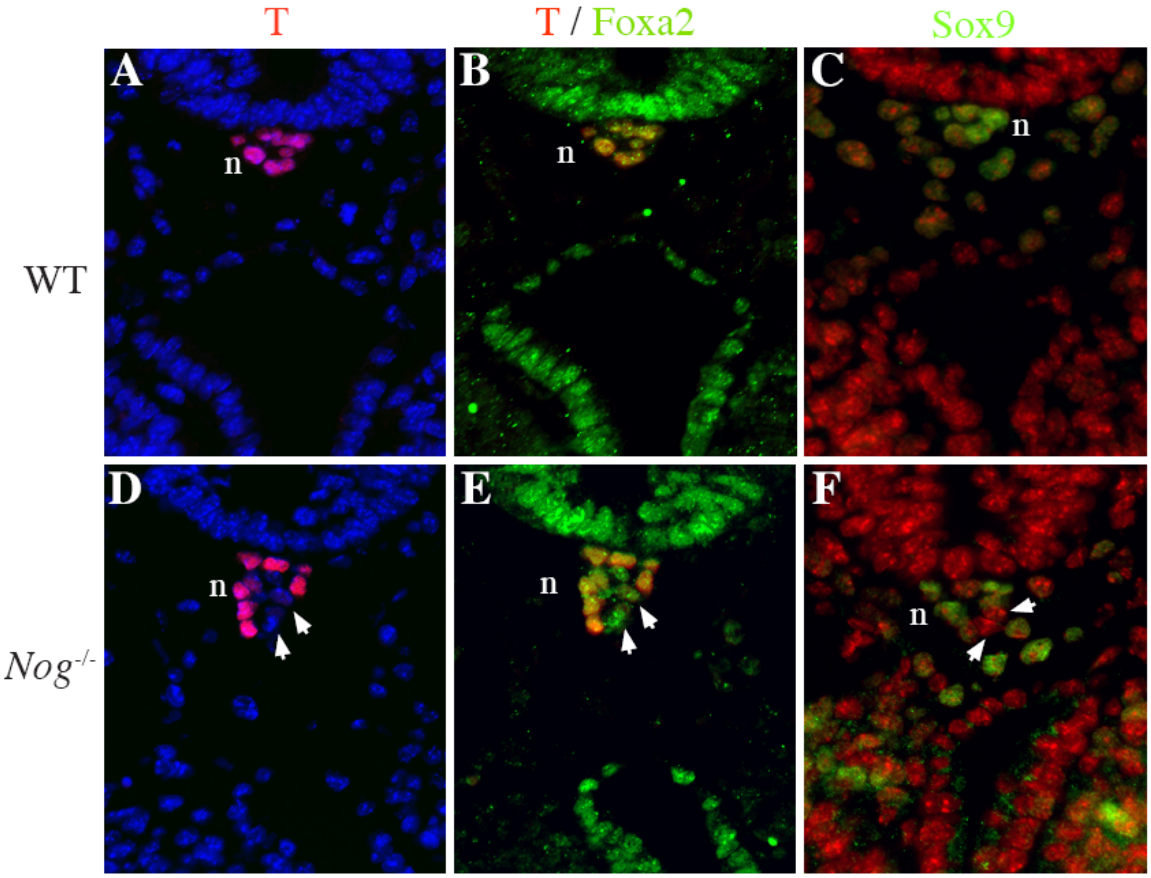

Figure 2.6 Presence of non-notochordal cells in *Nog*$^{-/-}$ notochord.
T (Brachyury) and Foxa2 double immunostaining of E9.0 embryos shows T-negative and Foxa2-positive cells in the *Nog*$^{-/-}$ notochord (D, E, arrowheads), but not in WT notochord. In agreement, *Nog*$^{-/-}$ notochord contains Sox9-negative cells (F, arrowheads), indicative of non-notochordal cells. Immunofluorescence color designations are: T (red), Foxa2 (green), Merge (yellow), Sox9 (green) and nuclei are stained with Hoechst dye. n, notochord. Magnification: 400X.

endoderm (Stolt, Lommes et al. 2003).We therefore took advantage of this differential expression to examine whether *Nog*$^{-/-}$ notochord contained cells that do not express Sox9. As predicted, we found that Sox9^{-} cells were consistently present in the *Nog*$^{-/-}$ notochord which likely indicate endodermal cell types (Figure 2.6E, F**,** arrowheads). Taken together, these results are suggestive of the presence of non-notochordal cells, likely Foxa2^{+} foregut endodermal cells, intermingled with notochord cells in *Nog*$^{-/-}$ embryos.

Nog$^{-/-}$ dorsal foregut endoderm displayed concomitant cell loss, alteration in intercellular adhesion and matrix disruption

To investigate whether the *Nog*$^{-/-}$ dorsal foregut endoderm cells displayed alterations in cell-cell adhesion, we performed immunohistochemistry with epithelial markers such as E-cadherin, a component of cell adherens junctions, to highlight the foregut tube at E9.0 (17-18s). We consistently observed loosening or loss of dorsal foregut cells in *Nog*$^{-/-}$ embryos concomitant with reduced E-cadherin level (Figure2.7 A, B). We observed similar disruption of dorsal foregut endoderm by immunolabeling with an antibody against zona occludens-1 (ZO-1), a tight junction protein (Figure 2.7 C, D). We also observed basement membrane disruption as highlighted by laminin immunostaining in the dorsal foregut of *Nog*$^{-/-}$ embryos (Figure 2.7 E, F). Collectively, these results are in agreement with our findings above that dorsal foregut endoderm cells are likely displaced into the notochord resulting in dorsal foregut reduction in *Nog*$^{-/-}$ embryos.

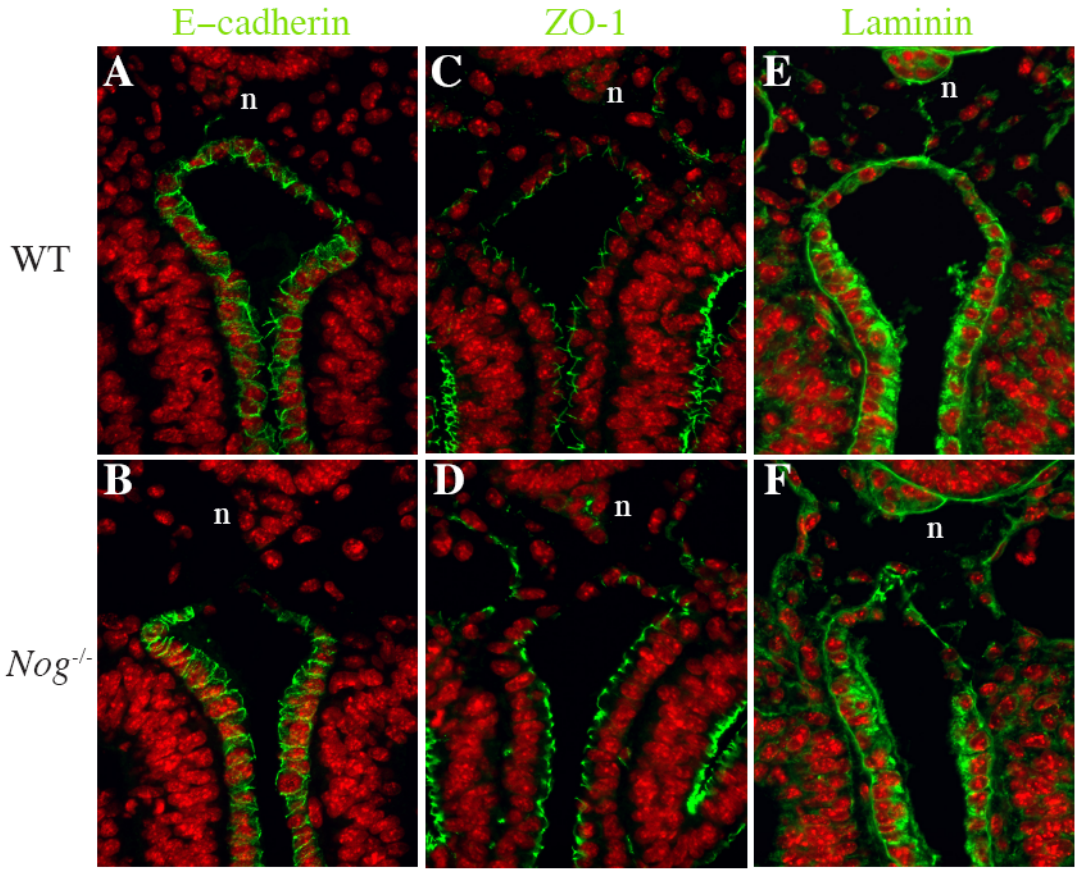

Figure 2.7 *Nog*$^{-/-}$ dorsal foregut displays cell loss, alteration in intercellular adhesion and matrix disruption.
Immunohistochemistry of foregut sections from E9.0 WT and *Nog*$^{-/-}$ embryos with E-cadherin (A, B, green) and ZO-1(C, D, green) to highlight disrupted epithelial cell adhesion in the *Nog*$^{-/-}$ dorsal foregut region. Staining with basement membrane marker laminin (E, F,green) reveals disruption of matrix and apparent loosening of dorsal foregut cells in *Nog*$^{-/-}$ embryos compared to WT embryos. n, notochord. Magnification 400X.

Noggin-mediated Bmp7 antagonism in the pathogenesis of EA/TEF

In order to gain insight into the spatial and temporal requirement of Noggin-mediated Bmp antagonism during notochord-foregut separation, we compared expression patterns of Noggin and Bmps during early foregut development. Among a few Bmps that are expressed in the gastrulating embryo, *Bmp7* expression shows a close association with that of *Noggin* in the anterior primitive streak and in the node where prospective notochordal cells are clustered and both *Noggin* and *Bmp7* continue to be expressed in the notochordal plate during its delamination from the roof of the dorsal foregut endoderm (Lyons, Hogan et al. 1995; Dudley and Robertson 1997; McMahon, Takada et al. 1998) (Figure 2.8A). By immunolabeling with an affinity-purified antibody against phosphorylated Smad1/5/8 (pSmad1), we detected increased Bmp signaling in the notochord of *Nog*$^{-/-}$ embryos at E8.5 (somite 11-12) with reduced level by E9.0 (somite 17-18) (Figure 2.8B) consistent with loss of Noggin function and in agreement with a critical role of Bmp antagonism during notochord-foregut detachment. By contrast, we did not detect ectopic Bmp signaling in the *Nog*$^{-/-}$ dorsal foregut endoderm and its surrounding mesenchyme (Figure 2.8B).

We reasoned that if Noggin-mediated Bmp7 antagonism is critical for proper notochord-foregut separation, then ablating *Bmp7* would be expected to alleviate abnormal notochord detachment, thus rescuing the dorsal foregut defect and EA/TEF in *Nog*$^{-/-}$ mutants. We found that ablating *Bmp7* in *Nog*$^{-/-}$ embryos significantly rescued notochordal defects at E9.5 and we did not observe notochord branches in 8 of 9

Figure 2.8 Overlapping expression of *Nog-lacZ* and *Bmp7*, and ectopic Bmp signaling in *Nog*$^{-/-}$ notochord.

(A) Expression of *Noggin-lacZ* and *Bmp7* is detected in the node (arrow) and its derivative the notochordal plate (brackets).

(B) Increased Bmp signaling as determined by phosphorylated-Smad1/5/8 (p-Smad1) antibody staining (green) in *Nog*$^{-/-}$ notochord (arrow) at E8.5. By E9.0, p-Smad1 staining, although detectable, appears to be reduced in *Nog*$^{-/-}$ notochord. Note that p-Smad1 is also detected in the ventral foregut but not in the dorsal foregut endoderm in WT and *Nog*$^{-/-}$ embryos. n, notochord; fg, foregut. Magnification: A (E7.75), 630X; all other panels, 200X.

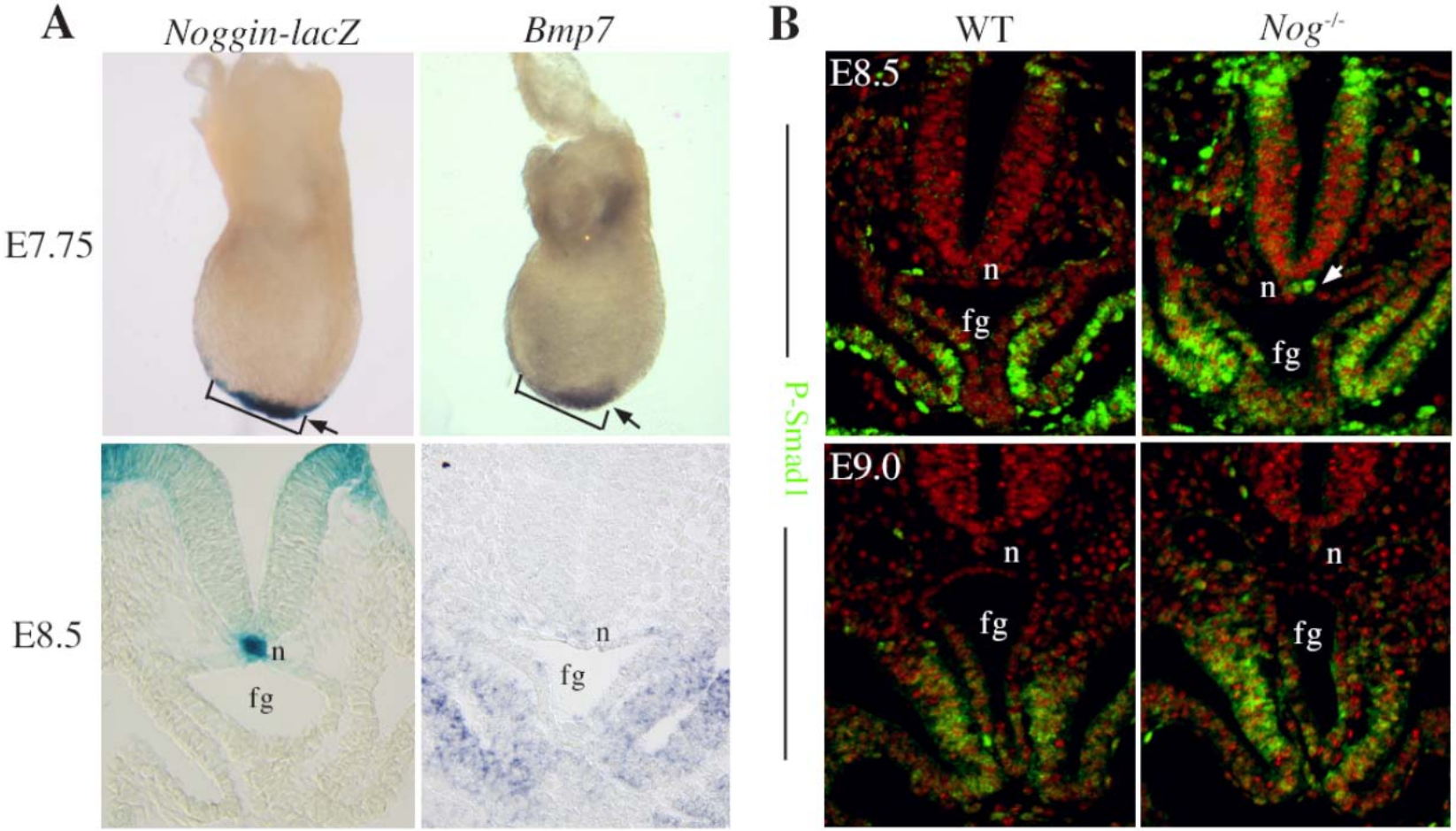
A
Noggin-lacZ
Bmp7
E7.75
E8.5
n
fg
n
fg
B
WT
Nog-/-
E8.5
E9.0
P-Smad1
n
fg
n
fg
n
fg
n
fg

Nog$^{-/-}$;*Bmp7*$^{-/-}$ embryos (Figure 2.9E-H); one embryo showed a small branch in its notochord (inset in Figure 2.9H). As predicted, at E9.5, *Bmp7*$^{-/-}$;*Nog*$^{-/-}$ foregut tubes showed rescue of the narrowing defect (Figure 2.9G, H). By contrast, *Nog*$^{-/-}$ littermates showed remarkable notochord defects in 16 of 19 embryos consistent with findings in Figure 2.1F. At E11.5, *Bmp7*$^{-/-}$;*Nog*$^{-/-}$ embryos (8/8) showed rescue of EA/TEF (Figure 2.9I-L); the caudal neural tube which was also defective in *Nog*$^{-/-}$ displayed a relatively normal phenotype in *Bmp7*$^{-/-}$;*Nog*$^{-/-}$ (Figure 2.9A-D, arrowheads). We also observed normal E-cadherin expression in the dorsal foregut and only T cells in the notochord of *Bmp7*$^{-/-}$;*Nog*$^{-/-}$ double mutant embryos (Figure 2.9M). Although the notochord branches observed in *Nog*$^{-/-}$ embryos were significantly reduced in *Bmp7*$^{-/-}$;*Nog*$^{-/-}$, notochords in the double mutants still appeared slightly hypertrophic compared to WT, suggesting that removing Bmp7 is not sufficient to completely counteract the effect of Noggin loss in the notochord.

Screening for point mutations in *NOG* locus in patients with EA/TEF

The human *NOG* gene is localized to chromosome 17q22. While browsing the literature, we found three EA/TEF patients with interstitial deletions of chromosome 17 that spans the *NOG* locus (Table 2.1). The deletion del(17)(q22q23.3) reported by Marsh et al. (Marsh, Wellesley et al. 2000) represents the minimal breakpoints for the EA/TEF phenotype, which is not observed in q23.2q24.3 and q23.1q23.3 deletions that fall outside of the *NOG* locus (Table 2.1). Therefore, 17q22 represents a critical chromosomal

Figure 2.9 The EA/TEF phenotype, foregut reduction and notochord defects in *Nog*$^{-/-}$ embryos are rescued by ablation of *Bmp7*.
(A-D), external views of WT (A), *Bmp7*$^{-/-}$;*Nog*$^{+/+}$ (B), *Bmp7*$^{+/+}$;*Nog*$^{-/-}$ (C) and *Bmp7*$^{-/-}$;*Nog*$^{-/-}$ (D) embryos at E11.5. *Bmp7*$^{+/+}$;*Nog*$^{-/-}$ embryos displays characteristic open brain and caudal neural tube (arrowhead, C) phenotypes. In *Bmp7*$^{-/-}$;*Nog*$^{-/-}$ mutants, the open caudal neural tube is rescued (arrowhead, D). As revealed by whole-mount Foxa2 immunostaining, ablating *Bmp7* in *Nog*$^{-/-}$ embryos significantly rescues notochord defects at E9.5 (H: 8/9 showed no obvious notochord branches; 1/9 showed a small branch in the notochord, see inset-arrowhead) as compared to the *Nog*$^{-/-}$ littermates (G). As in WT embryos (E), no foregut defects are observed in *Bmp7*$^{-/-}$;*Nog*$^{+/+}$ mutants (F). The foregut narrowing defect in *Nog*$^{-/-}$ (G, arrowheads) is rescued in *Bmp7*$^{-/-}$;*Nog*$^{-/-}$ (H, arrowheads). At E11.5, while the *Bmp7*$^{+/+}$;*Nog*$^{-/-}$ littermates displays either EA/TEF (K: 20/22) or a milder phenotype of esophageal stenosis (2/22), *Bmp7*$^{-/-}$;*Nog*$^{-/-}$ foregut shows rescue of EA/TEF (L: 8/8). (M) Expression of E-cadherin in *Bmp7*$^{-/-}$;*Nog*$^{-/-}$ dorsal foregut endoderm appears to be comparable with WT endoderm. Additionally, all cells in the *Bmp7*$^{-/-}$;*Nog*$^{-/-}$ notochord are stained with T, like in WT. es, esophagus; tr, trachea. Magnification: A-D, 125X; E-H, 630X; I-L, 500X; M, 400X.

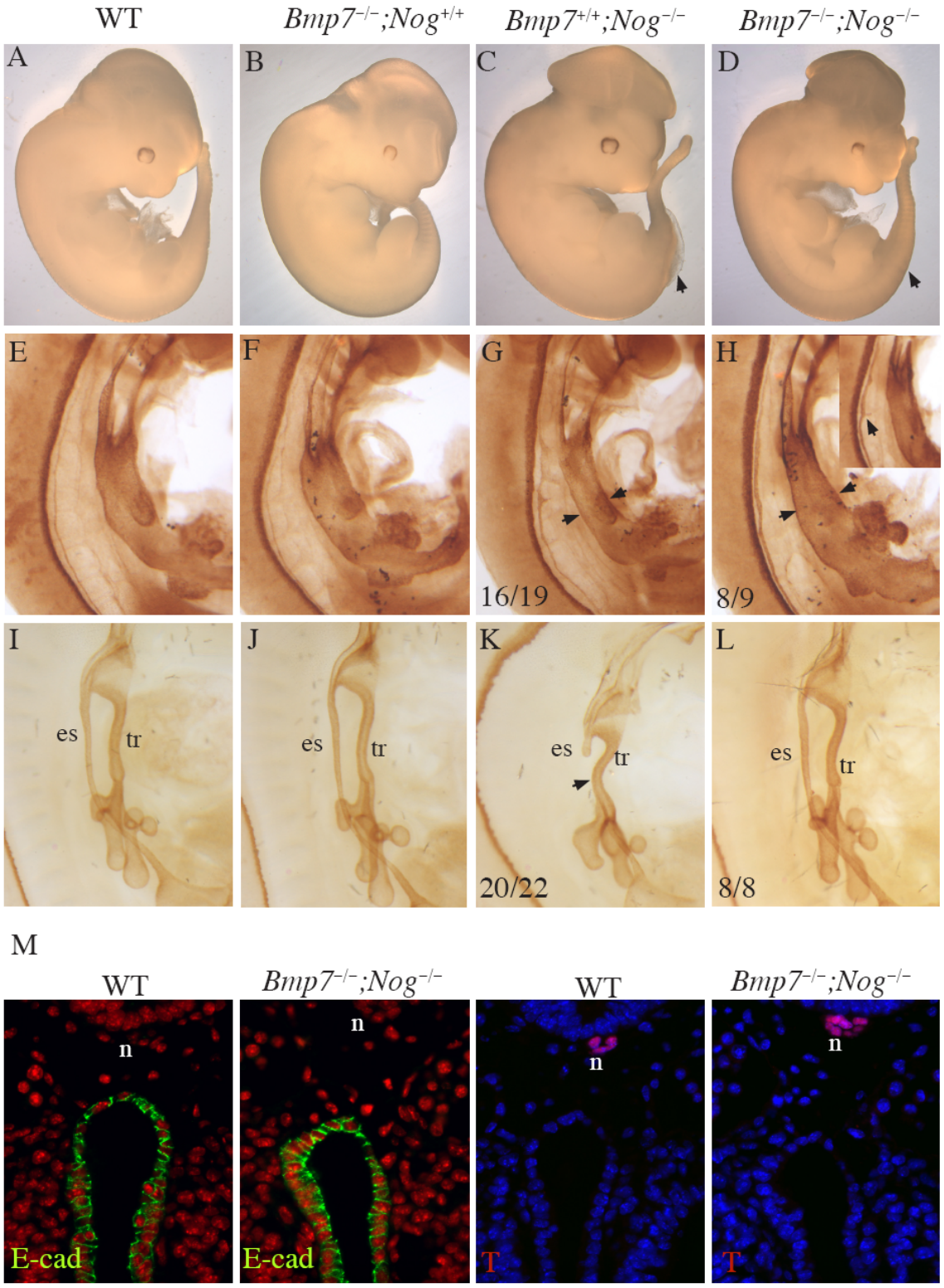
WT
Bmp7-/-;Nog+/+
Bmp7+/+;Nog-/-
Bmp7-/-;Nog-/-
A
B
C
D
E
F
G
16/19
H
8/9
I
es
tr
J
es
tr
K
es
tr
20/22
L
es
tr
8/8
M
WT
Bmp7-/-;Nog-/-
WT
Bmp7-/-;Nog-/-
n
E-cad
n
E-cad
n
T
n
T

location for the EA/TEF gene(s). Notably, the majority of EA/TEF patients also have symphalangism (fused digits), a prominent feature in SYM1 and SYNS1, autosomal dominant disorders that affect skeletal development and known to be linked with *NOG* mutations (Krakow, Reinker et al. 1998; Gong, Krakow et al. 1999). It is also worth noting that the breakpoints in 17q22 reported by Khalifa et al (Khalifa, MacLeod et al. 1993) are not associated with EA/TEF, and could be explained by differences in expressivity possibly caused by different genetic background. Taken together, the specific chromosomal aberrations identified in humans as well as our findings from *Nog*$^{-/-}$ mouse embryos provide a tentative link between EA/TEF and *NOG* mutations in humans.

In collaboration with Dr. Harold Lovvorn (Department of Pediatrics, Vanderbilt University), 50 blood samples from patients with EA/TEF were collected and screened for point mutations within the *NOG* coding region, using REVEAL/TGCE (Temperature Gradient Capillary Electrophoresis) analysis. One sample (#5) turned out positive for heteroduplex formation (Figure 2.10), which is suggestive of mismatched nucleotides between two DNA strands. DNA sequencing revealed this sample carried a single nucleotide polymorphism (SNP) at position 468, i.e. T instead of C, which still makes proline, rather than a point mutation.

Table 2.1 Comparison of interstitial deletions at chromosome 17q 21-23

References	Park et al (Park, Moeschler et al. 1992)	Dallapiccola et al (Dallapiccola, Mingarelli et al. 1993)	Khalifa et al (Khalifa, MacLeod et al. 1993)	Marsh et al (Marsh, Wellesley et al. 2000)	Levin et al (Levin, Shaffer et al. 1995)	Mickelson et al (Mickelson, Robinson et al. 1997)
Karyotype	46,XX,del(17)(q21.3q23)	46,XY,del(17)(q21.3q24.2)	46,XY,del(17)(q21.3q23)	46,XY,del(17)(q22q23.3)	46,XY,del(17)(q23.2q24.3)	46,XY,del(17)(q23.1q23.3)
EA/TEF	+	+	– (poor feeder)	+	–	–
Symphalangism	+	+	+	?	–	+

The deletion del(17)(q22q23.3) reported by March et al. (Marsh, Wellesley et al. 2000) represents the minimal breakpoints for the EA/TEF phenotype, which is not observed in q23.2q24.3 and q23.1q23.3 deletions that fall outside of the *NOG* locus. Therefore, 17q22 represents a critical chromosomal location for the EA/TEF gene.

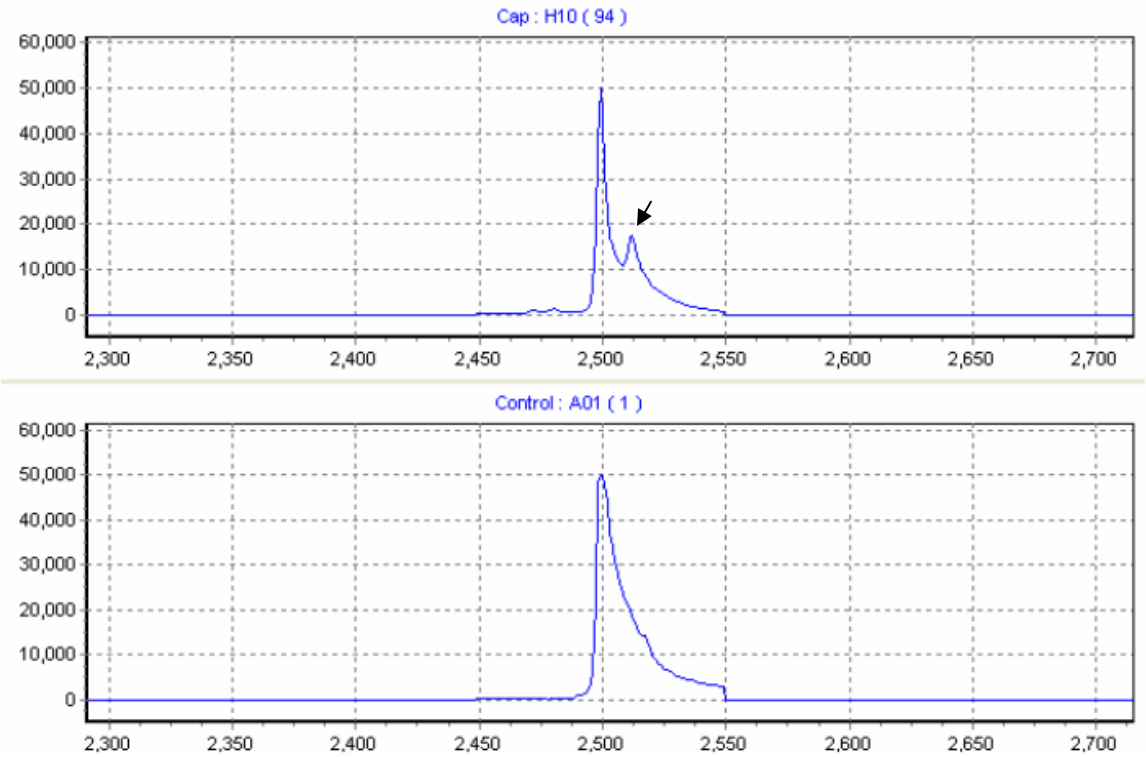

Figure 2.10 TGCE/REVEAL analysis identifies Sample #5 positive for a SNP. Arrow in the upper panel indicates an additional peak which is absent in the control, suggesting a mismatched nucleotide between two DNA strands.

Discussion

Human foregut malformations known as EA/TEF occur in 1 in 4,000 live births and are of unknown etiology. We found that mouse embryos nullizygous for *Noggin*, which encodes a Bmp antagonist, exhibit the Type C condition (Figure 2.1). This novel finding constitutes the first genetic evidence linking Bmp signaling to Type C EA/TEF, suggesting perhaps this common foregut malformation in humans is associated with alterations in Bmp signaling.

Our results indicate that Type C EA/TEF found in *Nog*$^{-/-}$ embryos at E10.5 and E11.5 correlate with a specific dorsal endoderm reduction observed at E9.5 (Figure 2.1 and 2.2), which likely occurred after formation of the foregut tube (Figure 2.3). In addition to Type C EA/TEF, we also observed abnormal notochord branches making contact with the dorsal foregut in *Nog*$^{-/-}$ embryos, similar to those reported in the adriamycin-induced rat embryos (Possoegel, Diez-Pardo et al. 1999; Qi and Beasley 1999; Orford, Manglick et al. 2001; Qi, Beasley et al. 2001; Williams, Qi et al. 2001; Mortell, O'Donnell et al. 2004). In support of the hypothesis that prolonged association of notochord with dorsal foregut may account for the dorsal foregut endoderm loss, we found non-notochordal (T^-/Foxa2$^+$ and sox9$^-$), likely foregut endodermal cells were present in the *Nog*$^{-/-}$ notochord, mingled with notochord cells (Figure 2.6). In contrast to the ventral foregut domain which is cellularly dense, only a few cells make up the dorsal foregut domain (Figure 2.2 K, L); therefore, it is possible that loss of just a few dorsal endodermal cells during notochord detachment can result in significant reduction of the

dorsal foregut at later stages. The possibility remains that T^- or $Sox9^-$ cells in *Nog*$^{-/-}$ notochord may represent a subpopulation of aberrant notochord cells that failed to express these markers; however, it is unlikely that these cells would display selective loss of T or Sox9 expression while maintaining Foxa2 expression. This notion argues in favor of the presence of endodermal cells that are $Foxa2^+$but T^- within the *Nog*$^{-/-}$ notochord. Ideally, the fate of dorsal foregut endoderm cells in *Nog*$^{-/-}$ mutants should be traced but, to our knowledge, no dorsal foregut endoderm-specific gene promoter has been identified. We also investigated several markers such as *Sox2, Sox3, Foxg1*, Foxp4 (data not shown), but these markers were expressed in the notochord as well as the gut endoderm, likely due to a common mesendodermal origin during gastrulation (Kinder, Tsang et al. 2001).

While *Nog*$^{-/-}$ embryos displayed Type C EA/TEF, embryos with loss of Chordin (*Chrd*$^{-/-}$), another Bmp antagonist, displayed a relatively normal esophagus and trachea (Figure 2.11), indicating a distinct function of *Nog* for proper notochord delamination from the dorsal foregut endoderm. *Nog* and *Chrd* share overlapping expressions in the anterior primitive streak during gastrulation. Ablation of both *Nog* and *Chrd* results in defective formation of ADE, the precursor of the foregut endoderm (Bachiller, Klingensmith et al. 2000). Formation of the foregut endoderm appeared normal in *Nog*$^{-/-}$ (Figure 2.3 and 2.4), implicating functional compensation by Chrd in *Nog*$^{-/-}$ embryos during gastrulation. Taken together, our finding suggests that while largely redundant with *Chrd* (Bachiller, Klingensmith et al. 2000), *Nog* also exhibits distinct and indispensable functions during development.

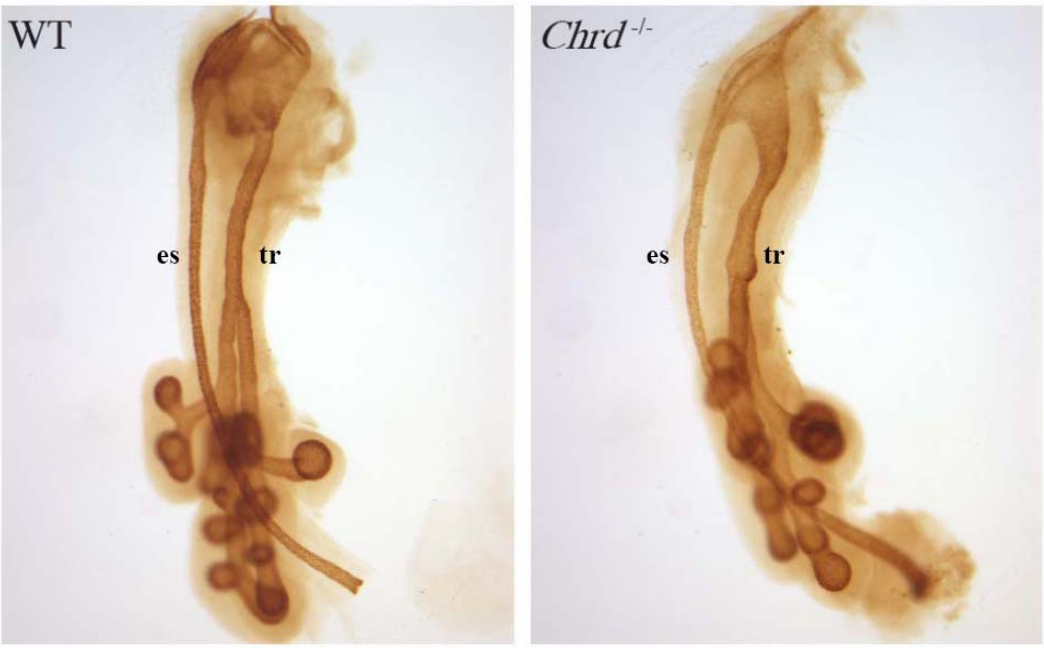

Figure 2.11 *Chrd*$^{-/-}$ embryos displayed normal esophagus and trachea.
es, esophagus; tr, trachea. Magnification: 500X

We have shown that ablating *Bmp7* alleviated the EA/TEF and foregut endoderm reduction observed in *Nog*$^{-/-}$ embryos (Figure 2.9). It remains possible, however, that other Bmps secreted from the ventral foregut mesoderm may also contribute to an increase in Bmp signaling in the notochord. During the course of this work, another group also reported a similar phenotype using *Noggin* mutant mice (Que et al., 2006). In their study, they rescued EA/TEF defect by partial removal of *Bmp4*, which is normally present in the ventral foregut mesoderm.

Our genetic screen for point mutations within the human *NOG* locus did not identify any point mutation, except a single nucleotide polymorphism (SNP) in one patient. However, since we have not examined potential mutations in the promoter region, it remains possible that *NOG* gene could be misregulated (suppressed) in some of these patients due to abnormal promoter activity. Another plausible explanation is that most EA/TEF cases may be the result of misregulated Bmp signaling caused by environmental influences, such as exposure to certain teratogenic drugs or presence of a disease condition, other than genetic inheritance. This is supported by the fact that familial occurrence of the congenital defect with associated anomalies is not common (Auchterlonie and White 1982; McMullen, Karnes et al. 1996; Nezarati and McLeod 1999).

Based on our results, we propose a model for the role of Noggin-mediated Bmp antagonism in dorsal foregut development and the pathogenesis of EA/TEF. We found

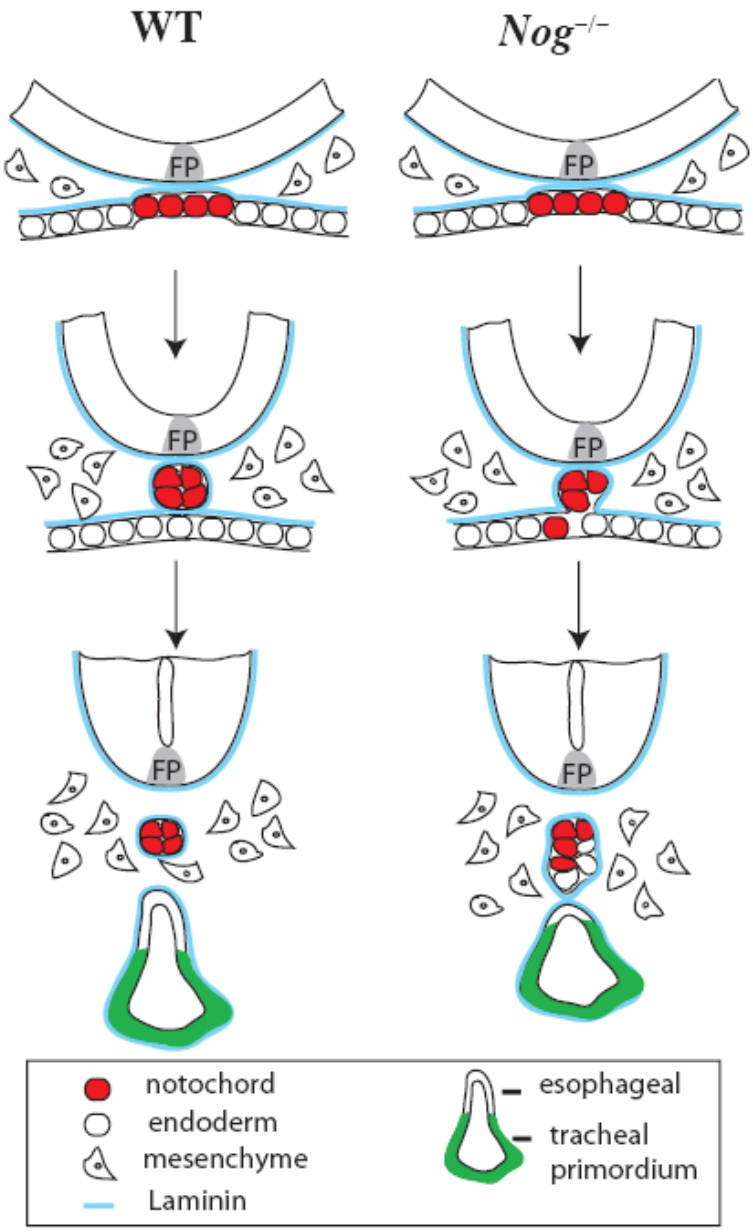

Figure 2.12 Schematic diagram showing abnormal notochord detachment and dorsal foregut reduction in *Nog*$^{-/-}$ embryos. FP, floorplate.
The domain of tracheal primordium (green) is based on Nkx2.1 expression data.

that elevated Bmp signaling in the notochord results in its prolonged attachment to the roof of the dorsal foregut endoderm (Figure 2.12). While the molecular activity downstream of unregulated Bmp signaling that results in delay and improper notochord delamination remains to be elucidated, it is likely associated with perturbation of cell-cell interaction between notochord and the foregut endoderm as disruption of basement membrane is evident in *Nog*$^{-/-}$ embryos (Figure 2.2 and 2.7). This effect is likely due to ectopic Bmp signaling in the notochord as the mesenchyme in close proximity to the dorsal foregut endoderm did not show ectopic Bmp signaling (Figure 2.8). However, we cannot exclude the possibility that the interstitial mesenchyme may indirectly contribute to the notochord detachment and/or the dorsal foregut defect.

The spectrum of foregut malformations, in particular, Type C EA/TEF characteristically displays a fistula between the narrowed esophagus and trachea. It is plausible to suggest that reduction of the dorsal foregut, which occurred prominently in the upper region, would result in a severely thin esophagus which may be disrupted at its weakest point forming a fistula to the trachea in close proximity. This notion is consistent with the observation that fistula formation can occur at different locations along the trachea and that a small fraction of *Nog*$^{-/-}$ embryos exhibited esophageal stenosis without TEF as expected if esophageal disruption did not occur. In human patients, acquired TEF, as opposed to congenital TEF, can occur from a variety of causes that result in injury to the esophagus and/or trachea such as aspiration of gastric contents, presence of foreign body in the esophagus, and prolonged mechanical ventilation (Pelc, Prigogine et al. 2001;

Reed and Mathisen 2003; Imamoglu, Cay et al. 2004). Acquired TEF can also occur as a complication secondary to esophageal or pulmonary malignancy. Thus, it appears that TEF can occur as a consequence of esophageal perturbations but the cellular mechanism of fistula formation remains to be determined.

Acknowledgements

We thank Dr. Richard Harland for the *Noggin* mice. We also thank Dr. Michael Wegner for the Sox9 antibody, Dr. Edward Morrisey for the Foxp4 antibody and Dr. Peter ten Dijke for the phosphorylated Smad1/5/8 antibody. We thank Dr. Hiroshi Sasaki for providing the Foxa2 expression plasmid. We also thank Dr. Gary Olson and Virginia Winfrey for their help in the preparation of histological thin sections and Sean Schaffer for help with confocal microscopy.

CHAPTER III

CONDITIONAL ABLATION OF BMP SIGNALING IN THE VENTRAL FOREGUT RESULTS IN TRACHEAL AGENESIS

Introduction

Development of the respiratory system, the trachea and lung, begins with ventral outpocketing of primitive lung buds from the anterior foregut endoderm, which is clearly discernible at E9.5 in mouse embryos (Kauffman 1992). Concomitant with primary lung bud formation, the tracheal primordium arises ventrally from a relatively more anterior portion of the foregut, and separates from the dorsal foregut, the primitive esophagus, in a complex process that is poorly understood. Division between the trachea and esophagus is complete by E11.5 (Kauffman 1992; Cardoso and Lu 2006). Defective development of these organs can lead to a spectrum of congenital malformations in humans ranging from esophageal atresia and tracheoesophageal fistula (EA/TEF) to tracheal agenesis (TA). The study described in this chapter focuses on TA which is characterized by complete absence of trachea (agenesis) or severe reduction of the trachea (atresia), such that communication between the larynx proximally and the lungs distally is lacking (Kerschner and Klotch 1997; Evans, Greenberg et al. 1999; Sparey, Jawaheer et al. 2000; Saleeby, Vustar et al. 2003; Lander, Schauer et al. 2004). It has been proposed that TA occurs due to failure of the tracheal tube to elongate (Effmann, Spackman et al. 1975; Lander, Schauer et al.

2004); however, the etiology and molecular pathogenesis of TA remain poorly understood.

During anterior foregut development, inductive signals emanating from the underlying mesoderm, such as Fgfs and Bmps, are thought to pattern the ventral aspect of the foregut resulting in outgrowth of rudimentary buds that give rise to structures such as the lung, liver and ventral rudiment of the pancreas during an active period of organogenesis (Min, Danilenko et al. 1998; Sekine, Ohuchi et al. 1999; Rossi, Dunn et al. 2001; Zaret 2002; Kumar, Jordan et al. 2003). For instance, during hepatogenesis, *Bmp4* produced in the septum transversum mesenchyme is required both for the induction of liver genes in the endoderm which would otherwise adopt a pancreatic fate, and the morphogenesis of the hepatic endoderm into a liver bud (Rossi, Dunn et al. 2001).

Bmp4 belongs to the Tgfβ superfamily of cytokines, and has been implicated in various developmental processes (Hogan 1996; Zhao 2003; Pogue and Lyons 2006). Bmp signaling is mediated by receptor complexes consisting of type 1 (BMPR-1A/Alk3, BMPR-1B/Alk6 and ActR-I/Alk2) and type 2 (BmpRII, Act-RII and Act-RIIb) transmembrane receptor serine-threonine kinases. Type I receptor for Bmps phosphorylates R-Smad1/5/8, which then form heteromeric complexes with Smad4 to translocate to the nucleus where they bind *cis* elements associated with specific gene expressions in the regulation of diverse cellular processes such as proliferation, apoptosis, growth arrest and cell migration. (Massague 2000; Mishina 2003; Aubin, Davy et al. 2004; Chen, Zhao et al. 2004; Kishigami and Mishina 2005).

Previous studies have shown that *Bmp4* is expressed in the ventral foregut mesenchyme surrounding the lung primordium and the future trachea (Weaver, Yingling et al. 1999); however, the biological significance of this finding has not been assessed since *Bmp4* null mutants exhibit early lethality, which hardly survive past the egg cylinder stage (E6.5) (Lawson, Dunn et al. 1999; Fujiwara, Dunn et al. 2001; Fujiwara, Dehart et al. 2002). We found that the distribution of phosphorylated-Smad1/5/8 (p-Smad1), indicative of Bmp signaling, is restricted to the ventral foregut endoderm and mesenchyme, raising the possibility that Bmp signaling may be important in tracheal morphogenesis. In order to address the role of Bmp4 signaling in the ventral anterior foregut, we circumvented the early lethality of *Bmp4* null embryos by conditionally ablating *Bmp4* with *Foxg1Cre* (*Bmp4*^{cko}), which, interestingly, resulted in the absence of trachea. Further analysis of *Bmp4*-deficient embryos indicated that specification of the tracheal primordium was unaffected; however, its outgrowth was severely compromised and was associated with significantly reduced tracheal epithelial and mesenchymal proliferation. The expression level of Sonic hedgehog (Shh), a proproliferative signaling molecule, was found to be significantly downregulated in *Bmp4*^{cko} foregut. Consistently, we also found that expression of Cyclin D1, a key cell cycle regulator and known Shh downstream target, was reduced in the *Bmp4*^{cko} foregut epithelium and mesenchyme. Taken together, these findings elucidate a critical role of Bmp signaling in tracheal morphogenesis and implicate potential Bmp-Shh crosstalk in anterior foregut growth.

Materials and Methods

Mice and Embryos

Bmp4$^{loxp/loxp}$ and *Bmp4*$^{lacZ/+}$ mice were kindly provided by Drs. Brigid Hogan and Holger Kulessa. The *Foxg1Cre* transgene, *ROSA*^{26R} and *Top-Gal* transgene were obtained from the Jackson Laboratory. All mouse strains were maintained in a C57BL/6 background, except for *ROSA*^{26R}, which is maintained in a mixed background. To characterize *Foxg1* expression, *Foxg1Cre* was crossed with *ROSA*^{26R}. *Bmp4* conditional knockout (*Bmp4*^{cko}) embryos were generated by crossing *Bmp4*$^{flox/flox}$ mice with *Bmp4*$^{lacZ/+}$*; Foxg1Cre* mice and identified by *Cre* and *Bmp4-lacZ* PCRs (Figure 3.1), using the following primers:

Cre (forward):5'-TCGATGCAACGAGTGATGAG-3';

Cre (reverse): 5'-TTCGGCTATACGTAACAGGG-3';

Bmp4-lacZ (forward): 5'-CAGGGCGATTCTTACTTTCG-3';

Bmp4-lacZ (reverse): 5'-AGCTTGGCGTAATCATGGTC-3'.

Conditions for PCRs were: 94°C for 4minutes; 32 cycles of (94°C for 30 seconds, 55°C for 30 seconds, 72°C for 40 seconds); 72°C for 10 minutes. Amplifications of *Cre* and *Bmp4-lacZ* allele generate a 480-bp product and a 339-bp product, respectively.

To study the effect of Bmp4 ablation on Wnt signaling, the *Top-Gal* transgene was introduced into *Bmp4*$^{lacZ/+}$*;Foxg1Cre* before mating with *Bmp4*$^{flox/flox}$ homozygotes. *Bmp4*^{cko} embryos containing *Top-gal* were determined by lacZ staining (see Results).

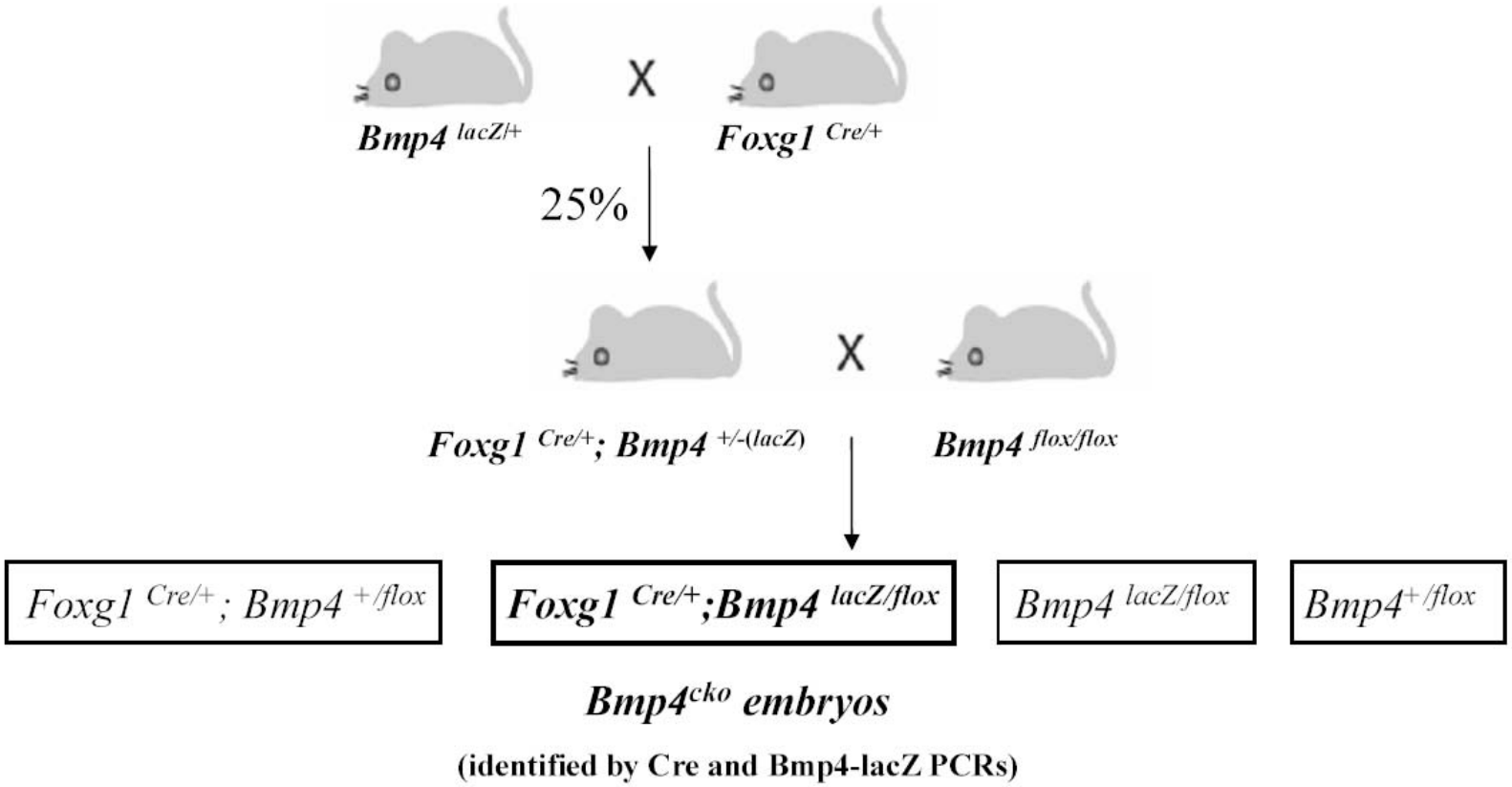

Figure 3.1 Strategy for generation and identification of *Bmp4*^{cko} embryos

Immunohistochemistry and lacZ staining

Immunohistochemistry and lacZ staining were performed as described in Chapter II (Li, Zhang et al. 2004), except for immunostaining of Nkx2.1 in embryos younger than E10 which was performed using cryosections. Briefly, embryos were fixed in 4% PFA at 4°C for 40 minutes, washed in PBS 3 times, 10 minutes each, and embedded in Tissue-Tek® OCT compound in cold ethanol-dry ice bath and stored at -80°C. Cryosections at 15μm thickness containing the desired embryonic regions were collected on Superfrost Plus slides and dried in a 37°C incubator for 10 minutes. After three 10 minute washes in PBS, slides were incubated in blocking solution (PBS+10% goat serum) containing 0.1% Triton-X100 for 1 hour at RT, prior to overnight incubation with primary antibody in blocking solution at 4°C. The remaining steps are the same as in immunohistochemistry for paraffin sections as described in Chapter II. Primary antibodies were used at the following dilutions: rabbit anti-phospho-Smad1/5/8 (gift of Dr. Laufer 1:1500); rabbit anti-Foxa2 (1:50); mouse anti-Nkx2.1 (Lab Vision, 1:200); rabbit anti-Shh (Santa Cruz H-160, 1:200); rat anti-E-cadherin (Zymed, 1:200); mouse anti-CylinD1 (BD pharmingen, 1:100); rabbit anti-CyclinD2 (Santa Cruz, M20, 1:150); and mouse anti-CyclinD3 (Lab Vision, 1:200).

Analysis of cell proliferation and cell death

Pregnant female mice at E9.5 were injected intraperitoneally with 5-Bromodeoxyuridine (BrdU; 50mg per kg body weight) and sacrificed 30 minutes later.

Embryos were collected in cold PBS, fixed in 4% PFA for 1 hour at 4°C, dehydrated in a series of methanol washes (25%, 50%, 75% methanol/PBS+0.1%Tween, and 2X 100% methanol), and embedded in paraffin (as described in Chapter II). Sections of 5μm thickness were collected on Superfrost Plus slides (Fisher). BrdU detection was performed as previously described (Litingtung, Lei et al. 1998). Briefly, slides were dewaxed in xylenes (3X, 5 minutes each) and rehydrated through a series of ethanol/PBS washes (2X 100% ethanol, 2X 95% ethanol, 1X 70% ethanol, 3X PBS, 3 minutes each). Endogenous peroxidase activity was blocked using 3% H_2O_2 in methanol for 10 minutes at RT. After washing in PBS for 3 times, sections were treated with 2N HCl at 37°C to expose the double-strand DNA. HCl treatment was stopped by several quick washes in water, followed by three 5 minute washes in PBS. After blocking in PBS containing 10% goat serum for 1 hour at RT, samples were incubated with mouse anti-BrdU antibody (Roche, 1:15 diluted in PBS+10% goat serum) overnight at 4°C. Slides were washed in PBTw (PBS+0.1% Tween20) 3 times for 10 minutes each, and incubated with goat anti-mouse horseradish peroxidase (HRP) conjugated secondary antibody (Jackson ImmunoResearch, 1:300) for 1.5 hours at RT in the dark. Following extensive wash in PBS, slides were incubated in the dark with chromogenic substrate DAB (Invitrogen) until signals were detected (normally 3-10 minutes). Samples were counterstained with hematoxylin (Thermo Shandon) for 30 seconds, dehydrated in ascending ethanol series and mounted with Permount (Fisher).

TUNEL assay was used for detection of apoptotic cells in embryo sections according to manufacturer's instruction (ApopTag Apoptosis Detect Kit, Chemicon).

Statistic analysis

Sections processed for BrdU detection were photographed at 200X magnification. Total number and percentage of BrdU-positive cells in *Bmp4*^{cko} embryonic foreguts compared with WT littermates on five sequential sections of the upper foregut (anterior to lung primordium) per mutant or WT embryo were counted, with three pairs of embryos. All values were represented as means +/- standard error of the mean (SEM). Student's t-test was applied to determine statistical significance of differences between WT and *Bmp4*^{cko} embryos. Statistical significance was defined as $P<0.05$.

***In situ* hybridization**

Cryosection *in situ* hybridizations were performed as described in Chapter II. The following cDNAs were used as templates for synthesizing DIG-labeled riboprobes: *Pax9* (R. Balling), *mCol2a* (Y. Yamada), and *Id1-3* (R. Benezra).

Results

Conditional ablation of *Bmp4* in the ventral foregut by *Foxg1Cre* transgene

We observed that expression of *Bmp4*^{lacZ} in the embryonic foregut was restricted to the ventral mesenchyme as early as E8.5 (Figure 3.2A). This restricted pattern remained until later stages when the trachea and esophagus are completely separated (Figure 3.2 E9.5-E11.5, B-D). Similarly, immunostaining of phosphorylated-Smad1/5/8 (p-Smad1) was found restricted to the ventral mesoderm and endoderm in the anterior foregut at E9.0 (Figure 3.4 A, B). The role of this ventrally-restricted Bmp4 expression and signaling in anterior foregut growth and patterning has not been studied. We reasoned that morphogenesis of the trachea, a ventral endoderm derivative, would likely involve epithelial-mesenchymal interactions involving Bmp signaling. Therefore, to investigate the role of Bmp signaling in tracheal morphogenesis, we took advantage of a *Foxg1Cre* transgenic mouse line to specifically delete Bmp4 function in the ventral foregut domain. *Foxg1* is expressed in the foregut endoderm as early as E8.5 (Figure 3.3 A-C), which is earlier than previously reported (Hebert and McConnell 2000). *Foxg1* expression became more uniform and robust in both the foregut endoderm and mesoderm by E9.5, as highlighted by lacZ staining of embryos generated by crossing *Foxg1Cre* with *ROSA*^{26R} (Figure 3.3 D-F). We generated conditional deletion of *Bmp4* in the ventral foregut by crossing *Bmp4*$^{lacZ/+}$*;Foxg1Cre* mice with *Bmp4*$^{flox/flox}$ mice (Figure 3.1). *Foxg1*-mediated *Cre* activity is predicted to ablate Bmp4 function in the ventral foregut by E9.5

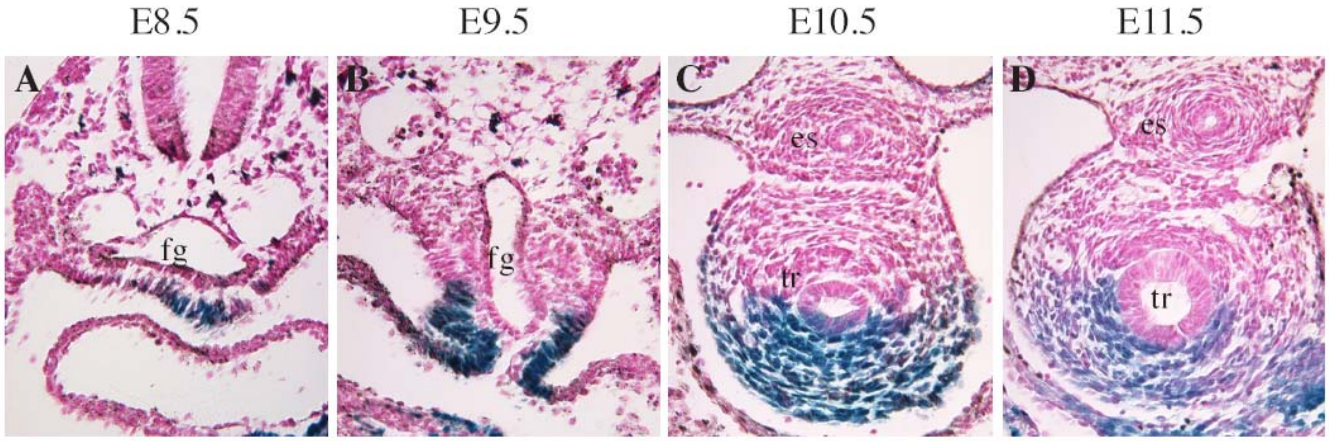

Figure 3.2 *Bmp4-lacZ* expression is restricted to the ventral foregut during tracheal morphogenesis. fg-foregut; es-esophagus;tr-trachea. Magnification: A to C-200X; D:100X.

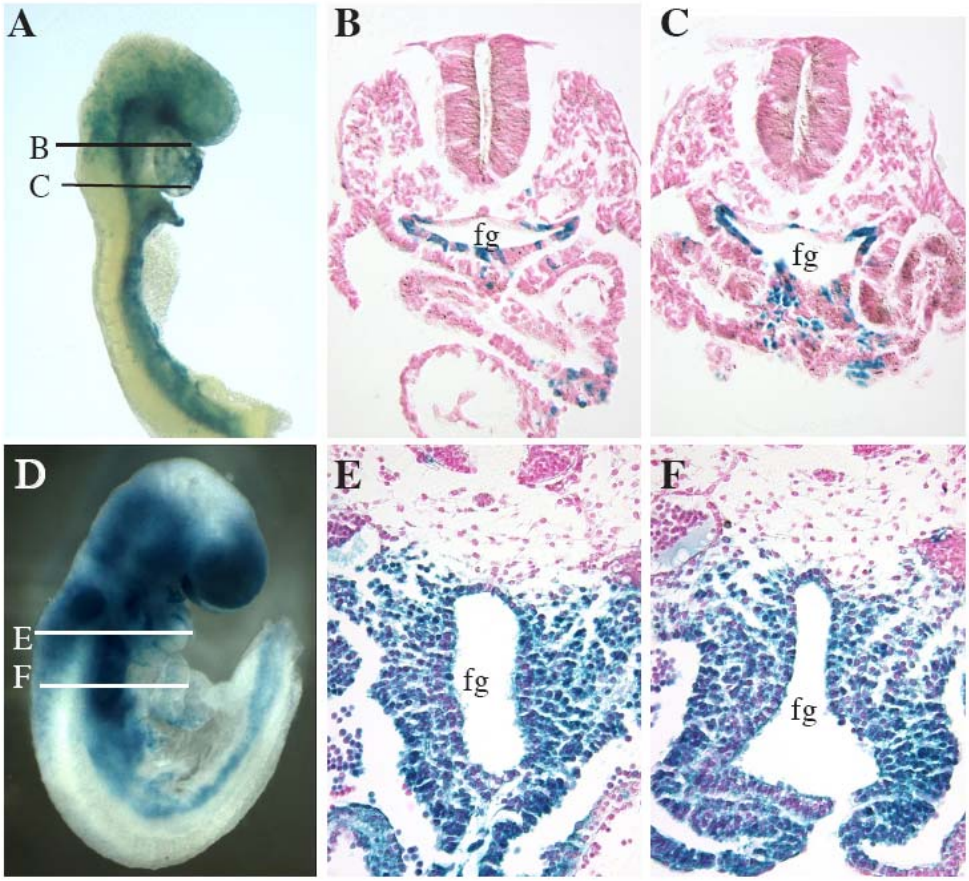

Figure 3.3 *Foxg1* expression at E8.5 (A-C) and E9.5 (D-F), by lacZ staining of embryos from *Foxg1Cre*X*Rosa26R*.
Lines in A and D denote the cross-section planes of B, C, E and F. *Foxg1* is expressed in the foregut endoderm as early as E8.5 (A-C). Its expression becomes more uniform in both the endoderm and mesenchyme by E9.5 (D-F). fg-foregut. Magnification: A-400X; D-250X; B, C, E, F-200X.

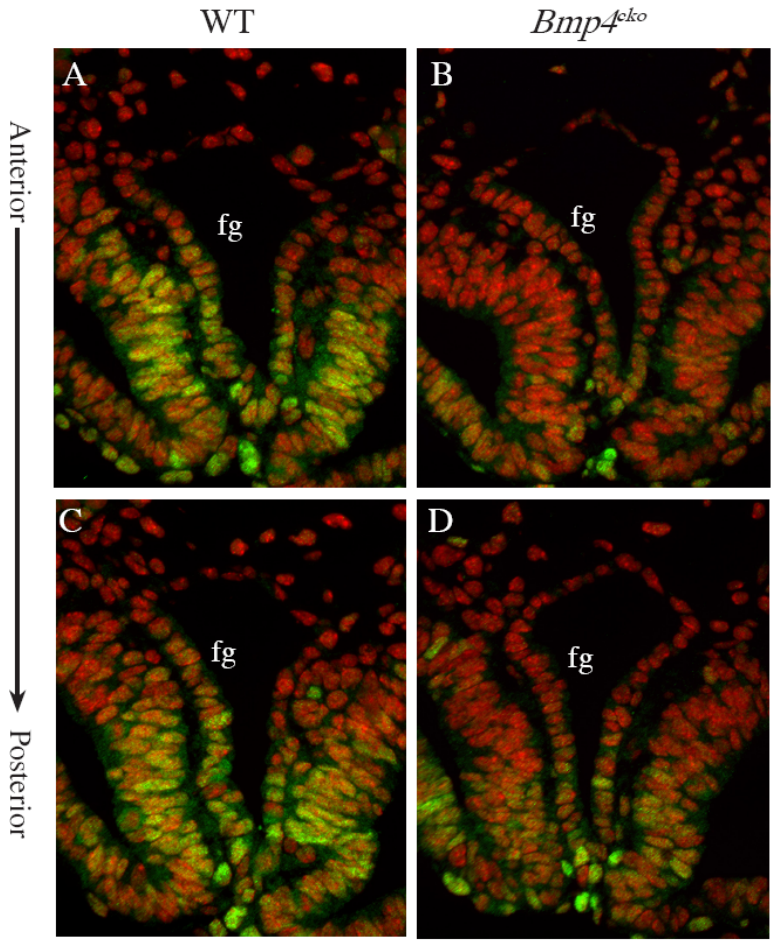

Figure 3.4 Expression of p-Smad1/5/8, indicative of activated Bmp signaling, is reduced in E9.0 *Bmp4^{cko}* foregut compared with WT foregut.
(A, C) sections of WT embryos show ventrally restricted p-Smad1/5/8 expression (green) throughout the anterior foregut. (B, D) p-Smad1/5/8 staining is significantly reduced in the *Bmp4^{cko}* embryos. The posterior half of the ventral foregut, close to the future lung bud level, displays some reduction in pSmad1/5/8 while loss of Bmp signaling appears to be even more dramatic in the anterior portion of the ventral foregut. fg-foregut. Manification: 400X.

(Kulessa and Hogan 2002).

Based on the early pattern of *Bmp4* expression in the ventral mesoderm (Figure 3.2), *Foxg1Cre*-mediated *Bmp4* ablation in this tissue would likely affect Bmp4-mediated signaling in the ventral foregut mesoderm (autocrine) and in the endoderm (paracrine). We found substantial loss of Bmp signaling as demonstrated by significantly reduced p-Smad1/5/8 immunostaining in the ventral foregut endoderm and mesoderm in *Bmp4*^{cko} compared with WT embryos at E9.0, prior to the emergence of the respiratory primordium (Figure 3.4). We observed that the posterior half of the ventral foregut, at the future lung bud level, displayed some reduction in pSmad1/5/8 (Figure 3.4 C, D)while loss of Bmp signaling appeared to be more pronounced in the anterior portion of the ventral foregut (Figure 3.4 A, B). Based on pSmad1/5/8 staining, it appears that *Foxg1Cre*-mediated *Bmp4* deletion occurred effectively in the anterior ventral foregut of all embryos examined (n=3).

Expression of *Id* genes was downregulated in the *Bmp4*^{cko} foregut

To further confirm the conditional ablation of *Bmp4*, we also examined expression of *inhibitor of differentiation* (*Id*) genes, putative *Bmp* target genes in the ventral foreguts of *Bmp4*^{cko}. Bmp signaling can transcriptionally regulate expression of *Id* genes which encode negative regulators of basic helix-loop-helix (bHLH) transcription factors (Hollnagel, Oehlmann et al. 1999; Miyazono and Miyazawa 2002; ten Dijke, Korchynskyi et al. 2003; Ying, Nichols et al. 2003). Id proteins have distinct functions in

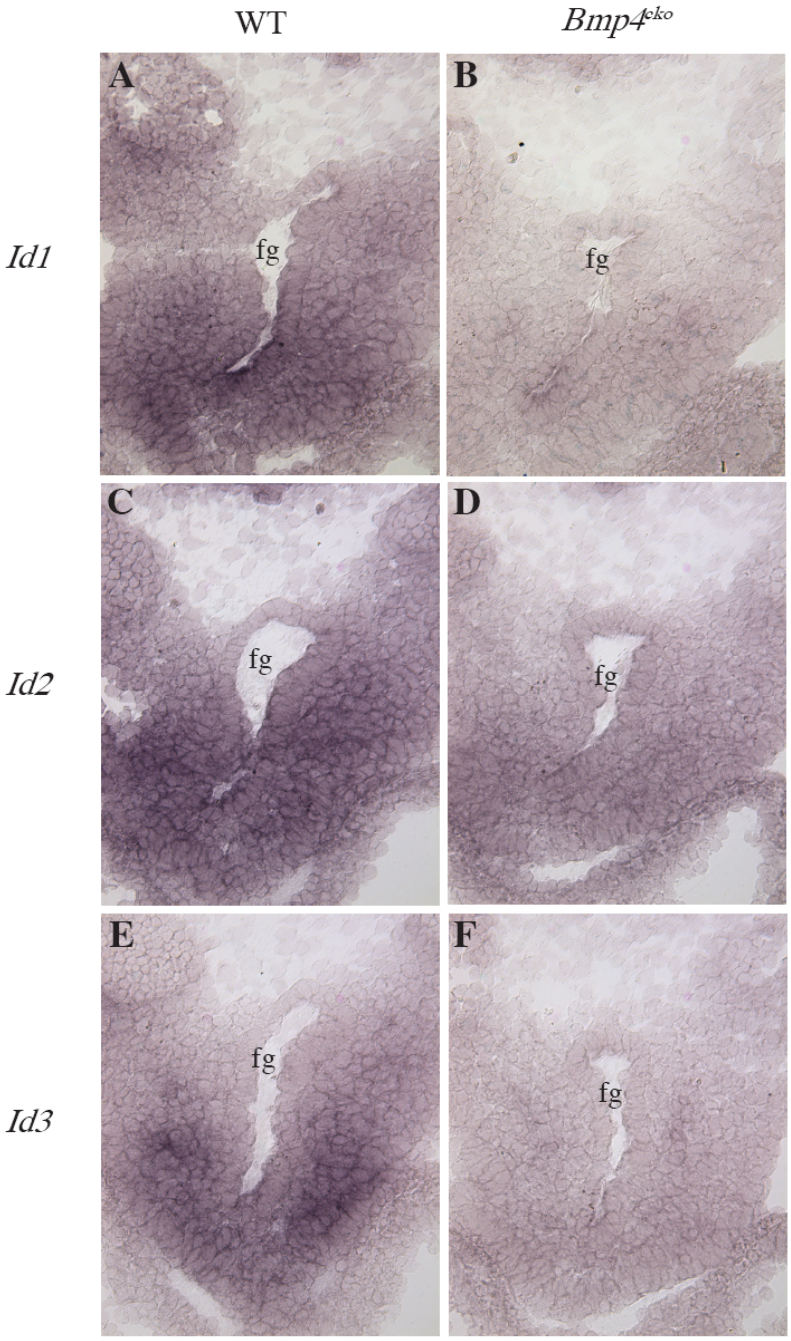

Figure 3.5 Expression of *Ids* 1, 2 and 3 is downregulated in *Bmp4*^{cko} foregut. fg-foregut. Manification: 200X.

development and disease, and have been implicated in cell cycle regulation, G1 progression and the control of growth induction (Barone, Pepperkok et al. 1994; Peverali, Ramqvist et al. 1994; Jen, Manova et al. 1997; Lyden, Young et al. 1999; Bain, Cravatt et al. 2001; Benezra, Rafii et al. 2001; Lasorella, Uo et al. 2001; Fong, Itahana et al. 2003; Ruzinova and Benezra 2003; Sikder, Devlin et al. 2003; Li, Luo et al. 2005). We found that all the *Id* genes (Id1, 2, 3) were expressed in both the ventral foregut mesoderm and endoderm while *Id3* expression is relatively higher in the ventral foregut mesoderm compared to the endoderm (Figure 3.5 A, C, E). Therefore, we examined expression of *Id1*, *Id2* and *Id3* in the ventral foregut of *Bmp4*^{cko} embryos by *in situ* hybridization on tissue sections at E9.25-9.5, compared with WT foreguts. In *Bmp4*^{cko} embryos, expression of all three *Ids* was significantly downregulated in the ventral foregut (Figure 3.5 B, D, F), consistent with downregulation of Bmp signaling detected by pSmad1/5/8 (Figure 3.4).

Bmp4-deficient foregut displayed trachea agenesis (TA)

To determine the functional significance of this specific ablation, we examined the gross morphologies of *Bmp4* conditional knockout (*Bmp4*^{cko}) embryos by Foxa2 immunohistochemistry to highlight the foregut endoderm (Litingtung, Lei et al. 1998). While there was no apparent morphological differences between WT and *Bmp4*^{cko} foregut at E9.0 (Figure 3.6 A, B), a stage prior to the appearance of tracheal primordium, all *Bmp4*^{cko} embryos displayed formation of a single tube, at E10.5 (n=3, Figure 3.6D) and E11.5 (n=3, Figure 3.6F), compared to WT littermates which exhibited two distinct gut

Figure 3.6 *Bmp4*-deficient foregut displays tracheal agenesis.
Bmp4^{cko} embryos display a single tube and hypoplastic lungs, at E10.5 (D) and E11.5 (F) while WT embryos display two distinct gut tube derivatives, the esophagus and trachea (C, E). Insets in E and F show the ventral views of lungs. Notably, no obvious defect is observed in *Bmp4*^{cko} foregut at E9.0 (A, B). Molecular analysis of E12.5 embryos indicates that the single tube in *Bmp4*^{cko} embryos adopts an esophageal fate and completely lacks the trachea identity, as it stains negatively for the respiratory/tracheal marker Nkx2.1 (brown, I and J) but is positively-labeled with *Pax9*, an esophageal specific marker, (purple, G and H). *mCol2a* expression, which normally surrounds the tracheal epithelium, is also lost in the ventral mesenchyme in *Bmp4*^{cko} foregut compared to WT foregut (purple, K and L). tr-trachea; es-esophagus; lu-lung. Magnification: A,B-900X; C, D-630X; E, F-500X; G to L-100X.

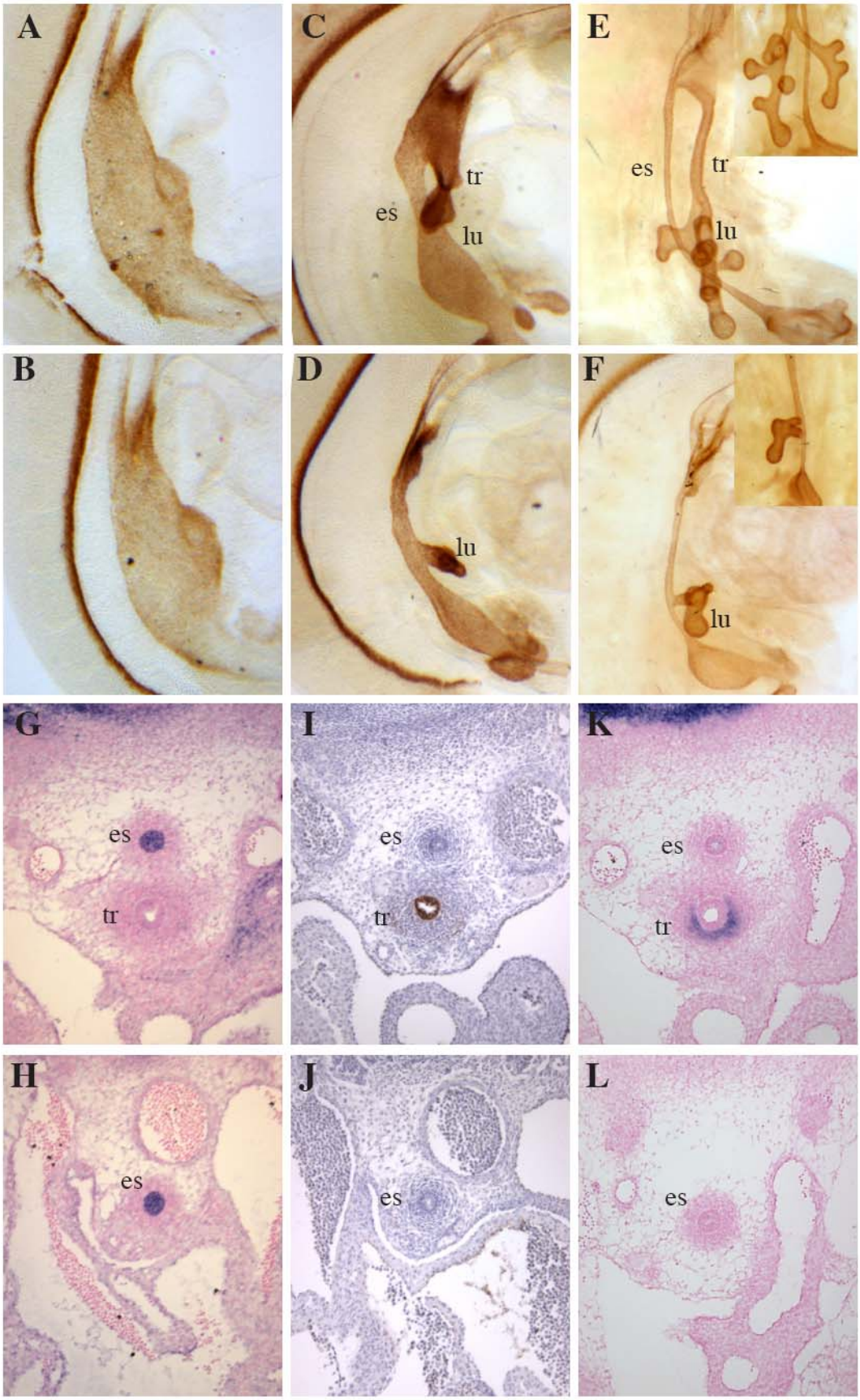
A
C
tr
es
lu
E
es
tr
lu
B
D
lu
F
lu
G
es
tr
I
es
tr
K
es
tr
H
es
J
es
L
es

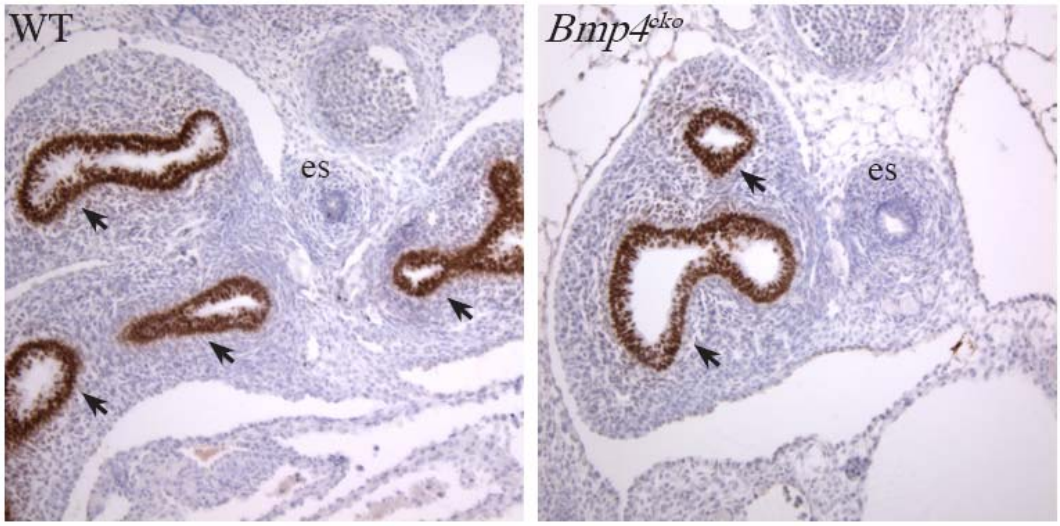

Figure 3.7 Nkx2.1 is expressed in the lung epithelium (arrows) of *Bmp4^{cko}* embryos. es-esophagus. Magnification: 100X.

tube derivatives, the esophagus and trachea (Figure 3.6 C, E). In addition, we also observed hypoplastic lungs in all the *Bmp4*^{cko} embryos examined (Figure 3.6 E, F insets), indicating an additional role of Bmp4 signaling during early lung bud growth.

Molecular analysis of E12.5 embryos showed that the single tube in the *Bmp4*^{cko} embryos did not stain with respiratory/tracheal specific marker Nkx2.1 (n=3, Figure 3.6 I, J), whereas Nkx2.1 expression could still be detected in the underdeveloped lung epithelium (Figure 3.7) (Minoo, Su et al. 1999). In contrast, *Pax9*, an esophageal specific marker, was able to label this endodermal tube (n=3, Figure 3.6 G, H). *mCol2a* expression, which normally surrounds the tracheal epithelium, was also lost in the ventral mesenchyme in *Bmp4*^{cko} foregut compared to WT foregut (Figure 3.6 K, L). Taken together, these findings indicated that the single tube in *Bmp4*^{cko} embryos has an esophageal characteristic and completely lacks tracheal identity, thus manifesting tracheal agenesis (TA).

Specification of the tracheal primordium appeared normal in *Bmp4*^{cko} embryos

To determine whether loss of trachea is due to a tracheal specification problem, we examined the ventral foregut endoderm in *Bmp4*^{cko} embryos by Nkx2.1 immunostaining at E9.0-E9.5 (20-25 somites). At E9.0-9.25 (20-22 somites), prior to the appearance of the respiratory rudiment, Nkx2.1 was expressed in the *Bmp4*^{cko} foregut and the extent of expression was quite comparable with WT foregut (Figure 3.8 A, B). As early as E9.25-9.5 (23-25 somites, Figure 3.8C, D), we observed a reduction in the

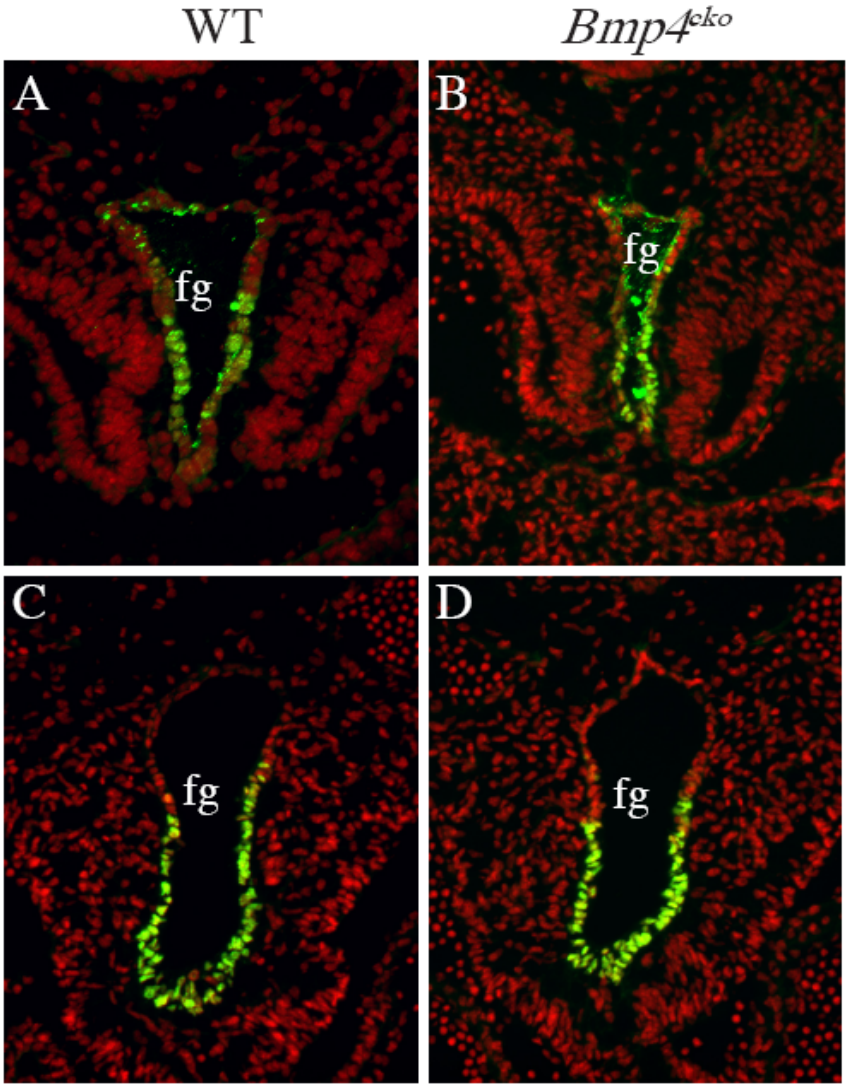

Figure 3.8 Specification of tracheal primordium appears normal in *Bmp4^{cko}* embryos. Nkx2.1-positive cells (green) are present in the endoderm of *Bmp4^{cko}* embryos at E9.0-9.5 suggesting that the initial specification of the tracheal primordium is not affected. (A, B) Nkx2.1 immunostaining at E9.0-E9.5 (20-25 somites) reveals the extent of Nkx2.1 expression is quite comparable in *Bmp4^{cko}* embryos compared to WT embryos at E9.0-9.25 (20-22 somites), prior to the appearance of the respiratory primordium. Note the fluorescence inside the lumen and close to the dorsal foregut is not nuclear and represents background staining. (C, D) Consistent with reduced growth capacity of the respiratory domain, the extent of Nkx2.1 expression, but not the expression level, is reduced in *Bmp4^{cko}* embryos as early asE9.25- E9.5 compared with WT (23-25 somites). fg-foregut. Magnification: 400X.

expression domain of Nkx2.1, but not the expression level, in *Bmp4*^{cko} embryos compared to WT embryos. The reduced extent of Nkx2.1 expression is consistent with the reduced foregut size in *Bmp4*^{cko} embryos. The presence of Nkx2.1-positive cells in the endoderm of *Bmp4*^{cko} embryos at E9.0 suggests that Bmp4-mediated signaling is required for the outgrowth, but not the initial specification, of the tracheal primordium.

Bmp4^{cko} foregut displays decreased cell proliferation but no significant alterations in cell survival and E-cadherin expression

To further investigate the decrease in growth potential of the *Bmp4*^{cko} foregut, we determined the proliferative capacity of E9.5 WT and mutant foreguts by *in vivo* pulse labeling with 5'-BromodeoxyUridine (BrdU), a nucleotide analog that is incorporated into replicating DNA. We counted the total number and percentage of BrdU-positive cells in *Bmp4*^{cko} embryonic foreguts compared with WT littermates on five sequential sections of the upper foregut per mutant or WT embryo in three pairs of embryos. WT and mutant embryos were paired based on somite number within the litters. We found a statistically significant difference in cell proliferation in the *Bmp4*^{cko} foregut endoderm and mesoderm. BrdU pulse-labeling revealed a relatively lower percentage of proliferating epithelial cells in the *Bmp4*^{cko} foregut (28.2-37.7%) compared with WT foregut (53.3-56.9 %). Mesenchymal cells in the *Bmp4*^{cko} foregut also displayed a lower proliferative capacity (25.0-41.6%) compared with WT foregut (48.8-52.2%) (Figure 3.9).

We also examined *Bmp4*^{cko} foregut sections at E9.0-10.25 for alterations in the

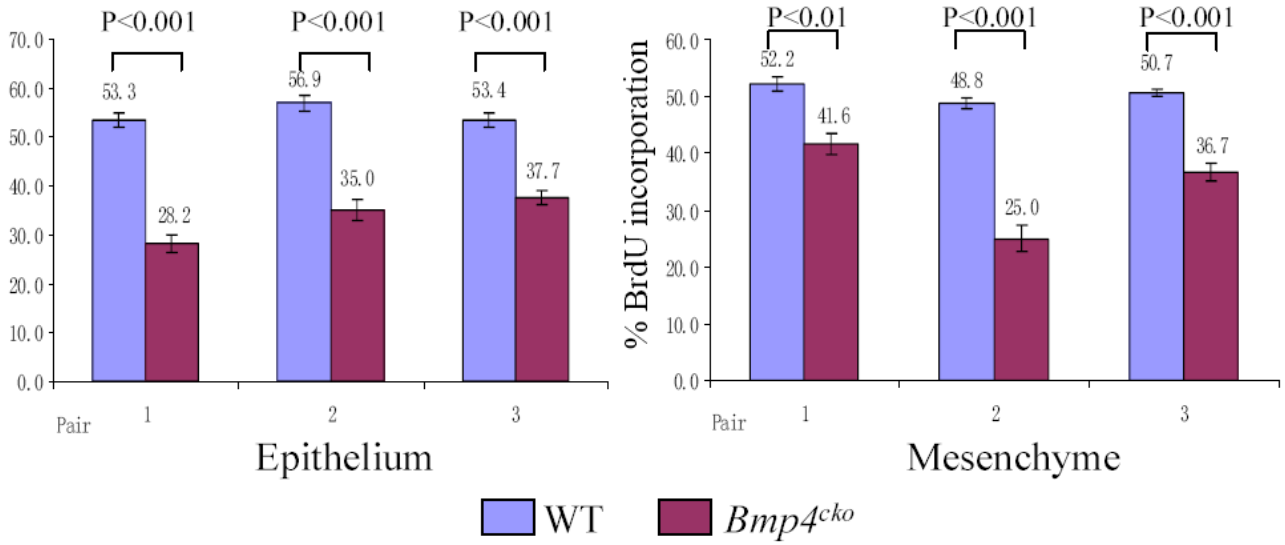

Figure 3.9 *Bmp4^{cko}* foregut displays reduced cell proliferation compared with WT foregut by *in vivo* BrdU pulse labeling. Histogram showing the percentage of BrdU-labeled cells in the epithelium and mesenchyme of E9.5 *Bmp4^{cko}* foregut compared with WT control. All the compared values are statistically significant, which is defined as $p<0.05$.

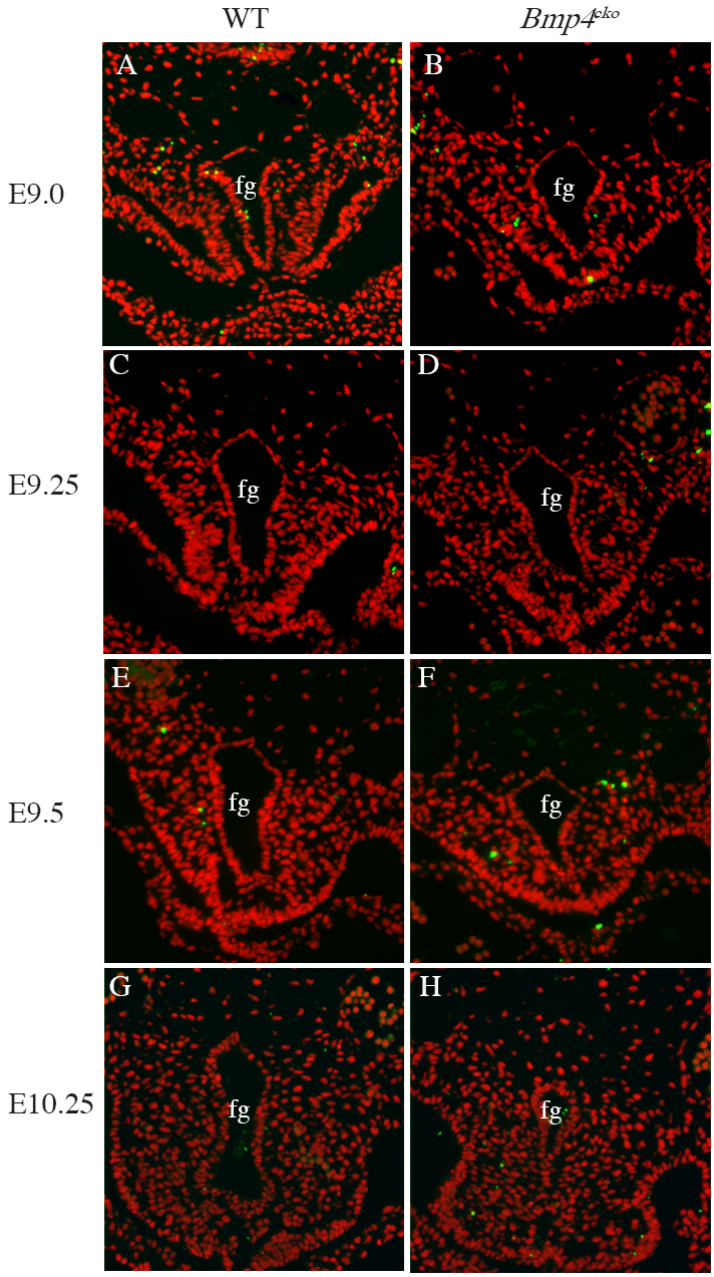

Figure 3.10 Programmed cell death is not affected in the *Bmp4*^{cko} foregut. fg-foregut. Magnification: 200X.

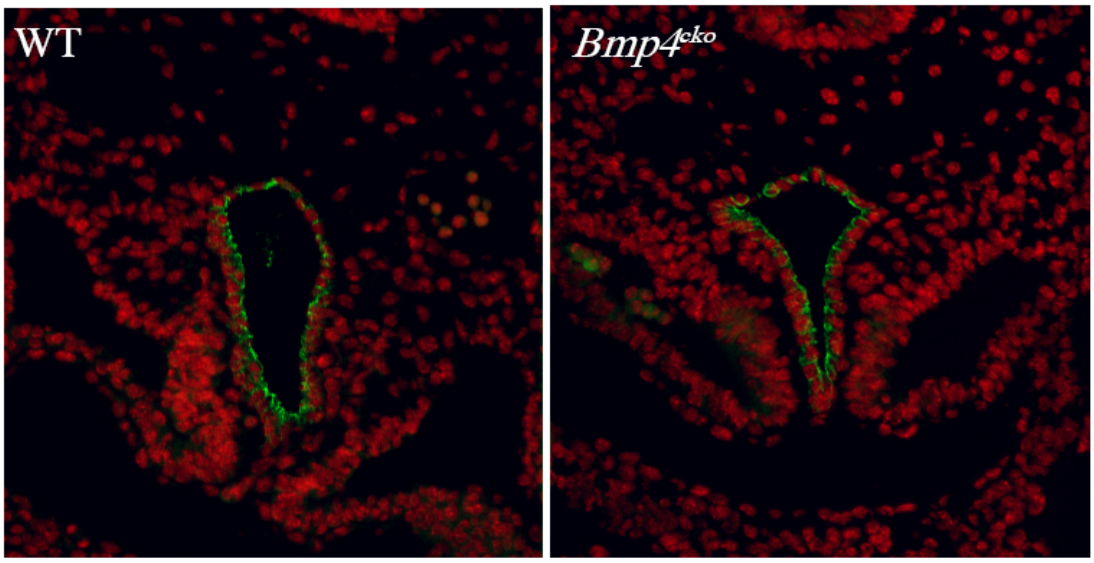

Figure 3.11 E-cadherin expression (green) is not altered in *Bmp4*^{cko} foregut. Magnification: 200X.

level of cell death by TUNEL assay, and found no significant difference in apoptotic cells in the ventral foregut endoderm of *Bmp4*^{cko} and WT embryos (Figure 3.10).

Initiation of morphogenesis of organs such as the trachea/lungs, teeth and hair follicles involves outgrowth/downgrowth of an epithelial bud. Downregulation of E-cadherin, an epithelial adherence junction protein, modulates Bmp and Wnt signaling to play a key role in epithelial bud outgrowth (Jamora, DasGupta et al. 2003). Although epithelial polarity and intercellular adhesion are essential to maintain epithelial integrity and function, it appears that disrupting epithelial adhesion is a critical step during epithelial bud morphogenesis. Therefore, we examined whether expression of E-cadherin may be altered in *Bmp4*^{cko}. However, we did not observe alterations in the expression or localization of E-cadherin (Figure 3.11).

Taken together, we propose that one critical role of Bmp4-mediated signaling in the foregut is to regulate cell proliferation during tracheal development.

Wnt signaling was not affected in the *Bmp4*^{cko} foregut epithelium

To explore the molecular mechanism underlying cell proliferation modulation by Bmp4 signaling, we next investigated the potential alteration of Wnt signaling in *Bmp4*^{cko} foregut, as several lines of evidence suggest that Bmp signaling may regulate cell proliferation/cell cycle progression via cross-talk with canonical Wnt signaling (Marcelle, Stark et al. 1997; Burstyn-Cohen, Stanleigh et al. 2004; Ovchinnikov, Selever et al. 2006). Transgenic Wnt/β-catenin signaling reporter *Top-Gal* expression can be detected at E9.5

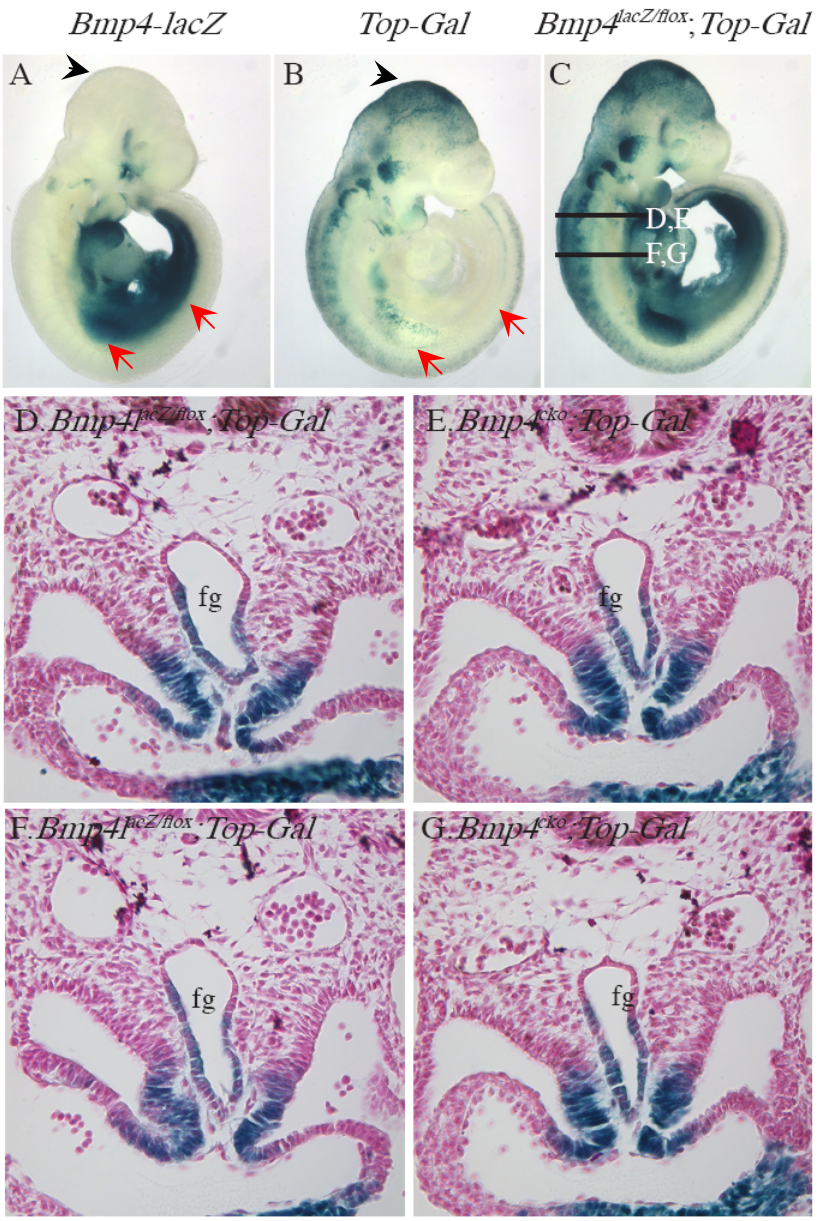

Figure 3.12 Wnt/β-catenin signaling remains unaffected in *Bmp4^{cko}* embryos.
(A-C) Whole-mount view of lacZ stained E9.0-9.25 (20-22 somites) *Bmp4-lacZ, Top-Gal* and *Bmp4-lacZ+Top-Gal* embryos. Note specific expression of *Top-Gal* in the mid-brain ectoderm (black arrowheads in A, B) and *Bmp4-lacZ* in the limb mesoderm and mid-hindgut (red arrows in A, B). Lines in C denote the cross-section planes of D-G. (D-G) Endodermal *Top-Gal* expression levels remain unaltered in the *Bmp4^{cko}* compared to control (*Bmp4$^{lacZ/flox}$*) littermates. The lacZ staining in the ventral mesenchyme is from *Bmp4-lacZ* allele (see Figure 3.2), which is present in both the control and *Bmp4^{cko}* embryos. fg-foregut. Magnification: A to C-250X; D to G-200X.

in the developing anterior foregut endoderm at the level of the laryngotracheal groove and canonical Wnt activity persists in foregut endoderm derivatives at later stages (Okubo and Hogan 2004; Shu, Guttentag et al. 2005), suggesting that canonical Wnt signaling may play a key role in anterior foregut morphogenesis. We therefore introduced *Top-Gal* transgene into *Bmp4*$^{lacZ/+}$; *Foxg1*$^{Cre/+}$ mice and mated them with *Bmp4*$^{flox/flox}$ to obtain *Bmp4*^{cko} embryos harboring *Top-Gal*. E9.0-9.25 (20-22 somites) embryos expressing both *Bmp4-lacZ* and *Top-Gal* upon lacZ staining were selected, based on specific *Bmp4-lacZ* expression in the limb mesoderm and mid-hind gut (red arrows in Figure 3.12 A, B) and distinct *Top-Gal* expression in the mid-brain ectoderm (black arrowheads in Figure 3.12 A, B). *Bmp4*^{cko} were identified by *Cre* PCR. At E9.0-9.25, while *Bmp4-lacZ* was restricted in the ventral foregut mesenchyme (also refer to Figure 3.2), *Top-Gal* expression was observed in the ventral endodermal layer, consistent with a previous report (Okubo and Hogan 2004) (Figure 3.12, D, F). To our surprise, we found that the *Top-Gal* expression in the *Bmp4*^{cko} foregut was largely comparable to control (*Bmp4*$^{lacZ/flox}$) littermates (Figure 3.12, E, G), indicating that Wnt/β-catenin signaling was not affected in *Bmp4*^{cko}.

Shh expression was reduced in the *Bmp4*^{cko} embryos

In addition to canonical Wnt signaling, there is also evidence suggesting that Bmp can cross-talk with Shh during palatogenesis and tooth germ development (Chen, Bei et al. 1996; Zhang, Zhang et al. 2000; Zhang, Song et al. 2002). Shh signaling has been

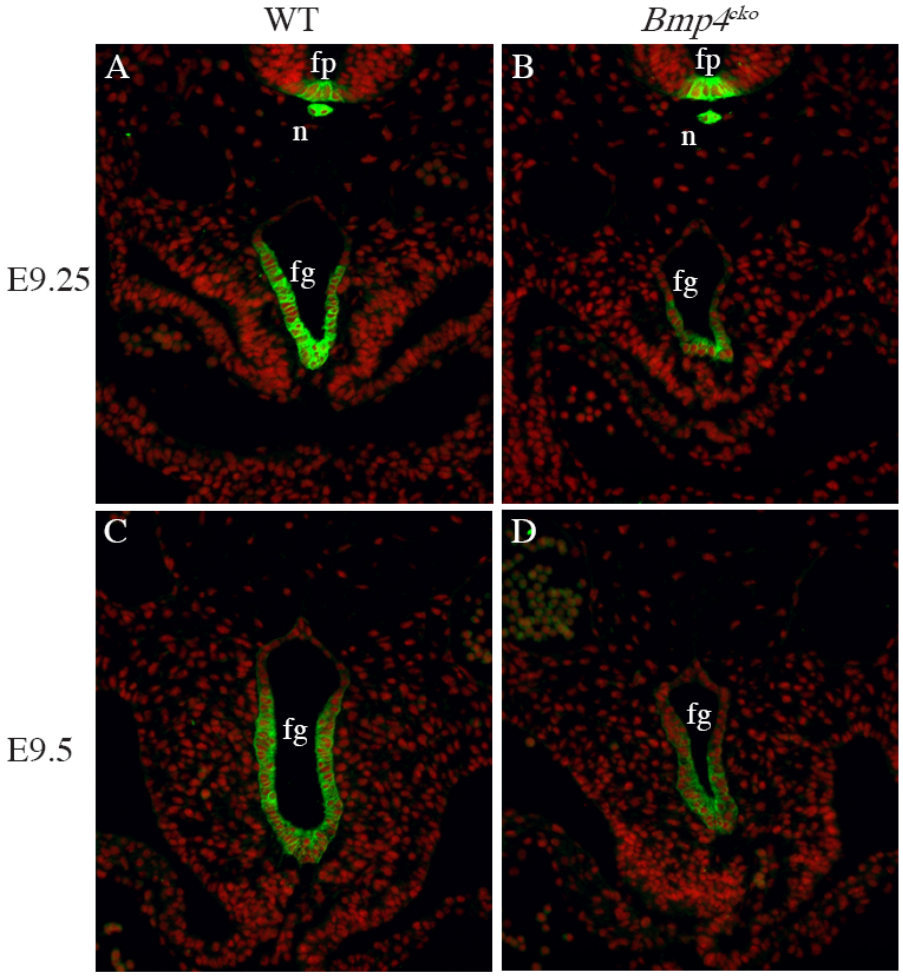

Figure 3.13 Expression levels of Shh are reduced in *Bmp4*^{cko} foreut.
Note decreased Shh expression levels occur only in the foregut region where Bmp4 is specifically ablated, but not in the notochord and floor plate. fg-foregut; n-notochord; fp-floor plate. Magnification: 200X.

implicated in the regulation of cell proliferation during normal developmental processes in various organs, as well as under pathological conditions (Litingtung, Lei et al. 1998; Pepicelli, Lewis et al. 1998; Wetmore 2003; Ingham and Placzek 2006). Embryos with loss of *Shh* or defective in Shh signaling components displayed severe esophagotracheal defects suggesting a critical role of Shh signaling in foregut morphogenesis (Litingtung, Lei et al. 1998; Motoyama, Liu et al. 1998; Pepicelli, Lewis et al. 1998). Shh expression is normally restricted to the ventral foregut endoderm (Figure 3.13A, C); expressions of its target genes such as *Gli1* and *Ptch1* revealed that signaling occurred in both the ventral epithelium and mesenchyme (Litingtung, Lei et al. 1998; Pepicelli, Lewis et al. 1998; and Yina Li and Chin Chiang, unpublished observation). We therefore examined the expression of Shh in *Bmp4*^{cko} embryos. In contrast to *Top-Gal* expression, Shh level was consistently reduced in the *Bmp4*^{cko} foregut at E9.25 and E9.5 (Figure 3.11B, D), and this reduction was specific in the foregut region where Bmp signaling was ablated, but not in the notochord and floor plate (Figure 3.13 A, B). This result suggests that the impaired proliferative capacity of *Bmp4*^{cko} foregut is, at least in part, due to compromised Shh expression level.

Expression of Cyclin D1 was downregulated in *Bmp4*^{cko}

Numerous publications have implicated the role of Shh signaling in the regulation of proproliferative genes such as *Cyclins*, which are evolutionarily conserved proteins essential for cell cycle control (Kenney and Rowitch 2000; Berman, Karhadkar et al.

2002; Ciemerych, Kenney et al. 2002; Mill, Mo et al. 2003; Yu, Mazerolle et al. 2006). Therefore, we next determined the expression of Cyclin D1-3, which are critical components for G1 to S progression. By performing immunohistochemistry on paraffin-embedded tissue sections of *Bmp4*^{cko} foreguts compared with WT at E9.5, we found the expression level and distribution of Cyclin D1 was reduced in both the epithelium and mesenchyme of *Bmp4*^{cko} foregut (Figure 3.14B), compared with WT (Figure 3.14A), which is consistent with the impaired growth capacity observed in the epithelium and mesenchyme of the *Bmp4*^{cko} foreguts (Figure 3.9). Compared to Cyclin D1, Cyclin D2 and D3 were expressed at low levels in only a few foregut cells (Figure 3.14 C, E). Examination of these two D type Cyclins did not reveal appreciable differences between WT and *Bmp4*^{cko} foreguts (Figure 3.14, C-F), suggesting that Shh signaling in developing foreguts does not affect cyclin D2 and D3, in contrast to its effect on Cyclin D1.

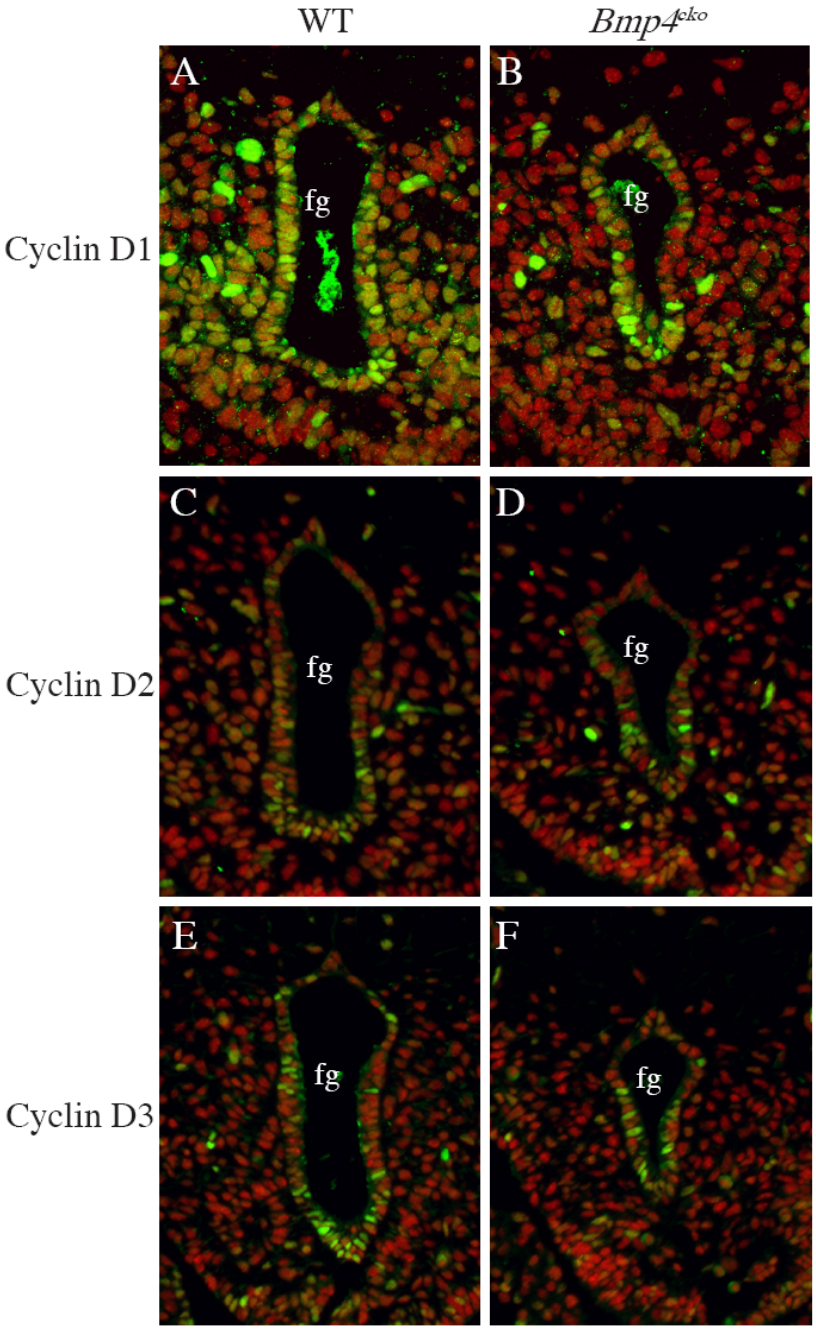

Figure 3.14 Expression of Cyclin D1-3 in the *Bmp4^{cko}* foregut.
Cyclin D1 expression in the foregut region is reduced in both the epithelium and mesenchyme in the E9.25-9.5 *Bmp4^{cko}* embryos. However, there are no appreciable differences of Cyclin D2 and D3 expression between WT and *Bmp4^{cko}* embryos. fg-foregut. Magnification: A, B-400X; C to F-200X.

Discussion

Tracheal atresia/agenesis is a rare but life-threatening foregut anomaly of unknown etiology (Diaz, Adams et al. 1989; Manschot, van den Anker et al. 1994; Kerschner and Klotch 1997). We found that mouse embryos with conditional ablation of Bmp4 in the ventral foregut domain by a *Foxg1Cre* transgene displayed tracheal agenesis (TA) (Figure 3.5). This novel finding provides the first genetic mouse model manifesting TA, and suggests perhaps TA in humans is associated with insufficient Bmp signaling during tracheal morphogenesis.

Like lung development, tracheal morphogenesis is also governed by a complex process of inductive interactions between the endoderm and its surrounding mesoderm. In mouse embryos nullizygous of fibroblast growth factor 10 (Fgf10), which is normally expressed in the foregut mesoderm, the respiratory primordium failed to grow out while the presumptive trachea was still formed (Min, Danilenko et al. 1998; Sekine, Ohuchi et al. 1999), suggesting alternative signaling(s) from the mesoderm is required to regulate tracheal formation. Here we show that conditional ablation of *Bmp4* in the ventral foregut domain led to a significant reduction in its growth capacity at E10.5 and E11.5 which resulted in loss of the trachea (Figure 3.6 C-F). Since we observed reduction in Bmp signaling in both the ventral foregut endoderm and mesenchyme (Figure 3.4), it is possible that mesenchymally-derived Bmp4 signals in a paracrine fashion to regulate the underlying foregut endodermal growth. In addition, it could also signal in an autocrine manner to affect the ability of mesenchymal cells to secrete growth factors or ECM

molecules which are critical for mesenchymal-epithelial interaction, epithelial growth and patterning. Bmp4 also appears to be expressed at low levels at a later stage in the ventral foregut endoderm (Figure3.2D, E10.5), therefore it is possible that *Foxg1Cre*-mediated ablation of epithelial-derived Bmp4 may also contribute to reduction of autocrine Bmp signaling in the epithelium at later stages.

We detected significant reduction in *Id1-3* expression in *Bmp4*^{cko} foregut, consistent with these regulatory factors being downstream targets of Bmp signaling. The role of Id factors in modulating epithelial cell proliferation has been reported in several studies (Coppe, Smith et al. 2003; Kowanetz, Valcourt et al. 2004; Asirvatham, Schmidt et al. 2006; Hua, Zhang et al. 2006; Langenfeld, Kong et al. 2006). Members of the *Id* family are expressed in the foregut region and share significant redundant functions during development (Lyden, Young et al. 1999; Kee and Bronner-Fraser 2001; Fraidenraich, Stillwell et al. 2004). *Id2* has also been implicated in distal lung epithelial growth (Komatsu, Shibuya et al. 2002). However, loss of *Id* function in the foregut as in *Id2*$^{-/-}$ (Mori, Nishikawa et al. 2000) or in *Id1*$^{-/-}$*;Id3*$^{-/-}$ (data not shown) embryos did not result in tracheal atresia. Therefore, the role of Id proteins in tracheal morphogenesis remains to be elucidated. Possibly, due to redundant functions, tracheal development might be impaired when all three *Id* genes are deleted.

The observation that Nkx2.1-expressing cells were still present in the *Bmp4*^{cko} foregut and the expression level was comparable with WT E9.0 embryos suggests that Bmp4 is not required for the initial tracheal specification; rather, it plays an indispensable

role in the subsequent outgrowth of the trachea. This finding is different from the role of Bmp signaling in liver development, in which Bmp signaling appears to be essential for both initial hepatic fate specification and subsequent outgrowth of hepatic endoderm into liver buds (Zaret 2000; Rossi, Dunn et al. 2001; Zaret 2001).

Consistent with the reduction in growth potential, we found that E9.5 *Bmp4*^{cko} foregut showed reduced cell proliferation in the epithelium and mesenchyme by BrdU labeling, indicative of impaired cell cycle progression, in particular, G1-S transition. Several studies indicate that Bmp can modulate components of canonical Wnt signaling in embryonic development and cancer (Nishanian, Kim et al. 2004; Yang, Yamasaki et al. 2006). Bmp has also been shown to regulate the cell cycle by controling Cyclin D1 expression and G1/S transition via activation of canonical Wnt signaling during neural crest delamination, in particular, via transcriptional activation of Wnt1 in the dorsal neural tube (Marcelle, Stark et al. 1997; Burstyn-Cohen, Stanleigh et al. 2004). Surprisingly, we did not observe changes in reporter *Top-Gal* expression suggesting that Wnt/β-catenin signaling was not affected in *Bmp4*^{cko} foregut.

In contrast to Wnt/β-catenin signaling, we detected consistent reduction of Shh expression level in *Bmp4*^{cko} foregut, suggesting that Bmp4 may regulate tracheal outgrowth via Shh. Shh has been implicated in the regulation of cell cycle genes such as *Cyclins* and we found that Cyclin D1 level was reduced in the epithelium and more pronounced reduction in the mesenchyme of *Bmp4*^{cko} foregut. It has been shown that in most tissues the D-type cyclins are largely exchangeable; when two of the three D-cyclins

are ablated, the remaining cyclin will be ubiquitously upregulated to compensate for the loss (Ciemerych, Kenney et al. 2002). However, we did not find upregulation of Cyclin D2 and D3 to compensate for the Cyclin D1 reduction, indicating reduced cell proliferation in *Bmp4*^{cko} is at least in part due to attenuated Cyclin D1 expression.

The *Bmp4*-deficient foregut showed impaired cell proliferation, without apparent alteration in cell death, whereas embryos with loss of *Shh* displayed severe esophagotracheal defects with reduced cell proliferation and elevated cell death (Litingtung, Lei et al. 1998; Pepicelli, Lewis et al. 1998; and Y.L. and C.C., unpublished observation). The difference between these two mutants suggests that low levels of Shh may be sufficient for cell survival while high levels of Shh may be required to promote cell proliferation.

While our data together with several other previous reports (Chen, Bei et al. 1996; Zhang, Zhang et al. 2000; Zhang, Song et al. 2002) suggest that Bmp4 acts upstream of Shh, it also appears that Shh signaling can conversely regulate the expression of Bmp4 in the developing lung mesenchyme (Litingtung, Lei et al. 1998; Pepicelli, Lewis et al. 1998; Weaver, Batts et al. 2003). Hence, these two highly conserved and ubiquitous signaling systems, Bmp and Shh, might cross-regulate each other during embryogenesis in promoting tissue outgrowth and patterning.

Acknowledgements

We would like to thank Drs. Brigid Hogan and Holger Kulessa for providing the *Bmp4*^{cko} mice and Dr. Robert Benezra for providing the *Id1* and *Id3* mutant mice. We thank Dr. Laufer for providing us the p-Smad1 antibody. This work was done in collaboration with Dr. Nancy Manley at the University of Georgia.

CHAPTER IV

GENERAL DISCUSSION

Development of the dorsal esophagus and the ventral trachea from a common anterior foregut endoderm is a complex process involving cell proliferation, programmed cell death, differentiation and migration, which requires appropriate and regulated interactions between two different interfaces, not only within the foregut tissue but between foregut and its adjacent tissues as well. In this dissertation work, I have focused on Bmp signaling and its role during anterior foregut patterning. Our studies have identified a pathogenic role of deregulated Bmp signaling resulting from loss of the Bmp antagonist Noggin in the formation of esophageal atresia, which involves inappropriately prolonged interaction between the foregut endoderm and the overlying notochord. In addition, we have elucidated an instructive/permissive role for mesodermally derived Bmp4 during tracheal outgrowth; this involves Bmp4-mediated reciprocal communications between tracheal foregut endoderm and mesoderm. Ablation of this Bmp4 function resulted in tracheal loss, a foregut malformation that has not been previously demonstrated in genetic mouse models. My work therefore sheds new insights into the relatively under-explored research area involving morphogenesis of the trachea and esophagus, and brings up interesting new questions that need to be addressed in the future.

Identification of new animal models with foregut anomalies

Our investigation of the role of Bmp signaling in anterior foregut patterning has revealed two new mouse models manifesting human foregut malformations. As mentioned in the introduction, several mouse mutant lines previously generated, such as *Shh*$^{-/-}$, *Gli2*$^{-/-}$*Gli3*$^{+/-}$ and *Nkx2.1*$^{-/-}$, show foregut defects (Table 1.2); however, they do not exhibit the typical phenotype of the most common form of EA/TEF, Type C, in which the upper esophagus ends in a blind pouch and the lower esophagus, normally stenosed, abnormally connects to the trachea via a fistula (Table 1.1). We found that mouse embryos lacking Noggin, a Bmp antagonist, displayed foregut defects that are highly reminiscent of Type C EA/TEF (Figure 2.1), thus providing genetic evidence linking deregulated Bmp signaling in the pathogenesis of the most prevalent form of EA/TEF. Tracheal atresia/agenesis (TA) is relatively rare (less than 1:50,000) but nevertheless represents a life-threatening malformation that produces respiratory distress due to partial or complete absence of the trachea (Manschot, van den Anker et al. 1994). So far, no one has reported genetic mouse models exhibiting TA. We identified that ablation of *Bmp4* in the ventral foregut domain by *Foxg1Cre* resulted in complete loss of trachea, therefore providing the first genetic mouse model representing the human TA condition. This finding suggests that insufficient Bmp signaling during tracheal morphogenesis is linked to the pathogenesis of TA.

Noggin-mediated Bmp antagonism in the pathogenesis of esophageal atresia

Our results indicate that the esophageal atresia in *Nog*$^{-/-}$ embryos (E11.5 and E10.5, Figure 2.2) correlate with a specific dorsal foregut endoderm reduction (Figure 2.1 and 2.2). Dorsal foregut defects in *Nog*$^{-/-}$ embryos appear to associate with abnormal notochord branches making contact with the dorsal foregut in *Nog*$^{-/-}$ embryos, similar to those reported in the adriamycin-induced rat embryos (Possoegel, Diez-Pardo et al. 1999; Qi and Beasley 1999; Orford, Manglick et al. 2001; Qi, Beasley et al. 2001; Williams, Qi et al. 2001; Mortell, O'Donnell et al. 2004). Consistent with our hypothesis that impresice detachment of notochord due to its prolonged contact with the dorsal foregut may contribute to the dorsal foregut endoderm loss, we found loosening or loss of cells in the dorsal foregut endoderm (Figure 2.7), and the presence of non-notochordal (T^{-}/Foxa2^{+} and sox9^{-}), likely foregut endodermal cells in the *Nog*$^{-/-}$ notochord, amongst notochord cells (Figure 2.6). Since the dorsal foregut endoderm is composed of only a few cells at E8.5-9.0 (Figure 2.2 E-L), it is conceivable that loss of just a few dorsal endodermal cells during notochord detachment can result in significant reduced dorsal foregut domain at later stages. While it remains possible that T^{-} or Sox9^{-} cells in *Nog*$^{-/-}$ notochord may represent a subpopulation of aberrant notochord cells that failed to express these markers, it is unlikely that these cells would display selective loss of T or Sox9 expression but not Foxa2 expression. This notion argues in favor of the presence of endodermal cells that are Foxa2^{+}but T^{-} within the *Nog*$^{-/-}$ notochord. Ideally, lineage tracing of dorsal foregut endoderm cells in *Nog*$^{-/-}$ mutants should be performed; however, so far no dorsal foregut

endoderm-specific gene promoter has been identified. In addition, we have not revealed any markers that are dorsal foregut endoderm specific, likely due to a common mesendodermal origin of the dorsal foregut and the notochord during gastrulation (Kinder, Tsang et al. 2001).

Our data imply a new role of Noggin-mediated Bmp antagonism in dorsal foregut development and in the pathogenesis of EA/TEF. Under physiological condition, Noggin is required to keep Bmp signaling silent in the notochord so it can properly detach from the dorsal foregut endoderm in a timely manner; in the absence of Noggin, elevated Bmp signaling in the notochord results in its prolonged attachment to the roof of the dorsal foregut endoderm, which contribute to dorsal foregut cell loss (Figure 2.12). We have not yet identified the molecular activity downstream of deregulated Bmp signaling that results in delay and improper notochord delamination in our current study; however, we think it is likely associated with perturbation of cell-cell interaction between notochord and the foregut endoderm since disruption of the basement membrane is obvious in *Nog*$^{-/-}$ embryos (Figure 2.2 and 2.7). The mechanism underlying the establishment of the cellular boundary between the roof of the foregut endoderm and notochord remains to be elucidated.

In our study, we show that ablating *Bmp7* completely rescued the EA/TEF and foregut endoderm reduction observed in *Nog*$^{-/-}$ embryos (Figure 2.9). Since other Bmps, such as Bmp4 secreted from the ventral foregut mesoderm, may also contribute to an increase in Bmp signaling in the notochord, we can not rule the possibility that other

Bmps may also be involved. Consistent with this notion, during the course of this work, another group also reported a similar phenotype using *Noggin* mutant mice (Que, Choi et al. 2006). In their study, they rescued the EA/TEF defect by partial removal of *Bmp4*, which is normally present in the ventral foregut mesoderm. The successful rescue of *Nog*$^{-/-}$ EA/TEF by two different Bmps suggests that *Bmps* expressed in overlapping domains may exhibit functional redundancies during development. In contrast, embryos with loss of Chordin (*Chrd*$^{-/-}$), another Bmp antagonist that shares several overlapping functions with Noggin (Bachiller, Klingensmith et al. 2000), displayed a fairly normal esophagus and trachea (Figure 2.11), indicating a distinct function of Noggin in proper notochord detachment.

To further explore the critical role of *Noggin*-mediated antagonism in EA/TEF pathogenesis that we established in the mouse model, we collaborated with Dr. Harold Lovvorn to perform a genetic screening of 50 patients with EA/TEF for point mutations within the human *NOG* coding region. Although we did not identify any point mutation, except a conservative polymorphism in one patient, it is possible that it is in part due to the relatively small sample size. In addition, we have not examined potential mutations in the promoter region, so it remains possible that *NOG* gene could be misregulated (suppressed) in some of these patients due to aberrant gene promoter activity. Another plausible explanation is that most of EA/TEF cases may be the result of misregulated Bmp signaling caused by environmental influences, such as exposure to certain teratogenic drugs or presence of a disease condition, other than genetic inheritance. This

is supported by the fact that familial occurrence of the congenital defect with associated anomalies is not common (Auchterlonie and White 1982; McMullen, Karnes et al. 1996; Nezarati and McLeod 1999).

The role of Bmp signaling in tracheal formation

Our results from the *Bmp4*^{cko} foregut study suggest a critical role of signaling by *Bmp4* produced in the ventral foregut mesoderm in the regulation of tracheal growth. In the *Bmp4*^{cko} embryos, *Bmp4* in the ventral foregut is selectively deleted with *Foxg1Cre*, which results in complete loss of the trachea, evident at E11.5 and E10.5 (Figure 3.6). Consistent with a reduction in growth potential, *Bmp4*^{cko} embryos display reduced cell proliferation in the foregut endoderm as well as the mesoderm (E9.5, Figure 3.9). However, the presence of Nkx2.1-positive cells in the endoderm of *Bmp4*^{cko} embryos at E9.0, a stage prior to the appearance of respiratory primordium, suggests that Bmp4-mediated signaling is required for the subsequent outgrowth but not the initial specification of the tracheal primordium. This newly identified Bmp signaling role is different from the role of Bmps in liver development, in which Bmp signaling appears to be essential both for initial hepatic fate specification and subsequent outgrowth of hepatic endoderm into liver buds (Zaret 2000; Rossi, Dunn et al. 2001; Zaret 2001).

Similar to morphogenesis of other organs such as lung, kidney and pancreas, tracheal development is also controlled by a complex process of inductive interactions between the endoderm and its surrounding mesoderm. We observe reduction in Bmp

signaling in both the ventral foregut endoderm and mesenchyme in the *Bmp4*^{cko} foregut (Figure 3.4); therefore, it is conceivable that mesenchymally-derived Bmp4 signals in both paracrine and autocrine fashions to respectively regulate the underlying foregut endoderm growth and affect mesenchymal cells to secrete growth factors or ECM molecules which are important for mesenchymal-epithelial interaction, epithelial growth and patterning. Consistent with this notion, we detect that expression levels of Shh in the ventral endoderm are significantly reduced in the *Bmp4*^{cko} foregut. Since Shh signals to both the mesoderm and the endoderm (Litingtung, Lei et al. 1998; Pepicelli, Lewis et al. 1998; and Y.L. and C.C., unpublished observation), and it has been implicated in the regulation of cell proliferation (Kenney and Rowitch 2000; Berman, Karhadkar et al. 2002; Ciemerych, Kenney et al. 2002; Mill, Mo et al. 2003; Yu, Mazerolle et al. 2006), the reduced Shh level is consistent with the observed reduction of cell proliferation in the *Bmp4*^{cko} foregut endoderm and mesoderm.

While the *Bmp4*-deficient foreguts display reduced cell proliferation, without apparent alteration in cell death, embryos with loss of *Shh* exhibit severe esophagotracheal defects with reduced cell proliferation and elevated cell death (Litingtung, Lei et al. 1998; Pepicelli, Lewis et al. 1998; and Y.L. and C.C., unpublished observation). The difference in cellular behaviors between these two mutants suggests that low levels of Shh may be necessary for cell survival while high levels of Shh are critical to promote cell proliferation.

Cross-regulation of signaling pathways

Cross-regulation between signaling pathways is thought to be critical during the growth and patterning of many organ systems. The relationship between Bmp and Shh can be either opposing or promoting, depending on different developmental contexts. For instance, in the developing central nervous system, Shh (located ventrally in the notochord and floor plate) and BMP (located dorsally in the boundary of neural/nonneural ectoderm and later in the roof plate) functionally oppose each other to properly pattern the dorsoventral aspect of the neural tube (Jessell and Sanes 2000). Similarly, in the developing limb field, Bmp signaling derived from the mesoderm needs to be modulated by its antagonist Gremlin, which is essential to maintain the Shh-Fgf4 feedback loop (Capdevila, Tsukui et al. 1999; Zuniga, Haramis et al. 1999; Khokha, Hsu et al. 2003). In contrast to the antagonistic interaction, during palate and tooth germ development, mesenchymally- derived Bmp4 is thought to act upstream of Shh. Bmp4-soaked bead can induce Shh expression in explant culture and transgenic expression of human *BMP4* under the *Msx1* promoter in *Msx1*$^{-/-}$ palatal mesenchyme restores Shh expression in the epithelium (Chen, Bei et al. 1996; Zhang, Zhang et al. 2000; Zhang, Song et al. 2002). Our analysis of *Bmp4*^{cko} foregut also indicates that Bmp can upregulate Shh expression during tracheal outgrowth. While our data, together with previous reports (Chen, Bei et al. 1996; Zhang, Zhang et al. 2000; Zhang, Song et al. 2002), suggest that Bmp4 acts upstream of Shh, it also appears that Shh signaling can conversely regulate the expression of *Bmp4*, as in the developing lung mesenchyme (Litingtung, Lei et al. 1998;

Pepicelli, Lewis et al. 1998; Weaver, Batts et al. 2003). Hence, these two highly conserved signaling systems, Bmp and Shh, can cross-talk during embryogenesis to promote tissue outgrowth and patterning.

FUTURE DIRECTIONS

Molecular and cellular distinction of foregut endoderm and notochord

Our results of the *Nog*$^{-/-}$ foregut, together with investigations in the adriamycin rat/mouse model (Possoegel, Diez-Pardo et al. 1999; Qi and Beasley 1999; Orford, Manglick et al. 2001; Qi, Beasley et al. 2001; Williams, Qi et al. 2001; Mortell, O'Donnell et al. 2004), implicate notochordal abnormalities in the pathogenesis of esophageal atresia, suggesting the importance of proper notochord delamination to the integrity of the dorsal foregut, which in turn is critical for the subsequent development of the dorsal structure, the esophagus. While our study has shed light on the essential role of *Noggin*-mediated Bmp antagonism in the appropriate notochord detachment from the roof of the foregut, we have not identified factors that control this process which could be altered by deregulated Bmp signaling. We think it is likely associated with perturbation of cell-cell interaction between notochord and the foregut endoderm as disruption of basement membrane is evident in *Nog*$^{-/-}$ embryos (Figure 2.1 and Figure 2.7). How the boundary between the notochord and the underlying dorsal foregut is defined and how it is affected by Bmp signaling are important future questions.

During development, the notochord is initially embedded in the dorsal foregut hence physically participate in the formation of the roof of the primitive gut tube; however, these two types of tissues are already predetermined and therefore intrinsically different from each other. As development proceeds, the foregut endodermal cells and the notochordal cells detach and the latter move dorsally to lie underneath the neural tube. How the foregut endoderm is molecularly programmed to be distinguished from the notochord is still unknown. In the mouse, all the genes so far found that are expressed in the foregut endoderm are also expressed in the notochord, likely due to a common mesendodermal origin during gastrulation (Kinder, Tsang et al. 2001). Recently, expression of *Panza*, a α2-macroglobulin (α2M), was found to be restricted to the dorsal domain of the primitive gut, but not the notochord, in *Xenopus laevis* (Pineda-Salgado, Craig et al. 2005). α2M is an abundant serum protein in vertebrates and arthropods with diverse functions, including inhibition of protease activity and binding of growth factors, cytokines, and disease factors (Borth 1992). It will be interesting to determine whether the mammalian counterpart is also selectively expressed in the endoderm. If so, this will provide some insight into how the transcriptional regulatory mechanism permits a foregut endoderm specific lineage expression.

The role of Bmp receptors in tracheal morphogenesis

Our study of conditional *Bmp4*-deficient foregut elucidates an essential role of Bmp signaling in tracheal outgrowth. There are three type I receptors, (BMPR-1A/Alk3,

BMPR-1B/Alk6 and ActR-I/Alk2), that bind and transduce signaling of Bmps. It is intriguing which type I receptor mediates Bmp signaling in tracheal outgrowth. While *Alk6* normally is not highly expressed in the anterior foregut, *Alk3* and *Alk2* are expressed in the developing primitive foregut (Yoshikawa, Aota et al. 2000, and Y.L and C.C unpublished observation). Mice with targeted mutation of *Alk6* are viable (Liu, Wilson et al. 2003), whereas those with mutations in *Alk2* and *Alk3* die before E9.5, exhibiting profound disruption in early embryonic development (Mishina, Suzuki et al. 1995; Mishina, Crombie et al. 1999). Taken together, it suggests that Bmp4 signaling in the ventral foregut is likely mediated via *Alk3* or *Alk2* or both. To decipher which receptor is involved in the Bmp4-mediated tracheal outgrowth, we could conditionally ablate *Alk2* and *Alk3* in the foregut region with the same strategy as for the Bmp4 conditional ablation by *Foxg1Cre*. Homozygous mice for $Alk3^{flox/flox}$ and $Alk2^{flox/flox}$ have been generated, and are viable with no discernable phenotype (Kaartinen and Nagy 2001; Mishina, Hanks et al. 2002). Prior to obtaining *Foxg1Cr*e transgene, I attempted to address this question by ablating *Alk3* or *Alk2* with *ShhCre* transgene. *Shh* expression is normally found in the ventral foregut endoderm (Litingtung, Lei et al. 1998; Pepicelli, Lewis et al. 1998); therefore, *ShhCre* will specifically delete receptors in the endoderm. The resulting conditional mutant foreguts revealed fairly normal formation of the esophagus and trachea, suggesting that deleting either receptor alone is not sufficient or endodermal Bmp4 signaling per se is not critical for tracheal outgrowth. To distinguish these two possibilities, we need to generate conditional mutants deficient for both

receptors by *ShhCre*. The comparison of mutants generated by *Foxg1Cre* and *ShhCre* will also provide us with new insights into whether paracrine (mesenchymal Bmp signaling to the endoderm) or autocrine (mesenchymal Bmp signaling to mesenchyme, which in turn affects the endoderm) or both is critical for tracheal morphogenesis, as *Foxg1Cre* deletes receptors in both layers whereas *ShhCre* only deletes receptors in the endoderm.

Specification of the tracheal and esophageal primordium

The *Bmp4*^{cko} foregut that we have generated is so far the only mutant that exhibit complete loss of the trachea. Our analysis of this mutant foregut suggests that Bmp signaling is likely not required for the initial tracheal specification but rather the subsequent growth of the respiratory primordium, thus implying that other still unidentified signal(s) is required for tracheal specification. In addition to questions regarding specification of the trachea, it is also not clear how foregut cells adopt the esophageal fate and what signals are involved. A major limitation is the lack of markers specific for the trachea or esophagus. Laser capture microdissection is a recently developed method for procuring pure cells from specific microscopic regions of tissue sections, which may be a tool to enable us to identify specific markers for the esophagus and trachea. We could extract tracheal and esophageal primordia from foregut tissue sections by performing laser capture microdissection and compare their mRNA expression profiles. Genes that are differentially expressed may be useful as tracheal/esophageal specific markers. Armed with these newly identified markers, we

could carry out definitive experiments to uncover signals that are important for anterior foregut patterning.

CHAPTER V

SONIC HEDGEHOG SIGNALING REGULATES GLI3 PROCESSING, MESENCHYMAL PROLIFERATION, AND DIFFERENTIATION DURING MOUSE LUNG MORPHOGENESIS

Introduction

Lung development involves a highly orchestrated series of growth and morphogenetic events, precisely regulated by complex interactions among signaling molecules and transcription factors (Whitsett 1998; Hogan 1999; Perl and Whitsett 1999; van Tuyl and Post 2000; Warburton, Schwarz et al. 2000; Cardoso 2001; Costa, Kalinichenko et al. 2001). Reports of lung abnormalities, both in humans and from mouse models, due to genetic aberrations, diseases and environmental factors abound in the literature. In severe cases, lung hypoplasia has also been shown concurrently with congenital diaphragmatic hernia (CDH) in humans, with an incidence of 1 in 2500 newborns (Causak, Zgleszewski et al. 1998; Zhang, Zgleszewski et al. 1998; Chinoy, Chi et al. 2001; Chinoy 2003; Unger, Copland et al. 2003).

The mammalian *Gli* gene family consists of three members, *Gli1*, *Gli2* and *Gli3* (Kinzler, Ruppert et al. 1988; Ruppert, Kinzler et al. 1988; Hui, Slusarski et al. 1994), which encode zinc finger transcription factors involved in both developmental regulation and human diseases (Vortkamp, Gessler et al. 1991; Kang, Graham et al. 1997; Wild, Kalff-Suske et al. 1997; Ming, Roessler et al. 1998; Villavicencio, Walterhouse et al.

2000). All three *Gli* genes are expressed in the lung mesenchyme during the pseudoglandular stage of development (Grindley, Bellusci et al. 1997) and mutations in the *Gli* genes give rise to various lung and foregut defects (van Tuyl and Post 2000). While *Gli1* is dispensable for lung development in the presence of other *Gli* genes (Park, Bai et al. 2000), *Gli2*$^{-/-}$ mutant lung exhibits right lobe hypoplasia, narrowing of the esophagus and trachea (Motoyama, Liu et al. 1998) and *Gli3*^{XtJ} mutant lung, with an intragenic deletion of *Gli3* (Vortkamp, Franz et al. 1992; Hui and Joyner 1993), shows an overall growth defect with a pronounced length reduction of the left lobe (Grindley, Bellusci et al. 1997). Compound mutants such as *Gli2* and *Gli3* null mice are severely defective in upper foregut structures lacking lung, trachea and esophagus. *Gli2*$^{-/-}$;*Gli3*$^{+/-}$ foregut displays tracheoesophageal fistula (TEF) and severe lung growth and lobation defects (Motoyama, Liu et al. 1998). Likewise, *Gli1* and *Gli2* compound homozygous mutants show severe lung defects (Park, Bai et al. 2000). These findings point to the critical role of the *Gli* genes in the development of foregut structures.

Shh is one among several important factors, derived from the lung endoderm, that is required for proliferation, differentiation and patterning of the mesenchyme and *Shh* null mice exhibit foregut anomalies including hypoplastic lungs due to defects in branching morphogenesis (Bellusci, Furuta et al. 1997; Litingtung, Lei et al. 1998; Pepicelli, Lewis et al. 1998). Shh signaling has been implicated in the regulation of *Gli* genes (Ruiz 1999), notably *Gli1* and *Gli3* transcription in the lung (Litingtung, Lei et al. 1998; Pepicelli, Lewis et al. 1998). *Gli2* has also been implicated in the regulation of

Ptch1 and *Gli1* (Motoyama, Liu et al. 1998), components of the Shh signaling cascade in the lung, although *Gli2* expression in the *Shh*$^{-/-}$ mutant lung mesenchyme is unaffected (Pepicelli, Lewis et al. 1998). It is possible that Gli2 activator function may be compromised in the absence of Shh signaling (Sasaki, Nishizaki et al. 1999; Mill, Mo et al. 2003). Shh signaling has also been shown to be activated in small cell lung cancer (SCLC) cell lines and cyclopamine, a hedgehog signaling antagonist, was shown to inhibit SCLC tumorigenicity (Watkins, Berman et al. 2003).

Gli3 is a bipotential transcription factor (Motoyama, Liu et al. 1998; Dai, Akimaru et al. 1999; Sasaki, Nishizaki et al. 1999; Dai, Shinagawa et al. 2002) and it has been shown the repressor form of Gli3 (Gli3R), generated as a result of proteolytic cleavage and lacking amino acids C-terminal to the zinc finger domain, is activated in the absence of Shh signaling in the developing limbs (Wang, Fallon et al. 2000; Litingtung, Dahn et al. 2002). Gli3R has been implicated in the regulation of growth and patterning of the ventral spinal cord (Litingtung and Chiang 2000; Persson, Stamataki et al. 2002; Wijgerde, McMahon et al. 2002) and limb (Litingtung, Dahn et al. 2002; te Welscher, Zuniga et al. 2002). It appears that while abrogating Shh function alone results in serious developmental defects, absence of the Shh signal combined with a lack of Gli3 function can result in an apparently less severe phenotype.

The effect of Shh signaling on Gli3 processing has been examined mainly in tissues known to be exposed to a long-range Shh gradient. However, it is not clear

whether Shh similarly regulates Gli3 processing in the lung. Furthermore, to what extent Shh-regulated Gli3 processing plays a role in lung development has not been addressed. Our findings shed light on the important role of Shh signaling on Gli3 processing and its role in proliferation and differentiation during lung growth and patterning, by directly or indirectly regulating the expression of critical developmental genes.

Material and Methods

Embryos

The generation and identification of *Shh* and *Gli3* mutant embryos and mice were performed as previously described (Litingtung and Chiang 2000).

Lung organ culture and Western blotting

The lung culture method used (Litingtung, Lei et al. 1998), production of amino-terminal-specific Gli3 (Gli3-N) antibody and Western analysis were performed essentially as previously described (Litingtung, Dahn et al. 2002). E11.5 wildtype (WT) lungs were cultured with cyclopamine (gift of W. Gaffield) in serum-free culture medium at a final concentration of 4 μg/ml for 24 hours, after which lung lysates were collected and resolved on 7.5% SDS-polyacrylamide gel, loading 150 μg total protein per lane. Lung lysates were also prepared from freshly dissected E12.5 WT and $Shh^{-/-}$ lungs and analysed by Western blotting with antibodies against Gli3-N, Cyclin D1 (BD Pharmingen, 1:250 dilution) or Cyclin E (Santa Cruz, 1:500 dilution).

Analysis of cell proliferation

5-bromodeoxyuridine (BrdU) *in vivo* labeling and detection were performed as previously described (Litingtung, Lei et al. 1998) (also see Chapter II). Cells in five different photomicrographs representing random portions of the WT, $Shh^{-/-}$ or $Shh^{-/-}$;$Gli3^{-/-}$ lungs were counted. The total number of epithelial cells counted were 1363, 1915 and

1900 and the total mesenchymal cells counted were 3911, 2734 and 3126, in WT, *Shh*$^{-/-}$ and *Shh*$^{-/-}$*;Gli3*$^{-/-}$, respectively. Statistic analysis was performed as described in Chapter III.

In situ hybridization

Whole-mount and cryosection *in situ* hybridizations were performed as previously described (Litingtung, Lei et al. 1998). The following cDNAs were used as templates for synthesizing digoxygenin-labeled riboprobes: *Ptch1* (Goodrich, Johnson et al. 1996), *Gli1* (Hui, Slusarski et al. 1994), *Wnt2* (Huguet, McMahon et al. 1994), *Foxf1* (Kalinichenko, Lim et al. 2001), *Tbx2*, *Tbx3*, *Tbx4*, *Tbx5* (Chapman, Garvey et al. 1996), c-*myc* and N-*myc* (Serra and Moses 1995).

Immunohistochemistry

Whole-mount staining was performed on E12.5 and E13.5 embryos using anti-Hnf-3β antibody (kindly provided by B. Hogan) as described (Litingtung, Lei et al. 1998). Labelings using antibodies against Cyclins D1, D2 and D3 were performed on 5μm tissue sections from paraffin-embedded embryos fixed in 4% paraformaldehyde overnight at 4°C. Paraffin sections were deparaffinized and rehydrated according to standard protocols. Endogenous peroxidase activity was blocked using 3% H_2O_2 in methanol for 10 minutes at room temperature. To reveal Cyclins D1, D2 and D3, sections were antigen-retrieved

using the DAKO target retrieval solution (pH 6.1), following DAKO's suggested protocol using a Black & Decker Handy Steamer. The antibodies used were: mouse anti-human Cyclin D1 (BD Pharmingen, 1:100 dilution); Cyclin D2 (Santa Cruz, 1:200 dilution); Cyclin D3 (Neomarkers, 1:200 dilution). For signal enhancement, a goat anti-mouse IgG-HRP or goat anti-rabbit IgG-AP polymer conjugated secondary antibody from ZYMED Picture-Double staining kit was used, following the company's suggested protocol. For studies on differentiation, E15.5 cryosections collected from embryos fixed in 4% paraformaldehyde for 4 hours at $4^{o}C$ were used for immunolabelings: sections were blocked in 10% goat serum in PBS containing 0.1% triton-X 100 at room temperature for 1 hour to reduce non-specific staining, followed by an overnight incubation at $4^{o}C$ with the following primary antibodies: rat anti-mouse PECAM-1/CD31 (BD Pharmingen, clone MEC 13.3, 1:100 dilution); rat anti-Flk-1 (BD Pharmingen, 1:50 dilution); mouse anti-Smooth Muscle Alpha-Actin (SMA) (Sigma, clone 1A4, 1:300 dilution); rabbit anti-Smooth Muscle Myosin II Heavy Chain (SMM) (BioMedical Technologies, 1:150 dilution). Sections were washed with several rinses of PBS containing 0.1% Tween-20 (Sigma). Alexa 488 (green)- or Alexa 568 (red)-conjugated secondary antibodies (Molecular Probes) were applied at 1:600 dilutions for 1 hour at room temperature.

RNA extraction, reverse transcription and Real-Time PCR

Total RNA was extracted from E12.5 WT and *Shh* $^{-/-}$ lungs using the RNeasy Mini

kit (Qiagen). cDNA was synthesized from 1 μg of total RNA with 4 units of Omniscript reverse transcriptase (RT) (Qiagen) in 20 μl, using 0.5 μg random hexamer primers (Invitrogen) according to the manufacturer's instructions. PCR was performed using 20 μl of a 1:10 dilution of a specific cDNA to confirm a single product with the desired length. Real-time PCR was performed in the iCycler Iq detection system (Bio-Rad): each reaction contained 25 μl of the 2X Quantitect SYBR Green (Qiagen) PCR Master Mix, 3 μl forward primer-f (5 μM), 3 ul reverse primer-r (5 μM), 5 μl of a 1:10 dilution of a specific wildtype or *Shh*$^{-/-}$ cDNA and 14 μl H_2O. PCR conditions: enzyme activation program (95°C for 15 min), amplification and quantification program repeated 45 times (94°C for 15 s, 58°C for 30 s, 72°C for 30 s) and melting curve program (55-95°C with a heating rate of 0.025°C/s). PCR primers, spanning two exons, are listed below followed by PCR product size (bp):

GAPDH:(f)5′-TTCACCACCATGGAGAAGGC-3′;

(r)5′-GGCATGGACTGTGGTCATGA-3′; 236.

Wnt2b: (f)5′-CACCCGGACTGATCTTGTCT3′;

(r)5′-GCCACAACACATGATTTCACA3′;142.

Wnt5a: (f)5′-AATCCACGCTAAGGGTTCCT-3′;

(r)5′-GAGCCAGACACTCCATGACA-3′;128.

Wnt2: (f)5-′GCAACACCCTGGACAGAGAT-3′;

(r)5′-ACAACGCCAGCTGAAGAGAT-3′;103.

Results and Discussion

Shh$^{-/-}$;*Gli3*$^{-/-}$ lung exhibits increased growth compared with *Shh*$^{-/-}$ lung

Gross morphological analyses of E12.5, E13.5 *Shh*$^{-/-}$;*Gli3*$^{-/-}$ double mutant lungs (Figure 5.1) by whole-mount immunolabeling with an antibody against Hnf-3β, an endodermal marker (Yasui, Sasaki et al. 1997), and E15.5 *Shh*$^{-/-}$;*Gli3*$^{-/-}$ lung sections by hematoxylin and eosin (H&E) staining (Figure 5.1), reveal that the *Shh*$^{-/-}$;*Gli3*$^{-/-}$ lungs show increased growth compared with age-matched *Shh*$^{-/-}$ lungs but patterning defects persist (Figure 5.1, 5.5, 5.6). There appears to be more epithelial buds with smaller lumens and a denser mesenchyme as shown in the E15.5 H&E-stained *Shh*$^{-/-}$; *Gli3*$^{-/-}$ sections than in E15.5 *Shh*$^{-/-}$ sections (Figure 5.1 g-i). Our finding that absence of Gli3 function in *Shh*$^{-/-}$;*Gli3*$^{-/-}$ lungs yields a mutant lung with enhanced growth potential compared with the *Shh*$^{-/-}$ lungs, demonstrates the interplay between Shh and Gli3 functions is conserved in the lung as in the limb and ventral neural tube. Albeit, the partial rescue in growth with persistent patterning defects in *Shh*$^{-/-}$;*Gli3*$^{-/-}$ lung (Figure 5.1, 5.5, 5.6) suggests there is a strict requirement for Shh (Litingtung, Lei et al. 1998; Pepicelli, Lewis et al. 1998) and Gli3 (Grindley, Bellusci et al. 1997; Motoyama, Liu et al. 1998) functions during lung development. Based on previous observations in the neural tube (Litingtung and Chiang 2000) and limb (Litingtung, Dahn et al. 2002)((te Welscher, Zuniga et al. 2002), it is postulated that the repressor form of Gli3 (Gli3R), which is generated at a higher level in the absence of Shh signaling, may contribute to growth

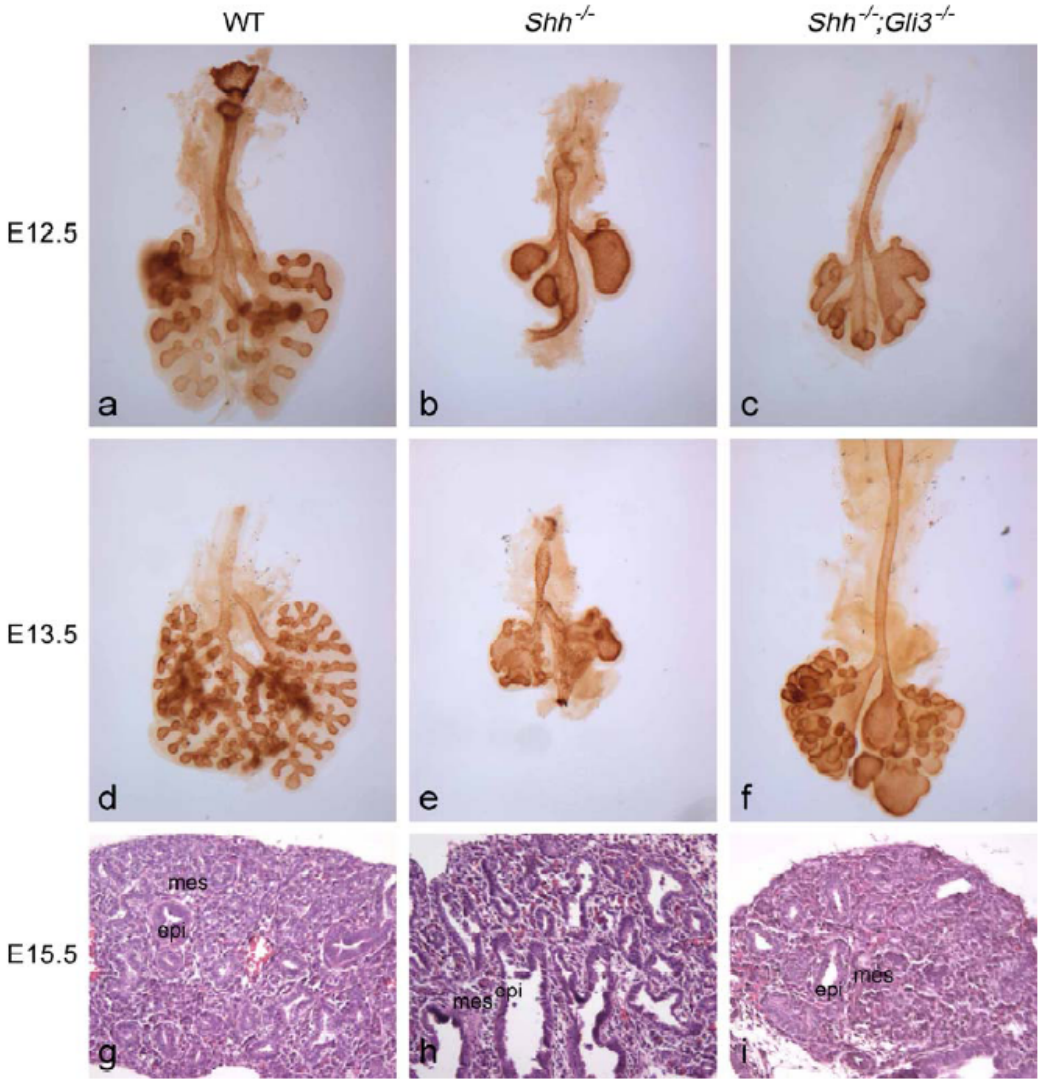

Figure 5.1 Morphology of *Shh*$^{-/-}$;*Gli3*$^{-/-}$ lung compared with *Shh*$^{-/-}$ and WT lungs. Foxa2 immunostaining of WT, *Shh*$^{-/-}$, and *Shh*$^{-/-}$;*Gli3*$^{-/-}$ E12.5 (a–c) and E13.5 (d–f) lungs, showing less severe hypoplasia of the *Shh*$^{-/-}$;*Gli3*$^{-/-}$ lungs (c,f) compared with *Shh*$^{-/-}$ (b,e) lungs. Hematoxylin and eosin staining of E15.5 WT, *Shh*$^{-/-}$, and *Shh*$^{-/-}$;*Gli3*$^{-/-}$ lung tissue sections (g–i). There appears to be more epithelial (epi) buds (c,f,i) with smaller lumen (i) and a more compact mesenchyme (mes) (i) in *Shh*$^{-/-}$;*Gli3*$^{-/-}$ compared with *Shh*$^{-/-}$ lungs (b,e,h). Magnification 400X for panels a–f and 200Xfor panels g–i.

suppression. Hence, one interpretation is that removing Gli3R, essentially by deleting *Gli3*, could enhance the growth potential of the *Shh*$^{-/-}$ lung, as has been observed in other organ systems, emphasizing the conserved role of Gli3R in growth regulation. Shh signaling, based on *Gli1* and *Ptch1* expressions, is not restored in the *Shh*$^{-/-}$;*Gli3*$^{-/-}$ double mutant lung (Figure 5.6 c,f). This initial finding suggests while lack of Shh signaling leads to severe lung hypoplasia, genetically deleting *Gli3* from the *Shh*$^{-/-}$ lung, hence abrogating Gli3R function, appears to have a positive effect on the overall growth of the resulting *Shh*$^{-/-}$; *Gli3*$^{-/-}$ double mutant lung.

Gli3R level is higher in *Shh*$^{-/-}$ lung *in vivo* and in wildtype cyclopamine-treated lung in culture

By Western analysis of freshly dissected E12.5 WT and *Shh*$^{-/-}$ lungs, we show that *Shh*$^{-/-}$ lungs exhibit higher levels of Gli3R compared with wildtype, with a concomitant decrease in the level of full length Gli3 (Gli3-190) (Figure 5.2A, lanes 1 and 2). The observation that a low level of Gli3R is normally present in wildtype lungs (Figure 5.2A, lane 2) suggests that the relative balance of Gli3R and full-length Gli3 may be important for normal lung development. This result is consistent with *in vivo* findings in the limb whereby a gradient of Gli3 processing exists across the limb bud, with the highest level of Gli3R in the anterior domain, furthest from the source of Shh which emanates from the posterior margin (Wang, Fallon et al. 2000; Litingtung, Dahn et al. 2002). Cyclopamine, a plant-derived steroidal alkaloid, has been shown in several studies to downregulate Shh

signaling (Cooper, Porter et al. 1998; Incardona, Gaffield et al. 1998; Chiang, Swan et al. 1999), by direct binding to Smoothened (Smo) (Chen, Taipale et al. 2002), a receptor that mediates Hedgehog signaling. Here, we show that cyclopamine treatment of E11.5 wildtype mouse lungs results in dissociation of mesenchymal cells from the epithelium (Figure 5.2B-b, arrows) and elevated levels of Gli3R (Figure 5.2C, compare lanes 1 and 2), consistent with the *in vivo* finding that *Shh*$^{-/-}$ lung contains higher levels of Gli3R (Figure 5.2A, lane 1), suggesting blockade in Shh signaling promotes Gli3 processing in the developing lung. As a control for the different species of Gli3 observed, we loaded protein lysates from *Gli3*$^{-/-}$ embryos which, as expected, did not show Gli3-specific protein bands (Figure 5.2A, lane 3).

Shh$^{-/-}$;*Gli3*$^{-/-}$ mesenchyme shows increased proliferation *in vivo*

To further investigate the increase in growth potential of the *Shh*$^{-/-}$;*Gli3*$^{-/-}$ lung compared with *Shh*$^{-/-}$ lung (Figure 5.1), we determined the proliferative capacity of WT and mutant lungs by *in vivo* labeling with bromodeoxyuridine (BrdU), a nucleotide analog that is incorporated into replicating DNA. BrdU pulse-labeling revealed a relatively higher percentage of proliferating mesenchymal cells in the *Shh*$^{-/-}$;*Gli3*$^{-/-}$ lung (43.9%) compared with the *Shh*$^{-/-}$ mutant (35.8%) (Figure 5.3), suggesting the increased Gli3R level in the *Shh*$^{-/-}$ lung mesenchyme (Figure 5.2A, lane 1) contributes, at least in part, to its lower proliferative capacity. The *Shh*$^{-/-}$;*Gli3*$^{-/-}$ lung epithelium also displayed a higher proliferative capacity (51.3%) compared with the *Shh*$^{-/-}$ epithelium (47.7%)

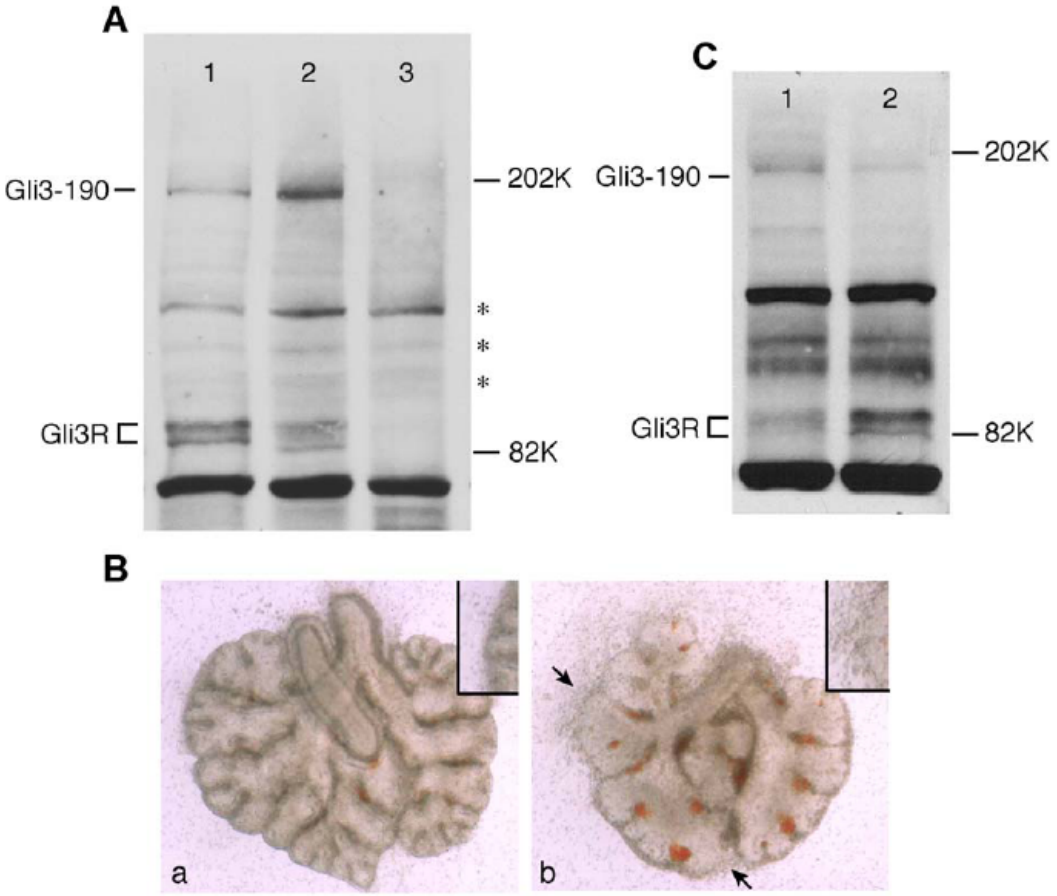

Figure 5.2 Shh signaling regulates Gli3 processing in the mouse lung.
(A) Protein extracts from freshly dissected E12.5 WT lungs (lane 2), *Shh*$^{-/-}$ lungs (lane 1), and *Gli3*$^{-/-}$ embryos (lane 3) were immunoblotted and probed with Gli3-specific antibody recognizing a prominent 190K band and several 83K to 86K bands, corresponding to full-length (Gli3-190) and processed repressor forms (Gli3R) of Gli3, respectively. Note *Shh*$^{-/-}$ lungs (lane 1) contain a higher level of Gli3R, with a corresponding reduction in Gli3-190, relative to WT lungs (lane 2). The Gli3 antibody recognizes several nonspecific proteins (asterisks). *Gli3*$^{-/-}$ embryo extracts were used as a control for the absence of Gli3-specific bands. (B) E11.5 WT lungs were treated with cyclopamine, a Shh signaling antagonist, at a final concentration of 4 µg/ml in serum-free lung medium for 48 h. The cyclopamine-treated lung (b) shows less epithelial branching and loosening of the mesenchymal tissue (arrows and inset) compared with control lung with no cyclopamine (a). Magnification 500X for a,b. (C) Protein extracts from E11.5 WT lungs, untreated (lane 1) or treated (lane 2) with cyclopamine, as described above, and cultured for 30 h, were immunoblotted and probed with Gli3-specific antibody.

(Figure 5.3). Gli3R has been shown to preferentially accumulate in the nucleus of expressing cells (Dai, Akimaru et al. 1999; Wang, Fallon et al. 2000), hence, it is anticipated that Gli3R could exert its effects by affecting the transcription of target genes related to growth and differentiation.

Cyclin D1 level appears downregulated in *Shh*$^{-/-}$ and derepressed in *Shh*$^{-/-}$;*Gli3*$^{-/-}$ lungs while Cyclins D2, D3 and *myc* levels remain unaltered

The Shh signaling pathway has been implicated in the regulation of pro-proliferative genes such as *myc* and *Cyclins* but whether their expressions are affected in the *Shh*$^{-/-}$ lung, and whether Gli3R plays a role, have not been documented. Cyclins and cyclin-dependent kinases (CDKs) are evolutionarily conserved proteins that are essential for cell cycle control in eukaryotes. Cyclin-CDK holoenzyme complexes such as Cyclin D-CDK4/6 and Cyclin E/CDK2 regulate G1/S cell cycle transitions. The activities of CDKs are also negatively regulated by specific CDK inhibitors (Sherr 1993; Nurse 1994; Sherr and Roberts 1999) (Miller and Cross 2001) ((Ekholm and Reed 2000). Numerous reports implicate Shh signaling in cell cycle regulation: the mitogenic effect of Shh during hair follicle development was found to be mediated by Gli2 activator which functions to upregulate Cyclins D1 and D2 (Mill, Mo et al. 2003); Shh opposes epithelial cell cycle arrest and promotes epidermal hyperplasia (Fan and Khavari 1999); N-*myc* and *Cyclins* D1 and D2 were found to be upregulated by Shh signaling in the proliferation of cerebellar granule neuron precursors in culture (Kenney and Rowitch 2000; Ciemerych,

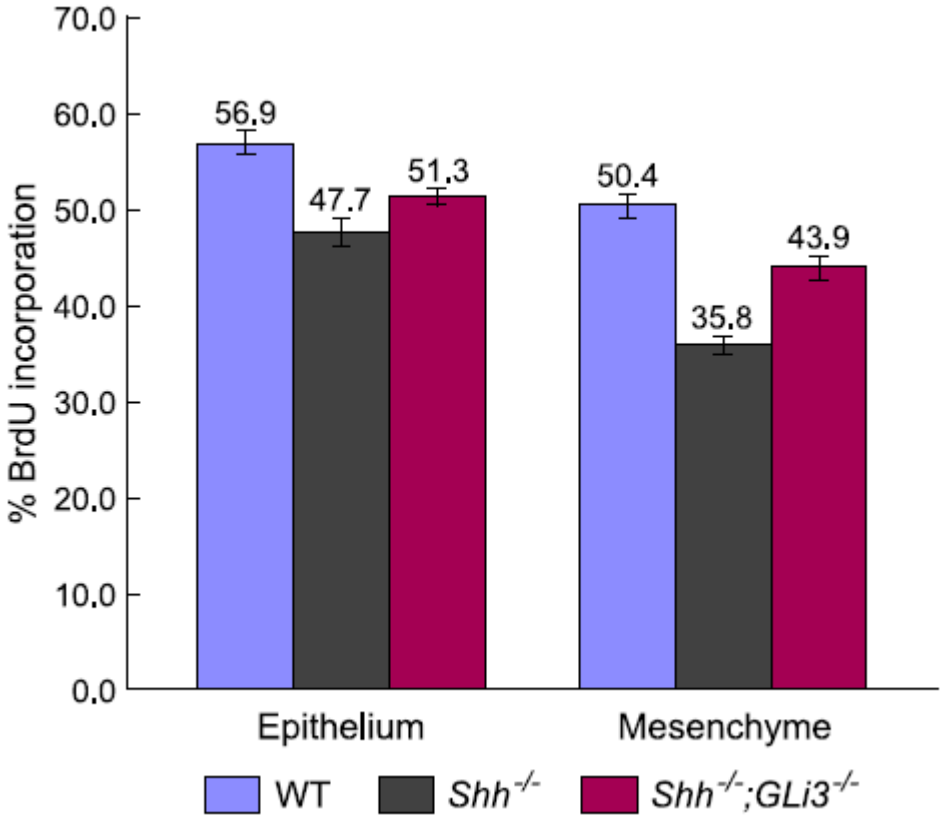

Figure5.3 *Shh*$^{-/-}$;*Gli3*$^{-/-}$ lung displays more cells at S phase compared with *Shh*$^{-/-}$ by *in vivo* BrdU pulse-labeling.
Histogram showing the percentage of BrdU-labeled cells in the epithelium and mesenchyme of E13.5 *Shh*$^{-/-}$;*Gli3*$^{-/-}$ lungs compared with *Shh*$^{-/-}$ and WT control.

Kenney et al. 2002; Kenney, Cole et al. 2003); Cyclopamine has been shown to block proliferation and downregulate *myc* and *Cyclins* D1, D2, E1 expression in a murine medulloblastoma cell line, implicating Shh signaling in regulating the expression of these genes, either directly or indirectly (Berman, Karhadkar et al. 2002); *Cyclin* D2 was identified as a target gene in Gli1-induced cellular transformation (Yoon, Kita et al. 2002) and overexpressing Shh in the developing lung leads to enhanced epithelial and mesenchymal cell proliferation (Bellusci, Furuta et al. 1997). The function of another mammalian hedgehog protein, Indian hedgehog (Ihh), has also been linked to chondrocyte proliferation during endochondral skeleton development and Cyclin D1 upregulation (Long, Zhang et al. 2001). Moreover, *Drosophila* Hedgehog (Hh) has been implicated in the control of cell growth and proliferation during eye development, by promoting the transcription of Cyclins D and E (Duman-Scheel, Weng et al. 2002).

The E-type cyclins partner with CDK2 and function during progression of mammalian cells through the G1/S phase. They show high expression patterns in many tissues such as the brain and lung during periods of active proliferation in the developing mouse embryo (Geng, Yu et al. 2001). Cyclin E level does not appear to be altered in *Shh*$^{-/-}$ lung compared with WT (Figure 5.4B); however, since the Western analysis represents overall expression of Cyclin E in whole lungs, we cannot rule out the possibility that Cyclin E may be expressed at lower levels in the wildtype lung mesenchyme compared with the epithelium, therefore, its decreased expression in *Shh*$^{-/-}$ lung mesenchyme could be masked by a higher unaltered level of Cyclin E expression in

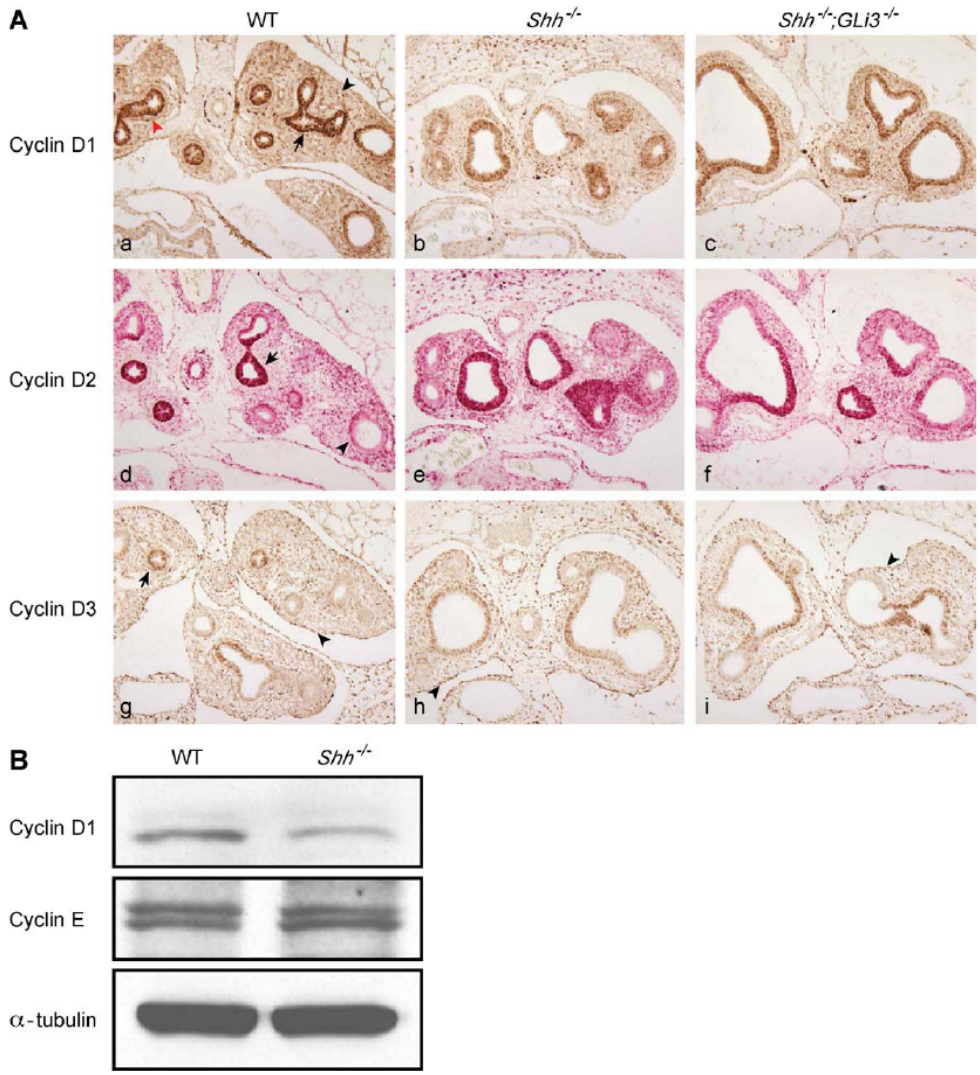

Figure 5.4 Expression of cyclin E and D-type cyclins in WT and mutant lungs. (A) Immunohistochemical labeling of E13.5 WT, *Shh*$^{-/-}$, and *Shh*$^{-/-}$;*Gli3*$^{-/-}$ lungs with Cyclin D1 (a–c), D2 (d–f), or D3 (g–i) antibodies. Cyclin D1 is expressed in both the epithelial (arrow) and mesenchymal (arrowheads) compartments of the developing lung. The bronchial smooth muscle is indicated by a red arrowhead. Expression of Cyclin D1 in the epithelium (epi) is higher than in the mesenchyme (mes). Expression of Cyclin D1 in *Shh*$^{-/-}$ lung is clearly downregulated in both epi and mes compartments and appears to be enhanced in the *Shh*$^{-/-}$;*Gli3*$^{-/-}$ lung (c), compared with *Shh*$^{-/-}$ lung (b). Cyclins D2 and D3 show higher expressions in the proximal epithelium, lower levels distally and throughout the mesenchyme in all three genotypes. High mesothelial expression of cyclin D3 is also evident (arrowheads in g–i). (B) Western blot analysis of E12.5 WT and *Shh*$^{-/-}$ lungs, probed with antibodies against Cyclins D1 and E, showing downregulation of Cyclin D1 but no significant alteration in Cyclin E expressions in the *Shh*$^{-/-}$ lungcompared to WT lung; α-tubulin was used as a control for loading. Magnification 100X for panel A.

the *Shh*$^{-/-}$ lung epithelium. To resolve this issue, we tested Cyclin E antibodies, from several sources, by immunohistochemistry on cryosections and antigen-retrieved paraffin sections, but failed to obtain positive staining indicating these Cyclin E antibodies were not suitable for tissue sections. In contrast, we found an overall reduction in the expression level of Cyclin D1, required for G1 progression (Quelle, Ashmun et al. 1993), in the E12.5 *Shh*$^{-/-}$ lung compared with WT lung by Western blot (Figure 5.4B). By immunohistochemistry, the decrease in Cyclin D1 expression was found in both the E13.5 *Shh*$^{-/-}$ lung epithelium and mesenchyme (Figure 5.4A-b), compared with WT lung which expresses Cyclin D1 in both epithelium (arrow) and mesenchyme (arrowheads) (Figure 5.4A-a). The expression of Cyclin D1 is strikingly higher in the lung epithelium than the mesenchyme **(**Figure 5.4A-a**)**, consistent with the notion that proliferation is important for expansion of the lung epithelium during branching morphogenesis, although bud outgrowth per se does not appear to require localized cell proliferation (Nogawa, Morita et al. 1998). The bronchial smooth muscle (Figure 5.4A-a, red arrowhead) also shows detectable Cyclin D1 staining. The expression level and distribution of Cyclin D1 appear to be elevated in both the epithelium and mesenchyme of *Shh*$^{-/-}$;*Gli3*$^{-/-}$ lung (Figure 5.4A-c), compared with *Shh*$^{-/-}$ (Figure 5.4A-b). These findings are consistent with the proliferative defects observed in *Shh*$^{-/-}$ lung and partial recovery of epithelial and mesenchymal proliferation in *Shh*$^{-/-}$;*Gli3*$^{-/-}$ (Figure 5.3), implicating Shh signaling, directly or indirectly, in the regulation of Cyclin D1 in the lung, as confirmed by Western analysis (Figure 5.4B). Since *Cyclin* D1 has also been identified

as a key transcriptional target of Wnt-β-catenin signaling (Morin 1999; Shtutman, Zhurinsky et al. 1999; Tetsu and McCormick 1999; Behrens 2000), which is operative during lung development (Tebar, Destree et al. 2001; Shu, Jiang et al. 2002; Mucenski, Wert et al. 2003), it is difficult to discern if alterations in Cyclin D1 expression observed in *Shh*$^{-/-}$ lung (Figure 5.4A-b and Figure 5.4B) are a direct consequence of lack of Shh signaling or indirectly due to aberrant canonical Wnt signaling. Other pathways have also been linked to *Cyclin* D1 transcriptional activation (Hu, Lee et al. 2001; Zhao, Pestell et al. 2001). Moreover, it is likely that the epithelial expression of Cyclin D1 (Figure 5.4A, a-c) is not regulated directly by Shh signaling since its targets, *Ptch1* and *Gli1*, are not normally expressed in the lung epithelium. Hence, it is plausible to suggest that lung epithelial Cyclin D1 expression is under the control of a mesenchymally-derived signal which appears to be affected in the *Shh*$^{-/-}$ but upregulated in the *Shh*$^{-/-}$;*Gli3*$^{-/-}$ lung. The *Drosophila* counterpart of vertebrate Gli proteins, Cubitus interuptus (Ci), which mediates Hh signaling, was shown to bind to the *Cyclin* E promoter in mediating transcriptional activation of the gene. Overexpression of Ci induces G1-arrested cells to progress through S-phase (Duman-Scheel, Weng et al. 2002). Whether Shh signaling directly regulates the expression of *Cyclin* D1, via Gli activation, in the mesenchyme remains to be determined.

We also examined the expression of other D-type cyclins, namely Cyclin D2 and D3 (Figure 5.4A d-f and g-i). Cyclin D2 shows high expression in the E13.5 wildtype lung (Figure 5.4A-d), predominantly in the proximal epithelium (arrow) with lower levels

distally (arrowhead). Cyclin D2 is also expressed throughout the lung mesenchyme (Figure 5.4A-d), but was not observed in the more proximal regions around the bronchial smooth muscles, unlike Cyclin D1. The expression levels of Cyclin D2 in E13.5 *Shh*$^{-/-}$ and *Shh*$^{-/-}$;*Gli3*$^{-/-}$ lungs seem comparable to wildtype and the proximal-distal differential distribution of Cyclin D2 in the epithelium is also maintained (Figure 5.4A-d-f). This finding suggests Shh signaling in the developing lung does not affect Cyclin D2 expression, in contrast to its effect on Cyclin D1 expression. Myc has been shown to activate Cyclin D2 expression (Bouchard, Thieke et al. 1999; Perez-Roger, Kim et al. 1999); likewise, loss of N-*myc* function in mice has been shown to disrupt *Cyclin* D2 expression in the cerebellar primordium (Knoepfler, Cheng et al. 2002). In the mouse fetal lung, N-*myc* expression (Serra, Pelton et al. 1994; Serra and Moses 1995) is restricted to the bronchial epithelium while c-*myc* is expressed exclusively in the mesenchyme (Hirning, Schmid et al. 1991). Both N-*myc* and c-*myc* expression coincide with regions undergoing proliferation (Schmid, Schulz et al. 1989; Hirning, Schmid et al. 1991). We did not observe significant alteration in the levels of N-*myc* or c-*myc* transcripts in E12.5 *Shh*$^{-/-}$ lung compared with WT, by *in situ* hybridization (Figure 5.5), suggesting that *myc* genes do not appear to play a significant role in the *Shh*$^{-/-}$ lung phenotype. This observation correlates with the finding that expression of Cyclin D2 is not altered in the *Shh*$^{-/-}$ lung (Figure 5.4A-e).

Cyclin D3 shows distinct expression at the periphery of the lung (Figure 5.4A-g-i, arrowheads), along the visceral pleura which consists of squamous epithelium also

known as the mesothelium (Colvin, White et al. 2001; Weaver, Batts et al. 2003). Cyclin D3 is also expressed in the epithelium, more proximally like Cyclin D2, and uniformly throughout the mesenchyme of the E13.5 lung (Figure 5.4A-g). Its expression was also detected in the bronchial smooth muscle region lining the bronchial epithelium (Figure 5.4A-g, arrow). The expression and distribution of Cyclin D3 in *Shh*$^{-/-}$ and *Shh*$^{-/-}$;*Gli3*$^{-/-}$ lungs were comparable to WT lungs (Figure 5.4A, g-i), except for a lack of bronchial smooth muscle cells (see Figure 5.9). While all three D-type cyclins show overlapping expression domains, they also display unique expression patterns in the developing lung at E13.5 suggesting some of their functions may be distinct. Findings from previous studies suggest that the D-cyclins are largely exchangeable in most tissues and complete functional ablation of two of the three D-cyclins results in ubiquitous upregulation of the remaining intact cyclin during embryogenesis, apparently via a compensatory feedback loop, the precise mechanism of which has not been unraveled. Hence, Cyclin D2-only mice displayed essentially normal development in most tissues (Ciemerych, Kenney et al. 2002). However, lower levels of one cyclin such as Cyclin D1 in the *Shh*$^{-/-}$ lung (Figure 5.4A-b) may not necessarily trigger the 'compensatory feedback'. By immunohistochemistry, we did not observe compensatory upregulation of Cyclin D2 or D3 in the *Shh*$^{-/-}$ lung (Figure 5.4A-e,h). However, we cannot rule out the possibility that there could be minor changes in Cyclins D2 and D3 expression that cannot be detected by immunolabeling. Hence, the downregulation of Cyclin D1 in *Shh*$^{-/-}$ lung and its relative increase in *Shh*$^{-/-}$;*Gli3*$^{-/-}$ could contribute, at least in part, to the proliferative defect and

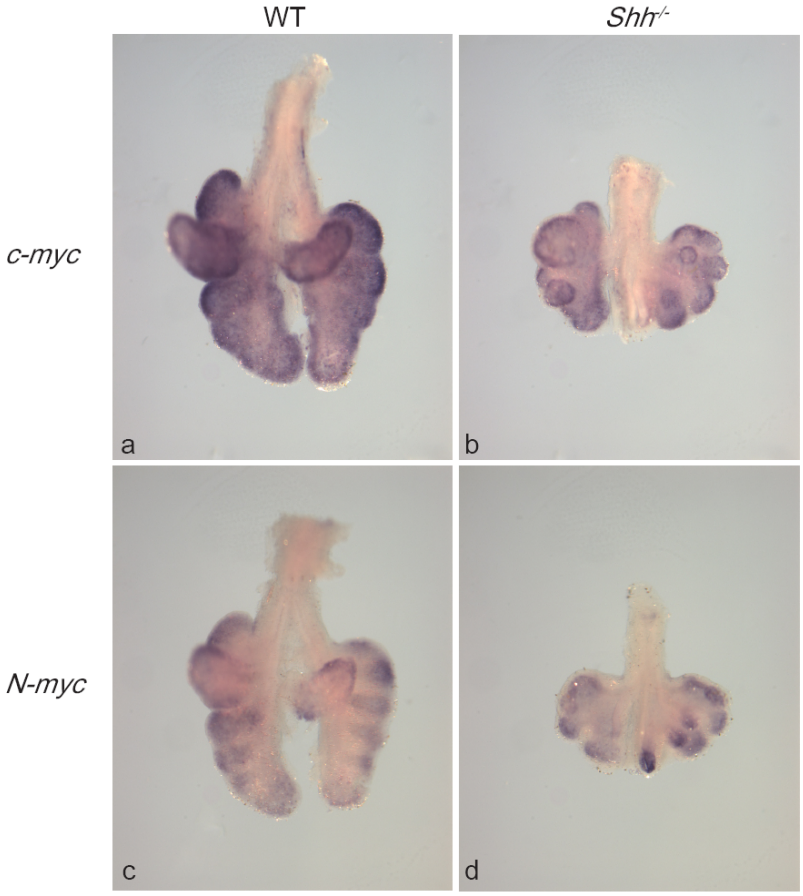

Figure 5.5 *c-myc* and *N-myc* are not altered in *Shh*$^{-/-}$ lungs.
Whole-mount *in situ* hybridization of WT and *Shh*$^{-/-}$ E12.5 lungs probed with *c-myc* (a, b) and *N-myc* (c, d). Magnification: 320X.

partial rescue in these mutant lungs, respectively. Certainly, the role of other cell cycle regulatory factors, such as CDKs, CDK inhibitors and tumor suppressors in the *Shh*$^{-/-}$ lung phenotype awaits further investigation.

Wnt expression is not significantly altered in _Shh_$^{-/-}$ lung, except _Wnt2_, which is partially restored in _Shh_$^{-/-}$;_Gli3_$^{-/-}$

Members of the *Wnt* gene family encode secreted glycoproteins that are involved in cell-cell interactions in tissue patterning and morphogenesis (Moon, Bowerman et al. 2002; van Es, Barker et al. 2003), by activating different intracellular signaling cascades such as the Wnt-β-catenin pathway, upon interaction with the Frizzled family of receptors (Miller and Moon 1996; Yang-Snyder, Miller et al. 1996; Moon, Brown et al. 1997; Hsieh, Rattner et al. 1999; Kalderon 2002). Activation of canonical Wnt pathway results in stabilization of β-catenin and its translocation into the nucleus, where it complexes with HMG box transcription factors TCF/LEF (Galceran, Farinas et al. 1999), to induce transcription of target genes in promoting cell cycle progression (Behrens, von Kries et al. 1996; Morin, Sparks et al. 1997; Eberhart and Argani 2001; Yokota, Nishizawa et al. 2002). Several *Wnt*s are expressed in the developing lung including mesenchymal *Wnt2* (Levay-Young and Navre 1992; Bellusci, Henderson et al. 1996), *Wnt2b* (*Wnt13*) (Zakin, Mazan et al. 1998; Lin, Liu et al. 2001), *Wnt5a* (Li, Xiao et al. 2002) and epithelial *Wnt7b* (Shu, Jiang et al. 2002). There are indications that modulating the Hedgehog

pathway can potentially affect canonical Wnt pathway and vice versa: *Wnt2b* and *Wnt5a* were candidate genes found to be upregulated in basal cell carcinomas with abnormal hedgehog signaling (Bonifas, Pennypacker et al. 2001; Mullor, Dahmane et al. 2001); Glycogen synthase kinase 3 (GSK3), a negative regulator of canonical Wnt signaling (Morin 1999; Kalderon 2002; Wharton 2003), has been shown to antagonize Hh signaling in *Drosophila*, by regulating the proteolysis of Ci (Aza-Blanc and Kornberg 1999), the invertebrate counterpart of Gli and effector of Hh signaling (Jia, Amanai et al. 2002; Price and Kalderon 2002).

Wnt2 expression was found to be dramatically downregulated in *Shh*$^{-/-}$ lungs (Pepicelli, Lewis et al. 1998); however, whether *Shh* induces *Wnt2* expression remains unclear since overexpression of *Shh* in the lung apparently did not result in *Wnt2* upregulation (Bellusci, Furuta et al. 1997). We show that some *Wnt2* expression is restored in the *Shh*$^{-/-}$;*Gli3*$^{-/-}$ (Figure 5.6 g-i), suggesting Gli3R contributes, in part, to *Wnt2* repression in *Shh*$^{-/-}$. We found expressions of *Wnt2b* and *Wnt5a* were not significantly altered in the *Shh*$^{-/-}$ lung by RT-PCR (data not shown) and *Wnt7b* expression in the lung epithelium, which has been shown to regulate lung mesenchymal proliferation (Shu, Jiang et al. 2002), is not altered in *Shh*$^{-/-}$ (Pepicelli, Lewis et al. 1998). Two potential Wnt targets, *Cyclin* D1 and c-*myc*, were examined in this study; while Cyclin D1 is downregulated (Figure 5.4A,b), c-*myc* appears unaltered in *Shh*$^{-/-}$ lung (Figure 5.5-b). Therefore, whether defective canonical Wnt signaling contributes to the hypoplastic *Shh*$^{-/-}$ lung phenotype remains unclear. Although we found that transcripts for several Wnt

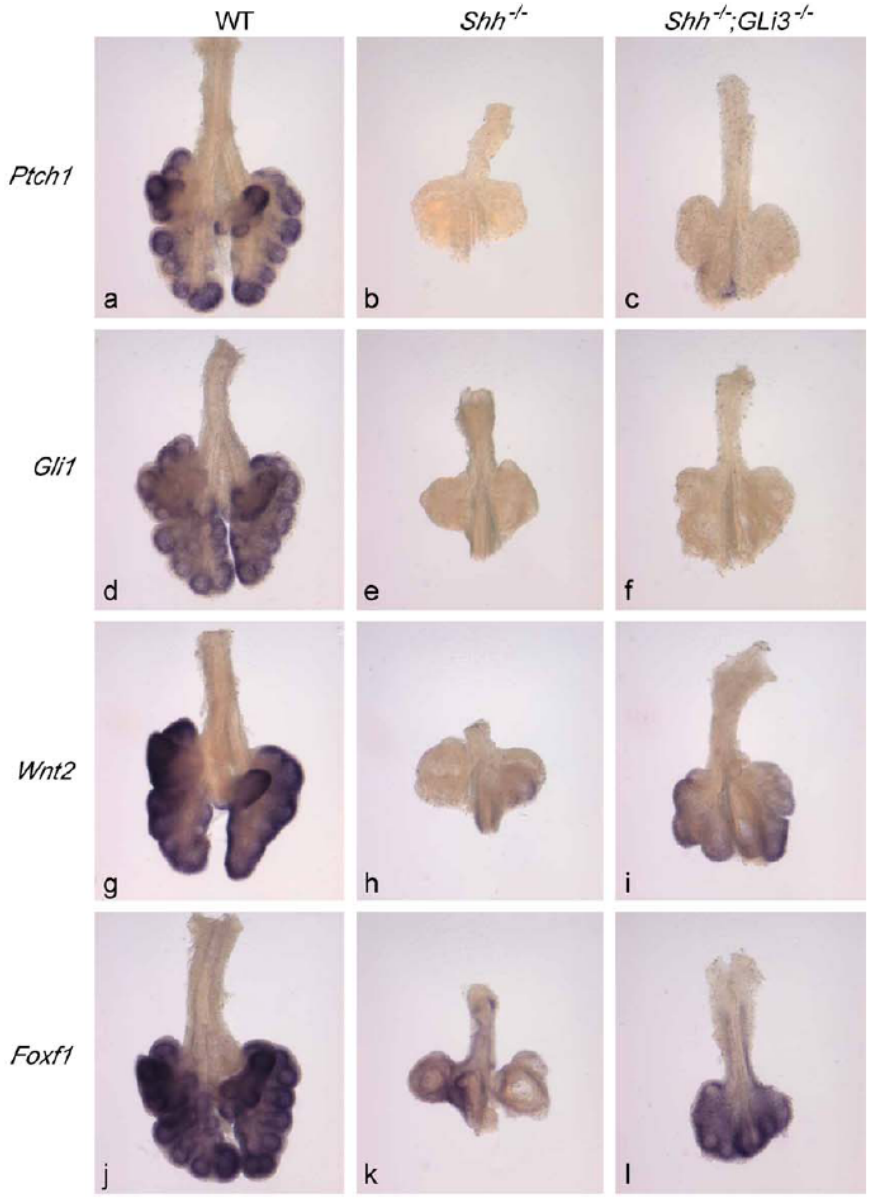

Figure 5.6 Expression of developmentally regulated genes in WT, *Shh*$^{-/-}$, and *Shh*$^{-/-}$;*Gli3*$^{-/-}$ lungs.
Whole-mount *in situ* hybridizations of WT, *Shh*$^{-/-}$, and *Shh*$^{-/-}$;*Gli3*$^{-/-}$ E12.5 lungs probed with *Ptch1* (a–c), *Gli1* (d–f), *Wnt2* (g–i) and *Foxf1* (j–l). As shown in e and f, *Gli1*, a Shh target, remains absent in *Shh*$^{-/-}$;*Gli3*$^{-/-}$, as in *Shh*$^{-/-}$ lungs. *Ptch1* expression appears to be detectable, albeit at very low levels, in the mutant lungs (b and c), compared to WT lungs (a). The expressions of mesenchymal genes *Wnt2* (g–i) and *Foxf1* (j–l) appear to be relatively higher in the *Shh*$^{-/-}$;*Gli3*$^{-/-}$ compared to *Shh*$^{-/-}$ lungs, although not as high as the expression in WT lungs (g,j). Magnification 320X.

ligands are not remarkably altered in *Shh*$^{-/-}$ lung, we ought to be circumspect given the possibility that the expressions or activities of Wnt mediators and signaling components such as the Frizzled family of receptors (Wang, Macke et al. 1996), Wnt antagonists such as secreted frizzled-related protein (sFRP) (Hsieh, Kodjabachian et al. 1999; Tebar, Destree et al. 2001; Heller, Dichmann et al. 2002) or other Wnt signaling effectors such as LEF1 and TCF transcription factors (Kengaku, Capdevila et al. 1998; Schmidt, Tanaka et al. 2000; Tebar, Destree et al. 2001; Kubo, Takeichi et al. 2003) may be altered in the *Shh*$^{-/-}$ lung and remain to be examined.

Gli3R contributes to the repression of *Foxf1* in the *Shh*$^{-/-}$ lung mesenchyme

The murine *Foxf1* gene (also known as *Freac1* or *Hfh8*) (Clevidence, Overdier et al. 1994; Pierrou, Hellqvist et al. 1994; Hellqvist, Mahlapuu et al. 1996) encodes a forkhead or winged helix DNA-binding domain transcription factor. During organogenesis, *Foxf1* is expressed in the splanchnic mesoderm adjacent to the gut endoderm, suggesting its potential involvement in epithelial-mesenchymal interactions (Peterson, Lim et al. 1997; Mahlapuu, Pelto-Huikko et al. 1998; Aitola, Carlsson et al. 2000; Costa, Kalinichenko et al. 2001). Indeed, *Foxf1* is downregulated in *Shh*$^{-/-}$ lung mesenchyme (Figure 5.6-k, E12.5 and Fig5.7-b, E15.5), although its expression in the *Shh*$^{-/-}$ lung has been previously reported absent (Mahlapuu, Enerback et al. 2001). This difference in *Foxf1* expression could be attributed to variations in the length of exposure to the color detection medium after *in situ* hybridization. Nevertheless, our conclusion

that Shh signaling is required for the activation of *Foxf1*, based on its repression in *Shh*$^{-/-}$ lung, agrees with the previous report that *Foxf1* is a target of Shh signaling (Mahlapuu, Enerback et al. 2001).

The present study on *Shh*$^{-/-}$;*Gli3*$^{-/-}$ lung reveals an interesting finding: *Foxf1* is derepressed in *Shh*$^{-/-}$ lung in the absence of *Gli3*, although not to the levels expressed in age-matched WT lung (Figure 5.6-l, E12.5 and Figure 5.7-c, E15.5). This finding suggests *Foxf1* transcriptional activation, in part, depends on Shh signaling and Gli2/3 functions as previously proposed (Mahlapuu, Enerback et al. 2001), but it also implicates Gli3R as a negative regulator of *Foxf1* transcription, emphasizing the critical role of Shh signaling in antagonizing Gli3R activity in the developing lung. Intriguingly, we also observed *Foxf1* expression in E15.5 bronchial epithelium of WT and *Shh*$^{-/-}$ lungs (data not shown). Since *Foxf1*$^{+/-}$ haploinsufficient lungs are hypoplastic (Kalinichenko, Lim et al. 2001; Mahlapuu, Enerback et al. 2001; Lim, Kalinichenko et al. 2002) and a WT level of *Foxf1* is required for normal lung development (Costa, Kalinichenko et al. 2001), we suggest upregulating *Foxf1* expression in the *Shh*$^{-/-}$;*Gli3*$^{-/-}$ lung may contribute, in part, to its increased growth potential compared with *Shh*$^{-/-}$ lung. *Foxf1* has been implicated in growth control since proliferation of the primitive streak mesoderm is reduced in *Foxf1* null embryos (Mahlapuu, Ormestad et al. 2001) and it has been suggested that Foxf1 may mediate the mitogenic effect of Shh in the developing lung (Mahlapuu, Enerback et al. 2001). However, the precise roles and targets of Foxf1 in governing cellular processes such as proliferation and differentiation in the developing lung await further investigation.

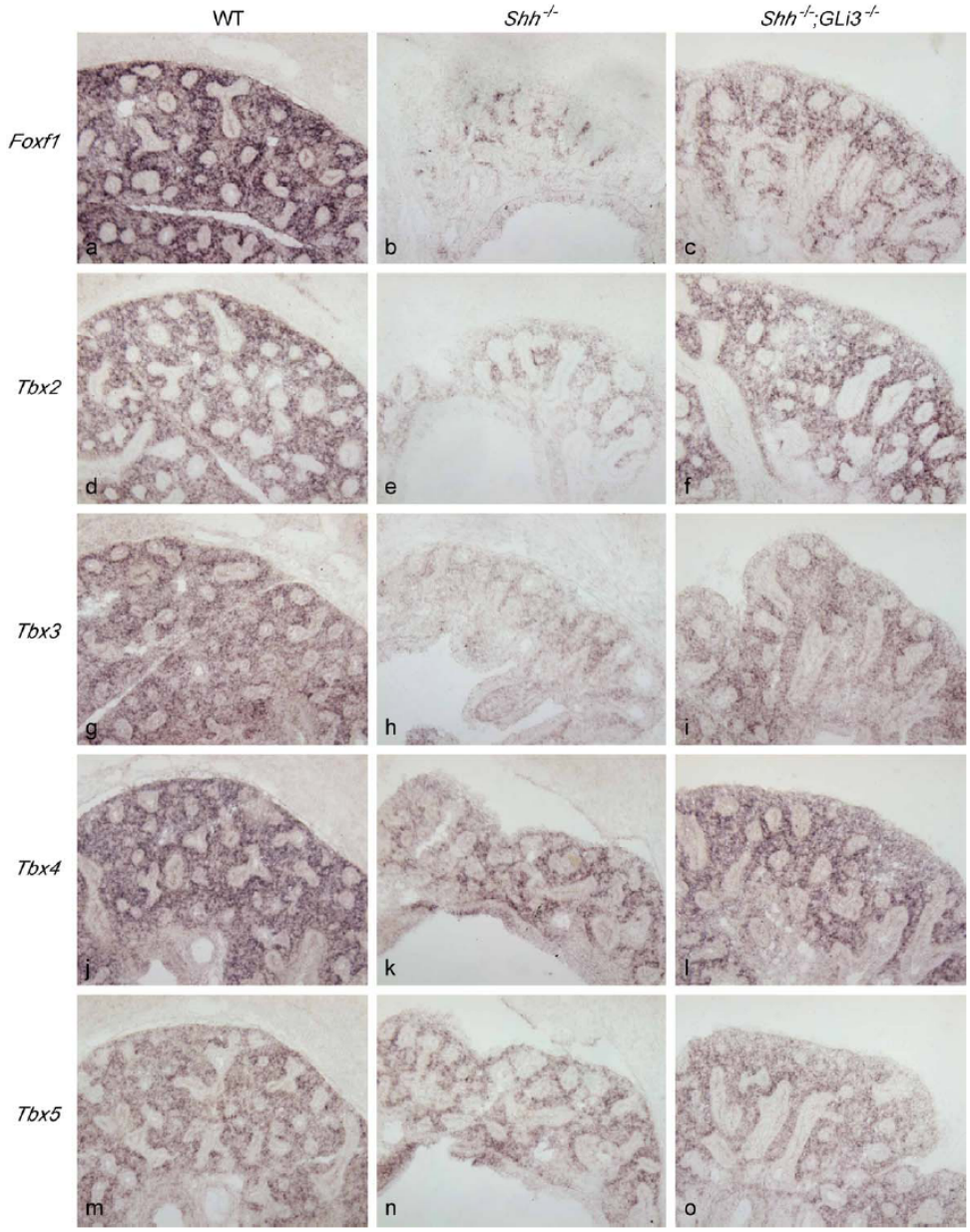

Figure 5.7 Expression of *Foxf1* and *Tbx* genes in WT, *Shh*$^{-/-}$, and *Shh*$^{-/-}$;*Gli3*$^{-/-}$ lungs.

Section *in situ* hybridizations on E15.5 WT, *Shh*$^{-/-}$ and *Shh*$^{-/-}$;*Gli3*$^{-/-}$ lungs with *Foxf1* (a–c), *Tbx2* (d–f), *Tbx3* (g–i), *Tbx4* (j–l), and *Tbx5* (m–o). The levels of *Foxf1*, *Tbx2*, and *Tbx3* transcripts are significantly reduced in *Shh*$^{-/-}$ but relatively higher in *Shh*$^{-/-}$;*Gli3*$^{-/-}$ lungs. *Tbx4* and *Tbx5* transcripts appear only slightly lower in *Shh*$^{-/-}$ lungs. Magnification100X.

Tbx2 and *Tbx3* expression are significantly repressed in *Shh*$^{-/-}$ and derepressed in *Shh*$^{-/-}$;*Gli3*$^{-/-}$ lungs

Based on recent literature, we next directed our efforts to examine the expression of *T-box* genes, which have been implicated as potential Fox targets (Kalinichenko, Lim et al. 2001; Yamagishi, Maeda et al. 2003), in the *Shh* mutant lungs. The T-box family comprises an ever-growing number of genes, now totaling eighteen in mammals (Gibson-Brown 2002). *T-box* genes (Tbx) encode DNA binding transcription factors which regulate the functions of tissues during embryogenesis, in particular, tissues undergoing inductive interactions such as the lung epithelium which expresses *Tbx1* and the mesenchyme which expresses two cognate gene sets: *Tbx2*; *Tbx3* and *Tbx4*; *Tbx5* (Chapman, Garvey et al. 1996; Cebra-Thomas, Bromer et al. 2003). The Tbx factors have been implicated in human birth defects and cancer (Jacobs, Keblusek et al. 2000; Papaioannou 2001; Gibson-Brown 2002); however, the transcriptional regulators and targets of Tbx remain largely unexplored.

By cDNA expression array analysis and RNase protection assay, the Tbx family of transcription factors such as Tbx2, 3, 4 and 5, which like Foxf1, are expressed in the lung mesenchyme (Chapman, Garvey et al. 1996), were found to be diminished in *Foxf1*$^{+/-}$ mutant background (Kalinichenko, Lim et al. 2001), implicating the potential role of Foxf1 in the transcriptional regulation of *Tbx* genes. Since *Foxf1* is downregulated in *Shh*$^{-/-}$ and partially derepressed in *Shh*$^{-/-}$;*Gli3*$^{-/-}$ lungs, we decided to analyze the expression of *Tbx2, 3* and *Tbx4,5* in these mutants.

By using antisense oligonucleotide to abrogate the functions of both Tbx4 and Tbx5 (Cebra-Thomas, Bromer et al. 2003), it was shown that these transcription factors are likely important for the expression of mesenchymal *Fgf10*, critical in lung epithelial branching (Bellusci, Grindley et al. 1997; Weaver, Dunn et al. 2000). *Fgf10* expression appears broader in *Shh*$^{-/-}$ lung (Litingtung, Lei et al. 1998; Pepicelli, Lewis et al. 1998); in agreement, expressions of *Tbx4* and *Tbx5* do not appear significantly altered in *Shh*$^{-/-}$ lung (Figure 5.7 k and n). In contrast *Tbx2* and *Tbx3* expression are significantly repressed in *Shh*$^{-/-}$ and enhanced in *Shh*$^{-/-}$;*Gli3*$^{-/-}$ lungs (Figure 5.7 e,h and f,i). Our finding suggests Shh signaling is important in the transcriptional regulation of *Tbx2* and *Tbx3*. While *Tbx2* and *Tbx3* transcriptional activation by a Shh mediator such as Gli cannot be ruled out, previous reports have implicated other factors in the transcriptional induction of *Tbx* genes such as Bmp2 induction of *Tbx2* in chick heart development (Yamada, Revelli et al. 2000), Foxa2 and Foxc2 induction of *Tbx1* in murine pharyngeal endoderm and head mesenchyme development, respectively (Yamagishi, Maeda et al. 2003). Shh signaling has been proposed to maintain the expression of *Foxa2* and *Foxc2* in the regulation of *Tbx1* (Yamagishi, Maeda et al. 2003). Our observation that *Tbx2* and *Tbx3* expressions are significantly repressed in *Shh*$^{-/-}$ (Figure 5.7 e,h) and derepressed in *Shh*$^{-/-}$;*Gli3*$^{-/-}$ lungs (Figure 5.7 f,i) bears good correlation with the *Foxf1* expression levels in these mutants (Figure 5.7 b,c). Therefore, we suggest that Shh signaling regulates *Tbx2* and *Tbx3* expression via *Foxf1* in the developing lung. Consistent with this notion, *Tbx2* and *Tbx3* expression are downregulated in *Foxf1*$^{+/-}$ lung (Kalinichenko, Lim et al. 2001).

Microarray analysis of *Tbx2*-induced gene expression revealed numerous, potentially interesting, transcriptional targets including genes involved in cell cycle control and cell adhesion (Chen, Zhong et al. 2001). Both *Tbx2* and *3* have been linked to inhibition of senescence in primary mouse embryonic fibroblasts (Jacobs, Keblusek et al. 2000; Brummelkamp, Kortlever et al. 2002). We suggest that *Tbx2* and *Tbx3* could also play a role in lung growth and proliferation; their downregulation could contibute, in part, to the *Shh*$^{-/-}$ hypoplastic lung phenotype. The specific role of *Tbx2* and *Tbx3* in lung development remains to be elucidated with the future identification of specific *Tbx2*- and *Tbx3*-regulated genes.

Vasculogenesis is significantly impaired in *Shh*$^{-/-}$ and partially restored in *Shh*$^{-/-}$; *Gli3*$^{-/-}$ lung

During mouse embryogenesis, the lung mesenchyme undergoes a series of differentiation events with development of the pulmonary capillary network beginning around E10. It is believed that the capillary network is established when a subpopulation of lung mesenchymal cells undergo a process known as vasculogenesis which involves the migration and coalescence of these mesenchymal cells into blood islands or hemangioblast clusters, which are precursors of endothelial and hematopoietic cells (deMello, Sawyer et al. 1997; Akeson, Wetzel et al. 2000; Gebb and Shannon 2000; Schachtner, Wang et al. 2000). This capillary network, formed by lumenal connections and assembly of endothelial cells, is thought to eventually make connections with the

major pulmonary blood vessels to establish the lung circulatory system (deMello and Reid 2000; Hislop 2002). We examined the expression of markers associated with endothelial cell function such as platelet endothelial cell adhesion molecule-1 (PECAM-1) and vascular endothelial growth factor R2 (VEGF-R2), a receptor tyrosine kinase also known as fetal liver kinase-1 (Flk-1), to investigate the role of Shh signaling in pulmonary vasculogenesis. Flk-1 mediates signaling by VEGF, an endothelial-specific mitogen secreted by the lung epithelium (Gebb and Shannon 2000; Healy, Morgenthau et al. 2000) and has been shown to be critical for vasculogenesis and hematopoiesis (Shalaby, Rossant et al. 1995; Shalaby, Ho et al. 1997).

Interestingly, we found the level of endothelial cell differentiation in the E15.5 *Shh*$^{-/-}$ lung mesenchyme is reduced, based on PECAM-1 and Flk-1 staining, while *Shh*$^{-/-}$;*Gli3*$^{-/-}$ lung mesenchyme displays a relatively increased distribution of PECAM-1- and Flk-1-positive cells (Figure 5.8 b-c and h-i). PECAM-1 and Flk-1 staining show less continuity in *Shh*$^{-/-}$ (Figure 5.8 b,h), suggesting possible defects in migration and/or coalescence of endothelial cells to form the capillary bed (Akeson, Wetzel et al. 2000), while in *Shh*$^{-/-}$;*Gli3*$^{-/-}$ lung, the severity of this problem appears alleviated based on the staining pattern of both endothelial markers (Figure 5.8 c,i). Flk-1 function has been linked to the movement of blood cell precursors (Shalaby, Ho et al. 1997). The present finding suggests that Shh signaling plays a critical role in the formation of the pulmonary capillary network. Moreover, the higher level of Gli3R in *Shh*$^{-/-}$ lung (Figure 5.2A, lane 1) appears to negatively regulate vasculogenesis which is less affected in *Shh*$^{-/-}$;*Gli3*$^{-/-}$ lung.

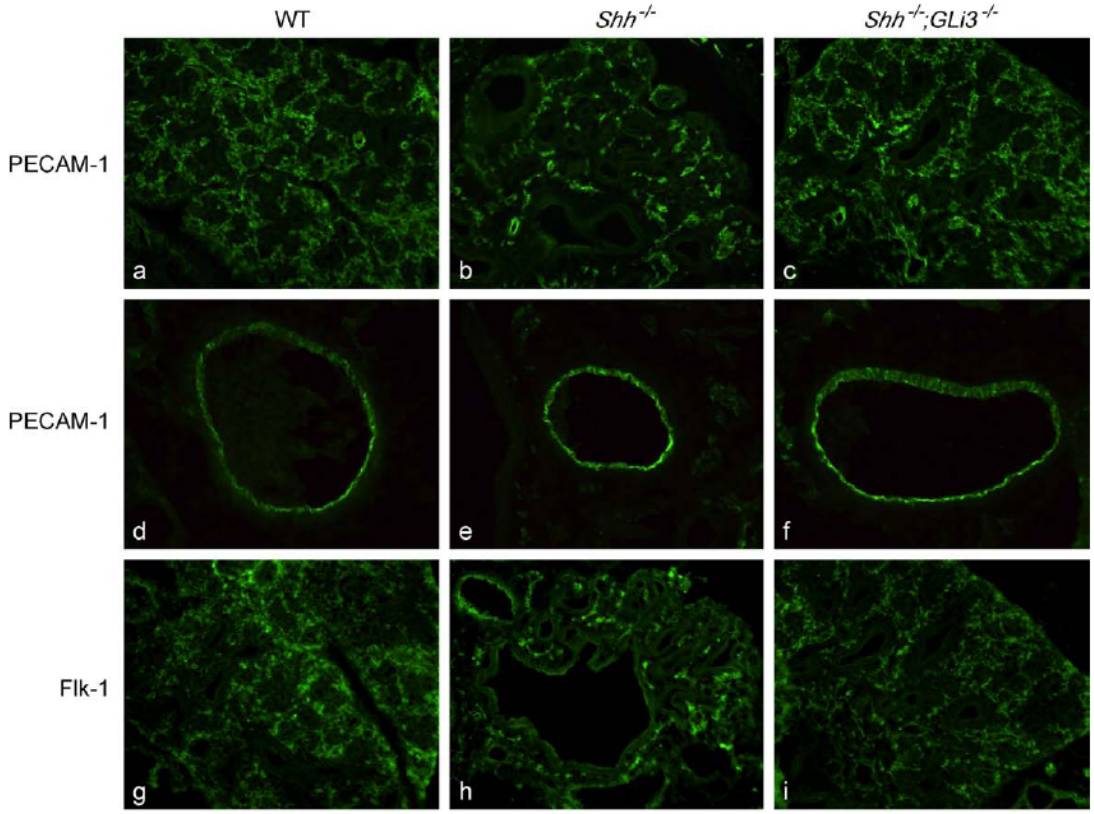

Figure 5.8 Vasculogenesis appears to be enhanced in *Shh*$^{-/-}$;*Gli3*$^{-/-}$ lung compared with *Shh*$^{-/-}$ lung.
Cryosections of WT, *Shh*$^{-/-}$, and *Shh*$^{-/-}$;*Gli3*$^{-/-}$ E15.5 lungs were labeled with antibodies against PECAM-1 (a–f) and Flk-1(g–i), both endothelial markers, followed by Alexa 488-conjugated secondary antibodies. PECAM-1-positive cells, in the interstitial mesenchyme, appear to be sparse in the *Shh*$^{-/-}$ but enhanced in *Shh*$^{-/-}$;*Gli3*$^{-/-}$ lung (compare b and c). However, the uniform distribution of PECAM-1-positive endothelia from major pulmonary blood vessels is evident in all three genotypes and is not significantly different in the WT and mutant lungs (d–f). Flk-1 immunolabeling also reveals enhanced Flk-1-expressing cells in the interstitial mesenchyme of the *Shh*$^{-/-}$;*Gli3*$^{-/-}$ lungs (i) compared with *Shh*$^{-/-}$ lungs (h). Magnification: a-c and g-I (100X), d-f (200X).

Foxf1 plays a critical role in pulmonary vasculogenesis because haploinsufficient *Foxf1*$^{+/-}$ embryos and newborn mice, expressing relatively low levels of *Foxf1* in the lung (20% of wildtype levels) die of severe alveolar hemorrhage due to defects in vasculogenesis and alveologenesis (Kalinichenko, Lim et al. 2001). These *Foxf1*$^{+/-}$ mice have diminished expression of PECAM-1 and Flk-1, whereas *Foxf1*$^{+/-}$ mice expressing near normal levels of *Foxf1* displayed normal levels of PECAM-1 and Flk-1 (Kalinichenko, Lim et al. 2001). In the adult mouse lung, *Foxf1*-expressing cells colocalized with PECAM-1-positive alveolar endothelial and peribronchiolar smooth muscle cells (Costa, Kalinichenko et al. 2001). PECAM-1 staining in the endothelium of large pulmonary blood vessels, which do not normally express *Foxf1* (Kalinichenko, Lim et al. 2001), were comparable in all three genotypes (Figure5.8 d-f). Among *Foxf1*$^{+/-}$ surviving adult mice, butylated hydroxytoluene (BHT) treatment causes fatal lung injury due to severe hemorrhage; BHT caused a 10-fold reduction in *Foxf1* level accompanied by increased alveolar endothelial cell apoptosis (Kalinichenko, Zhou et al. 2002). Hence, it is plausible to suggest that the defect in PECAM-1 and Flk-1 expressions observed in the *Shh*$^{-/-}$ may be linked to repressed *Foxf1* expression while *Shh*$^{-/-}$;*Gli3*$^{-/-}$ lung, which expresses a relatively higher level of *Foxf1*, shows a concomitant recovery of endothelial marker expressions (Figure 5.8 c,i). However, it is possible that other factors are involved such as vascular endothelial growth factor (VEGF) (Zeng, Wert et al. 1998; Gebb and Shannon 2000; Healy, Morgenthau et al. 2000; Ng, Rohan et al. 2001; Galambos, Ng et al. 2002) and TGF-beta1 (Zeng, Gray et al. 2001).

Foxf1$^{+/-}$ mice reported by another group also exhibited lung and foregut malformations resulting in 90% perinatal mortality but with apparently no significant defects in lung vascularization (Mahlapuu, Enerback et al. 2001). It is possible that the expression levels of *Foxf1* in these mutant mice was not low enough to cause vasculogenesis problems but sufficiently downregulated to cause lung hypoplasia. It is apparent that there is variability in the levels of *Foxf1* expressed from different *Foxf1*$^{+/-}$ embryos (Kalinichenko, Lim et al. 2001). This observation suggests that less than wildtype level of *Foxf1* is sufficient to promote near normal vasculogenesis during early embryogenesis (Mahlapuu, Enerback et al. 2001), at least based on endothelial marker expression and distribution. In agreement, we observed enhanced vasculogenesis in *Shh*$^{-/-}$;*Gli3*$^{-/-}$ lung (Figure 5.8 c,i), although its *Foxf1* transcript level is relatively less than wildtype (Figure 5.6 j, l and Figure 5.7 a,c). *Foxf1*, expressed in the mesenchyme, has been implicated in basement membrane extracellular matrix deposition and tight junction formation between cells of two interacting layers such as the mesenchymally-derived endothelial cell with Type I epithelial cell or the bronchial smooth muscle cell with the bronchiolar epithelium of the lung. Decreased *Foxf1* expression has also been linked to gall bladder defects and reduced expression of adhesion molecules, vascular cell adhesion molecule-1 (VCAM-1) and α5 integrin (Kalinichenko, Zhou et al. 2002). *Foxf1*$^{+/-}$ mice show tight junction disruptions which could result in impaired epithelial-mesenchymal interaction (Costa, Kalinichenko et al. 2001; Kalinichenko, Lim et al. 2001; Kalinichenko, Lim et al. 2001), hence providing one plausible mechanism by which *Foxf1* promotes

bronchial smooth muscle or endothelial cell homeostasis.

Bronchial myogenesis remains defective in *Shh*$^{-/-}$;*Gli3*$^{-/-}$ lung

The mesenchymal cells of the developing lung can give rise to visceral smooth muscle cells which express smooth muscle alpha-actin (SMA) and smooth muscle myosin (SMM) (Yang, Palmer et al. 1998; Yang, Relan et al. 1999). Since vasculogenesis defect is less impaired in the *Shh*$^{-/-}$;*Gli3*$^{-/-}$ lung compared to the *Shh*$^{-/-}$ lung, we thought it would be interesting to examine whether differentiation along another cell lineage, namely bronchial smooth muscle (BSM), which is absent in the *Shh*$^{-/-}$ lung (Pepicelli, Lewis et al. 1998), would be restored in *Shh*$^{-/-}$;*Gli3*$^{-/-}$ lung. Moreover, *Foxf1* expression is relatively higher in *Shh*$^{-/-}$;*Gli3*$^{-/-}$ lung compared with *Shh*$^{-/-}$ lung, so we wondered whether this increase would be accompanied by a concomitant recovery of BSM in *Shh*$^{-/-}$;*Gli3*$^{-/-}$ lung, since *Foxf1* is expressed in the peribronchiolar smooth muscle layer (Costa, Kalinichenko et al. 2001; Kalinichenko, Lim et al. 2001) and has been implicated in Shh-induced myogenesis in lung mesenchyme explants (Weaver, Batts et al. 2003). In *Foxf1*$^{+/-}$ newborn lung, a disruption of the cell interface between the BSM and epithelial layers was reported along with an increase in apoptosis of BSM cells (Kalinichenko, Lim et al. 2001). Our results, by immunohistochemistry using both SMA and SMM antibodies on E15.5 lungs, indicate that, while vascular smooth muscles lining the major pulmonary blood vessels (Hall, Hislop et al. 2000; Hall, Hislop et al. 2002; Hislop 2002) are present in both *Shh*$^{-/-}$ and *Shh*$^{-/-}$;*Gli3*$^{-/-}$ lungs (Figure 5.9 arrows in b,c,e,f), bronchial smooth

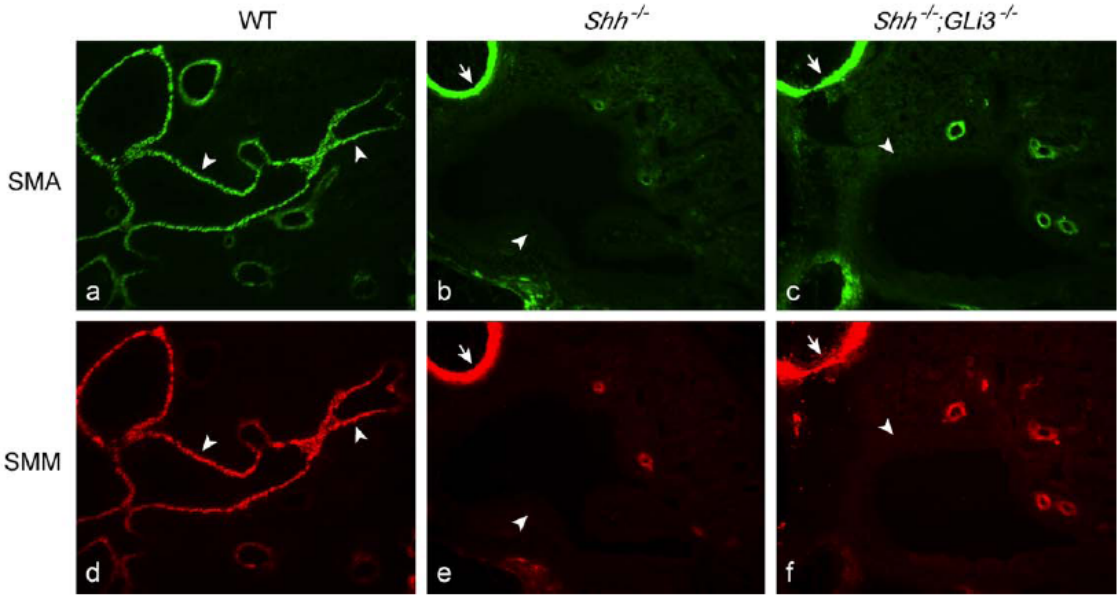

Figure 5.9 Bronchial myogenesis remains absent in *Shh*$^{-/-}$;*Gli3*$^{-/-}$ lung compared with *Shh*$^{-/-}$ lung.
Cryosections of wild-type (WT), *Shh*$^{-/-}$, and *Shh*$^{-/-}$;*Gli3*$^{-/-}$ E15.5 lungs were labeled with antibodies against smooth muscle actin (SMA) (a–c) and smooth muscle myosin (SMM) (d–f), followed by Alexa 488 (a–c) or Alexa 568 (d–f) conjugated secondary antibodies. While vascular smooth muscle is present in the mutants (arrows) and WT lungs (d–f), bronchial smooth muscle as highlighted by SMA (a–c) and SMM (d–f) is evident in the WT (arrowheads) but absent in the *Shh*$^{-/-}$;*Gli3*$^{-/-}$ lung (arrowheads), as in *Shh*$^{-/-}$ (arrowheads). Magnification: 100X.

muscle remains absent (Figure 5.9 arrowheads in b,c,e,f). The WT lung shows clear presence of bronchial smooth muscle as highlighted by the smooth muscle markers (Figure 5.9 arrowheads in a,d). This finding suggests that while differentiation along the alveolar capillary endothelial cell lineage is enhanced in *Shh*$^{-/-}$;*Gli3*$^{-/-}$ lungs, differentiation along the bronchial smooth muscle lineage remains defective. This observation implies that Gli3R does not contribute significantly to the lack of BSM in *Shh*$^{-/-}$ lung. In conclusion, our result suggests while upregulating *Foxf1*, implicated in pulmonary vasculogenesis, in *Shh*$^{-/-}$;*Gli3*$^{-/-}$ lung partially restored the distribution of PECAM-positive endothelial cell types, in contrast, that level of *Foxf1* is not sufficient to restore BSM. Hence, the role of *Foxf1* in bronchial myogenesis awaits further investigation.

Acknowledgements

We thank Dr. William Gaffield for gift of cyclopamine and Drs. B. Hogan, M. Scott, C-c. Hui, A. McMahon, R. Costa, V. Papaiannou and H. Moses for their generous gifts of cDNA probes and reagents. We also thank Yuan-Fang Wang for animal breeding and genotyping.

REFERENCES

Aberg, A., L. Westbom, et al. (2001). "Congenital malformations among infants whose mothers had gestational diabetes or preexisting diabetes." Early Hum Dev **61**(2): 85-95.

Aitola, M., P. Carlsson, et al. (2000). "Forkhead transcription factor FoxF2 is expressed in mesodermal tissues involved in epithelio-mesenchymal interactions." Dev Dyn **218**(1): 136-49.

Akeson, A. L., B. Wetzel, et al. (2000). "Embryonic vasculogenesis by endothelial precursor cells derived from lung mesenchyme." Dev Dyn **217**(1): 11-23.

Asirvatham, A. J., M. A. Schmidt, et al. (2006). "Non-redundant inhibitor of differentiation (Id) gene expression and function in human prostate epithelial cells." Prostate **66**(9): 921-35.

Aubin, J., A. Davy, et al. (2004). "In vivo convergence of BMP and MAPK signaling pathways: impact of differential Smad1 phosphorylation on development and homeostasis." Genes Dev **18**(12): 1482-94.

Auchterlonie, I. A. and M. P. White (1982). "Recurrence of the VATER association within a sibship." Clin Genet **21**(2): 122-4.

Aza-Blanc, P. and T. B. Kornberg (1999). "Ci: a complex transducer of the hedgehog signal." Trends Genet **15**(11): 458-62.

Bachiller, D., J. Klingensmith, et al. (2000). "The organizer factors Chordin and Noggin are required for mouse forebrain development." Nature **403**(6770): 658-61.

Bain, G., C. B. Cravatt, et al. (2001). "Regulation of the helix-loop-helix proteins, E2A and Id3, by the Ras-ERK MAPK cascade." Nat Immunol **2**(2): 165-71.

Balemans, W. and W. Van Hul (2002). "Extracellular regulation of BMP signaling in

vertebrates: a cocktail of modulators." Dev Biol **250**(2): 231-50.

Barone, M. V., R. Pepperkok, et al. (1994). "Id proteins control growth induction in mammalian cells." Proc Natl Acad Sci U S A **91**(11): 4985-8.

Beasley, S. W., M. Allen, et al. (1997). "The effects of Down syndrome and other chromosomal abnormalities on survival and management in oesophageal atresia." Pediatr Surg Int **12**(8): 550-1.

Beasley, S. W., J. Diez Pardo, et al. (2000). "The contribution of the adriamycin-induced rat model of the VATER association to our understanding of congenital abnormalities and their embryogenesis." Pediatr Surg Int **16**(7): 465-72.

Beddington, R. S. (1994). "Induction of a second neural axis by the mouse node." Development **120**(3): 613-20.

Behrens, J. (2000). "Control of beta-catenin signaling in tumor development." Ann N Y Acad Sci **910**: 21-33; discussion 33-5.

Behrens, J., J. P. von Kries, et al. (1996). "Functional interaction of beta-catenin with the transcription factor LEF-1." Nature **382**(6592): 638-42.

Bellusci, S., Y. Furuta, et al. (1997). "Involvement of Sonic hedgehog (Shh) in mouse embryonic lung growth and morphogenesis." Development **124**(1): 53-63.

Bellusci, S., J. Grindley, et al. (1997). "Fibroblast growth factor 10 (FGF10) and branching morphogenesis in the embryonic mouse lung." Development **124**(23): 4867-78.

Bellusci, S., R. Henderson, et al. (1996). "Evidence from normal expression and targeted misexpression that bone morphogenetic protein (Bmp-4) plays a role in mouse embryonic lung morphogenesis." Development **122**(6): 1693-702.

Benezra, R., S. Rafii, et al. (2001). "The Id proteins and angiogenesis." Oncogene **20**(58): 8334-41.

Berman, D. M., S. S. Karhadkar, et al. (2002). "Medulloblastoma growth inhibition by hedgehog pathway blockade." Science **297**(5586): 1559-61.

Blake, K. D., S. L. Davenport, et al. (1998). "CHARGE association: an update and review for the primary pediatrician." Clin Pediatr (Phila) **37**(3): 159-73.

Bonifas, J. M., S. Pennypacker, et al. (2001). "Activation of expression of hedgehog target genes in basal cell carcinomas." J Invest Dermatol **116**(5): 739-42.

Borth, W. (1992). "Alpha 2-macroglobulin, a multifunctional binding protein with targeting characteristics." Faseb J **6**(15): 3345-53.

Bouchard, C., K. Thieke, et al. (1999). "Direct induction of cyclin D2 by Myc contributes to cell cycle progression and sequestration of p27." Embo J **18**(19): 5321-33.

Boulet, A. M. and M. R. Capecchi (1996). "Targeted disruption of hoxc-4 causes esophageal defects and vertebral transformations." Dev Biol **177**(1): 232-49.

Brummelkamp, T. R., R. M. Kortlever, et al. (2002). "TBX-3, the gene mutated in Ulnar-Mammary Syndrome, is a negative regulator of p19ARF and inhibits senescence." J Biol Chem **277**(8): 6567-72.

Brunner, H. G. and H. van Bokhoven (2005). "Genetic players in esophageal atresia and tracheoesophageal fistula." Curr Opin Genet Dev **15**(3): 341-7.

Burstyn-Cohen, T., J. Stanleigh, et al. (2004). "Canonical Wnt activity regulates trunk neural crest delamination linking BMP/noggin signaling with G1/S transition." Development **131**(21): 5327-39.

Canalis, E., A. N. Economides, et al. (2003). "Bone morphogenetic proteins, their antagonists, and the skeleton." Endocr Rev **24**(2): 218-35.

Cano Garci-Nuno, A., G. Solis Sanchez, et al. (1992). "[Esophageal atresia and associated anomalies]." An Esp Pediatr **36**(6): 455-9.

Capdevila, J., T. Tsukui, et al. (1999). "Control of vertebrate limb outgrowth by the proximal factor Meis2 and distal antagonism of BMPs by Gremlin." Mol Cell **4**(5): 839-49.

Cardoso, W. V. (2001). "Molecular regulation of lung development." Annu Rev Physiol **63**: 471-94.

Cardoso, W. V. and J. Lu (2006). "Regulation of early lung morphogenesis: questions, facts and controversies." Development **133**(9): 1611-24.

Causak, R. A., S. E. Zgleszewski, et al. (1998). "Differential gene expression at gestational days 14 and 16 in normal and nitrogen-induced hypoplastic murine fetal lungs with coexistent diaphragmatic hernia." Pediatr Pulmonol **26**(5): 301-11.

Cebra-Thomas, J. A., J. Bromer, et al. (2003). "T-box gene products are required for mesenchymal induction of epithelial branching in the embryonic mouse lung." Dev Dyn **226**(1): 82-90.

Chapman, D. L., N. Garvey, et al. (1996). "Expression of the T-box family genes, Tbx1-Tbx5, during early mouse development." Dev Dyn **206**(4): 379-90.

Chen, D., M. Zhao, et al. (2004). "Bone morphogenetic proteins." Growth Factors **22**(4): 233-41.

Chen, J., Q. Zhong, et al. (2001). "Microarray analysis of Tbx2-directed gene expression: a possible role in osteogenesis." Mol Cell Endocrinol **177**(1-2): 43-54.

Chen, J. K., J. Taipale, et al. (2002). "Inhibition of Hedgehog signaling by direct binding of cyclopamine to Smoothened." Genes Dev **16**(21): 2743-8.

Chen, Y., M. Bei, et al. (1996). "Msx1 controls inductive signaling in mammalian tooth morphogenesis." Development **122**(10): 3035-44.

Chiang, C., R. Z. Swan, et al. (1999). "Essential role for Sonic hedgehog during hair follicle morphogenesis." Dev Biol **205**(1): 1-9.

Chinoy, M. R. (2003). "Lung growth and development." Front Biosci **8**: D392-415.

Chinoy, M. R., X. Chi, et al. (2001). "Down-regulation of regulatory proteins for differentiation and proliferation in murine fetal hypoplastic lungs: altered mesenchymal-epithelial interactions." Pediatr Pulmonol **32**(2): 129-41.

Ciemerych, M. A., A. M. Kenney, et al. (2002). "Development of mice expressing a single D-type cyclin." Genes Dev **16**(24): 3277-89.

Clark, D. C. (1999). "Esophageal atresia and tracheoesophageal fistula." Am Fam Physician **59**(4): 910-6, 919-20.

Cleaver, O. and P. A. Krieg (2001). "Notochord patterning of the endoderm." Dev Biol **234**(1): 1-12.

Clevidence, D. E., D. G. Overdier, et al. (1994). "Members of the HNF-3/forkhead family of transcription factors exhibit distinct cellular expression patterns in lung and regulate the surfactant protein B promoter." Dev Biol **166**(1): 195-209.

Colvin, J. S., A. C. White, et al. (2001). "Lung hypoplasia and neonatal death in Fgf9-null mice identify this gene as an essential regulator of lung mesenchyme." Development **128**(11): 2095-106.

Cooper, M. K., J. A. Porter, et al. (1998). "Teratogen-mediated inhibition of target tissue response to Shh signaling." Science **280**(5369): 1603-7.

Coppe, J. P., A. P. Smith, et al. (2003). "Id proteins in epithelial cells." Exp Cell Res **285**(1): 131-45.

Costa, R. H., V. V. Kalinichenko, et al. (2001). "Transcription factors in mouse lung development and function." Am J Physiol Lung Cell Mol Physiol **280**(5): L823-38.

Dai, P., H. Akimaru, et al. (1999). "Sonic Hedgehog-induced activation of the Gli1 promoter is mediated by GLI3." J Biol Chem **274**(12): 8143-52.

Dai, P., T. Shinagawa, et al. (2002). "Ski is involved in transcriptional regulation by the repressor and full-length forms of Gli3." Genes Dev **16**(22): 2843-8.

Dallapiccola, B., R. Mingarelli, et al. (1993). "Interstitial deletion del(17) (q21.3q23 or 24.2) syndrome." Clin Genet **43**(1): 54-5.

David, T. J. and S. E. O'Callaghan (1975). "Oesophageal atresia in the South West of England." J Med Genet **12**(1): 1-11.

Dawrant, M. J., S. Giles, et al. (2007). "Adriamycin mouse model: a variable but reproducible model of tracheo-oesophageal malformations." Pediatr Surg Int.

de Caestecker, M. (2004). "The transforming growth factor-beta superfamily of receptors." Cytokine Growth Factor Rev **15**(1): 1-11.

de Lorimier, A. A. and M. R. Harrison (1985). "Esophageal atresia: embryogenesis and management." World J Surg **9**(2): 250-7.

Degen, W. G., M. A. Weterman, et al. (1996). "Expression of nma, a novel gene, inversely correlates with the metastatic potential of human melanoma cell lines and xenografts." Int J Cancer **65**(4): 460-5.

del Rosario, J. F. and S. R. Orenstein (1998). "Common pediatric esophageal disorders." Gastroenterologist **6**(2): 104-21.

deMello, D. E. and L. M. Reid (2000). "Embryonic and early fetal development of human lung vasculature and its functional implications." Pediatr Dev Pathol **3**(5): 439-49.

deMello, D. E., D. Sawyer, et al. (1997). "Early fetal development of lung vasculature." Am J Respir Cell Mol Biol **16**(5): 568-81.

Diaz, E. M., Jr., J. M. Adams, et al. (1989). "Tracheal agenesis. A case report and literature review." Archives of Otolaryngology -- Head & Neck Surgery **115**(6): 741-5.

Diez-Pardo, J. A., Q. Baoquan, et al. (1996). "A new rodent experimental model of esophageal atresia and tracheoesophageal fistula: preliminary report." J Pediatr Surg **31**(4): 498-502.

Dudley, A. T., K. M. Lyons, et al. (1995). "A requirement for bone morphogenetic protein-7 during development of the mammalian kidney and eye." Genes Dev **9**(22): 2795-807.

Dudley, A. T. and E. J. Robertson (1997). "Overlapping expression domains of bone morphogenetic protein family members potentially account for limited tissue defects in BMP7 deficient embryos." Dev Dyn **208**(3): 349-62.

Duman-Scheel, M., L. Weng, et al. (2002). "Hedgehog regulates cell growth and proliferation by inducing Cyclin D and Cyclin E." Nature **417**(6886): 299-304.

Eberhart, C. G. and P. Argani (2001). "Wnt signaling in human development: beta-catenin nuclear translocation in fetal lung, kidney, placenta, capillaries, adrenal, and cartilage." Pediatr Dev Pathol **4**(4): 351-7.

Ebisawa, T., M. Fukuchi, et al. (2001). "Smurf1 interacts with transforming growth factor-beta type I receptor through Smad7 and induces receptor degradation." J Biol Chem **276**(16): 12477-80.

Effmann, E. L., T. J. Spackman, et al. (1975). "Tracheal agenesis." Am J Roentgenol Radium Ther Nucl Med **125**(4): 767-81.

Ein, S. H., B. Shandling, et al. (1989). "Esophageal atresia with distal tracheoesophageal fistula: associated anomalies and prognosis in the 1980s." J Pediatr Surg **24**(10): 1055-9.

Ekholm, S. V. and S. I. Reed (2000). "Regulation of G(1) cyclin-dependent kinases in the mammalian cell cycle." Curr Opin Cell Biol **12**(6): 676-84.

Engum, S. A., J. L. Grosfeld, et al. (1995). "Analysis of morbidity and mortality in 227 cases of esophageal atresia and/or tracheoesophageal fistula over two decades." Arch Surg **130**(5): 502-8; discussion 508-9.

Evans, J. A., C. R. Greenberg, et al. (1999). "Tracheal agenesis revisited: analysis of associated anomalies." Am J Med Genet **82**(5): 415-22.

Evans, J. A., J. Reggin, et al. (1985). "Tracheal agenesis and associated malformations: a comparison with tracheoesophageal fistula and the VACTERL association." American Journal of Medical Genetics **21**(1): 21-38.

Fan, H. and P. A. Khavari (1999). "Sonic hedgehog opposes epithelial cell cycle arrest." J Cell Biol **147**(1): 71-6.

Felix, J. F., R. Keijzer, et al. (2004). "Genetics and developmental biology of oesophageal atresia and tracheo-oesophageal fistula: lessons from mice relevant for paediatric surgeons." Pediatr Surg Int **20**(10): 731-6.

Fisher, M. C., Y. Li, et al. (2006). "Heparan sulfate proteoglycans including syndecan-3 modulate BMP activity during limb cartilage differentiation." Matrix Biol **25**(1): 27-39.

Floyd, J., D. C. Campbell, Jr., et al. (1962). "Agenesis of the trachea." American Review of Respiratory Disease **86**: 557-60.

Fluss, Z. and K. J. Poppen (1951). "Embryogenesis of tracheoesophageal fistula and esophageal atresia; a hypothesis based on associated vascular anomalies." AMA Arch Pathol **52**(2): 168-81.

Fong, S., Y. Itahana, et al. (2003). "Id-1 as a molecular target in therapy for breast cancer cell invasion and metastasis." Proc Natl Acad Sci U S A **100**(23): 13543-8.

Fraidenraich, D., E. Stillwell, et al. (2004). "Rescue of cardiac defects in id knockout embryos by injection of embryonic stem cells." Science **306**(5694): 247-52.

Fujiwara, T., D. B. Dehart, et al. (2002). "Distinct requirements for extra-embryonic and embryonic bone morphogenetic protein 4 in the formation of the node and primitive streak and coordination of left-right asymmetry in the mouse." Development **129**(20): 4685-96.

Fujiwara, T., N. R. Dunn, et al. (2001). "Bone morphogenetic protein 4 in the extraembryonic mesoderm is required for allantois development and the localization and survival of primordial germ cells in the mouse." Proc Natl Acad Sci U S A **98**(24): 13739-44.

Galambos, C., Y. S. Ng, et al. (2002). "Defective pulmonary development in the absence of heparin-binding vascular endothelial growth factor isoforms." Am J Respir Cell Mol Biol **27**(2): 194-203.

Galceran, J., I. Farinas, et al. (1999). "Wnt3a-/--like phenotype and limb deficiency in Lef1(-/-)Tcf1(-/-) mice." Genes Dev **13**(6): 709-17.

Gebb, S. A. and J. M. Shannon (2000). "Tissue interactions mediate early events in pulmonary vasculogenesis." Dev Dyn **217**(2): 159-69.

Geng, Y., Q. Yu, et al. (2001). "Expression of cyclins E1 and E2 during mouse development and in neoplasia." Proc Natl Acad Sci U S A **98**(23): 13138-43.

Gibson-Brown, J. J. (2002). "T-box time in England." Dev Cell **3**(5): 625-30.

Gibson-Brown, J. J., I. A. S, et al. (1998). "Expression of T-box genes Tbx2-Tbx5 during chick organogenesis." Mech Dev **74**(1-2): 165-9.

Gong, Y., D. Krakow, et al. (1999). "Heterozygous mutations in the gene encoding noggin affect human joint morphogenesis." Nat Genet **21**(3): 302-4.

Goodrich, L. V., R. L. Johnson, et al. (1996). "Conservation of the hedgehog/patched signaling pathway from flies to mice: induction of a mouse patched gene by Hedgehog." Genes Dev **10**(3): 301-12.

Griffith, D. L., P. C. Keck, et al. (1996). "Three-dimensional structure of recombinant human osteogenic protein 1: structural paradigm for the transforming growth factor beta superfamily." Proceedings of the National Academy of Sciences of the United States of America **93**(2): 878-83.

Grindley, J. C., S. Bellusci, et al. (1997). "Evidence for the involvement of the Gli gene

family in embryonic mouse lung development." Dev Biol **188**(2): 337-48.

Groppe, J., J. Greenwald, et al. (2002). "Structural basis of BMP signalling inhibition by the cystine knot protein Noggin.[see comment]." Nature **420**(6916): 636-42.

Hall, S. M., A. A. Hislop, et al. (2002). "Origin, differentiation, and maturation of human pulmonary veins." Am J Respir Cell Mol Biol **26**(3): 333-40.

Hall, S. M., A. A. Hislop, et al. (2000). "Prenatal origins of human intrapulmonary arteries: formation and smooth muscle maturation." Am J Respir Cell Mol Biol **23**(2): 194-203.

Healy, A. M., L. Morgenthau, et al. (2000). "VEGF is deposited in the subepithelial matrix at the leading edge of branching airways and stimulates neovascularization in the murine embryonic lung." Dev Dyn **219**(3): 341-52.

Hebert, J. M. and S. K. McConnell (2000). "Targeting of cre to the Foxg1 (BF-1) locus mediates loxP recombination in the telencephalon and other developing head structures." Dev Biol **222**(2): 296-306.

Heller, R. S., D. S. Dichmann, et al. (2002). "Expression patterns of Wnts, Frizzleds, sFRPs, and misexpression in transgenic mice suggesting a role for Wnts in pancreas and foregut pattern formation." Dev Dyn **225**(3): 260-70.

Hellqvist, M., M. Mahlapuu, et al. (1996). "Differential activation of lung-specific genes by two forkhead proteins, FREAC-1 and FREAC-2." J Biol Chem **271**(8): 4482-90.

Hicks, L. M. and P. B. Mansfield (1981). "Esophageal atresia and tracheoesophageal fistula. Review of thirteen years' experience." J Thorac Cardiovasc Surg **81**(3): 358-63.

Hirning, U., P. Schmid, et al. (1991). "A comparative analysis of N-myc and c-myc expression and cellular proliferation in mouse organogenesis." Mech Dev **33**(2): 119-25.

Hislop, A. A. (2002). "Airway and blood vessel interaction during lung development." J Anat **201**(4): 325-34.

Hogan, B., R. Beddington, et al. (1994). Manipulating the mouse embryo: A laboratory manual. New York, Cold Spring Harbor Laboratory Press.

Hogan, B. L. (1996). "Bone morphogenetic proteins in development." Current Opinion in Genetics & Development **6**(4): 432-8.

Hogan, B. L. (1999). "Morphogenesis." Cell **96**(2): 225-33.

Hollnagel, A., V. Oehlmann, et al. (1999). "Id genes are direct targets of bone morphogenetic protein induction in embryonic stem cells." J Biol Chem **274**(28): 19838-45.

Hsieh, J. C., L. Kodjabachian, et al. (1999). "A new secreted protein that binds to Wnt proteins and inhibits their activities." Nature **398**(6726): 431-6.

Hsieh, J. C., A. Rattner, et al. (1999). "Biochemical characterization of Wnt-frizzled interactions using a soluble, biologically active vertebrate Wnt protein." Proc Natl Acad Sci U S A **96**(7): 3546-51.

Hsu, D. R., A. N. Economides, et al. (1998). "The Xenopus dorsalizing factor Gremlin identifies a novel family of secreted proteins that antagonize BMP activities." Mol Cell **1**(5): 673-83.

Hsu, M. Y., S. Rovinsky, et al. (2005). "Bone morphogenetic proteins in melanoma: angel or devil?" Cancer Metastasis Rev **24**(2): 251-63.

Hu, G., H. Lee, et al. (2001). "Msx homeobox genes inhibit differentiation through upregulation of cyclin D1." Development **128**(12): 2373-84.

Hua, H., Y. Q. Zhang, et al. (2006). "BMP4 regulates pancreatic progenitor cell expansion through Id2." J Biol Chem **281**(19): 13574-80.

Huguet, E. L., J. A. McMahon, et al. (1994). "Differential expression of human Wnt genes 2, 3, 4, and 7B in human breast cell lines and normal and disease states of human breast tissue." Cancer Res **54**(10): 2615-21.

Hui, C. C. and A. L. Joyner (1993). "A mouse model of greig cephalopolysyndactyly syndrome: the extra-toesJ mutation contains an intragenic deletion of the Gli3 gene." Nat Genet **3**(3): 241-6.

Hui, C. C., D. Slusarski, et al. (1994). "Expression of three mouse homologs of the Drosophila segment polarity gene cubitus interruptus, Gli, Gli-2, and Gli-3, in ectoderm- and mesoderm-derived tissues suggests multiple roles during postimplantation development." Dev Biol **162**(2): 402-13.

Huse, M., T. W. Muir, et al. (2001). "The TGF beta receptor activation process: an inhibitor- to substrate-binding switch." Mol Cell **8**(3): 671-82.

Imamoglu, M., A. Cay, et al. (2004). "Acquired tracheo-esophageal fistulas caused by button battery lodged in the esophagus." Pediatr Surg Int **20**(4): 292-4.

Incardona, J. P., W. Gaffield, et al. (1998). "The teratogenic Veratrum alkaloid cyclopamine inhibits sonic hedgehog signal transduction." Development **125**(18): 3553-62.

Ingham, P. W. and M. Placzek (2006). "Orchestrating ontogenesis: variations on a theme by sonic hedgehog." Nat Rev Genet **7**(11): 841-50.

Ioannides, A. S., B. Chaudhry, et al. (2002). "Dorsoventral patterning in oesophageal atresia with tracheo-oesophageal fistula: Evidence from a new mouse model." J Pediatr Surg **37**(2): 185-91.

Jacobs, J. J., P. Keblusek, et al. (2000). "Senescence bypass screen identifies TBX2, which represses Cdkn2a (p19(ARF)) and is amplified in a subset of human breast cancers." Nat Genet **26**(3): 291-9.

Jamora, C., R. DasGupta, et al. (2003). "Links between signal transduction, transcription and adhesion in epithelial bud development." Nature **422**(6929): 317-22.

Jen, Y., K. Manova, et al. (1997). "Each member of the Id gene family exhibits a unique expression pattern in mouse gastrulation and neurogenesis." Dev Dyn **208**(1): 92-106.

Jessell, T. M. and J. R. Sanes (2000). "Development. The decade of the developing brain." Curr Opin Neurobiol **10**(5): 599-611.

Jia, J., K. Amanai, et al. (2002). "Shaggy/GSK3 antagonizes Hedgehog signalling by regulating Cubitus interruptus." Nature **416**(6880): 548-52.

Jurand, A. (1974). "Some aspects of the development of the notochord in mouse embryos." J Embryol Exp Morphol **32**(1): 1-33.

Kaartinen, V. and A. Nagy (2001). "Removal of the floxed neo gene from a conditional knockout allele by the adenoviral Cre recombinase in vivo." Genesis **31**(3): 126-9.

Kalderon, D. (2002). "Similarities between the Hedgehog and Wnt signaling pathways." Trends Cell Biol **12**(11): 523-31.

Kalinichenko, V. V., L. Lim, et al. (2001). "Differential expression of forkhead box transcription factors following butylated hydroxytoluene lung injury." Am J Physiol Lung Cell Mol Physiol **280**(4): L695-704.

Kalinichenko, V. V., L. Lim, et al. (2001). "Defects in pulmonary vasculature and perinatal lung hemorrhage in mice heterozygous null for the Forkhead Box f1 transcription factor." Dev Biol **235**(2): 489-506.

Kalinichenko, V. V., Y. Zhou, et al. (2002). "Haploinsufficiency of the mouse Forkhead Box f1 gene causes defects in gall bladder development." J Biol Chem **277**(14): 12369-74.

Kalinichenko, V. V., Y. Zhou, et al. (2002). "Wild-type levels of the mouse Forkhead Box f1 gene are essential for lung repair." Am J Physiol Lung Cell Mol Physiol **282**(6): L1253-65.

Kallen, B., P. Mastroiacovo, et al. (1996). "Major congenital malformations in Down

syndrome." Am J Med Genet **65**(2): 160-6.

Kang, S., J. M. Graham, Jr., et al. (1997). "GLI3 frameshift mutations cause autosomal dominant Pallister-Hall syndrome." Nat Genet **15**(3): 266-8.

Kauffman, M. H. (1992). The Atlas of Mouse Development, Academic Press, New York.

Kavsak, P., R. K. Rasmussen, et al. (2000). "Smad7 binds to Smurf2 to form an E3 ubiquitin ligase that targets the TGF beta receptor for degradation." Mol Cell **6**(6): 1365-75.

Kawabata, M., A. Chytil, et al. (1995). "Cloning of a novel type II serine/threonine kinase receptor through interaction with the type I transforming growth factor-beta receptor." J Biol Chem **270**(10): 5625-30.

Kee, Y. and M. Bronner-Fraser (2001). "The transcriptional regulator Id3 is expressed in cranial sensory placodes during early avian embryonic development." Mech Dev **109**(2): 337-40.

Kengaku, M., J. Capdevila, et al. (1998). "Distinct WNT pathways regulating AER formation and dorsoventral polarity in the chick limb bud." Science **280**(5367): 1274-7.

Kenney, A. M., M. D. Cole, et al. (2003). "Nmyc upregulation by sonic hedgehog signaling promotes proliferation in developing cerebellar granule neuron precursors." Development **130**(1): 15-28.

Kenney, A. M. and D. H. Rowitch (2000). "Sonic hedgehog promotes G(1) cyclin expression and sustained cell cycle progression in mammalian neuronal precursors." Mol Cell Biol **20**(23): 9055-67.

Kerschner, J. and D. W. Klotch (1997). "Tracheal agenesis: a case report and review of the literature." Otolaryngol Head Neck Surg **116**(1): 123-8.

Khalifa, M. M., P. M. MacLeod, et al. (1993). "Additional case of de novo interstitial deletion del(17)(q21.3q23) and expansion of the phenotype." Clin Genet **44**(5):

258-61.

Khokha, M. K., D. Hsu, et al. (2003). "Gremlin is the BMP antagonist required for maintenance of Shh and Fgf signals during limb patterning." Nat Genet **34**(3): 303-7.

Kimura, N., R. Matsuo, et al. (2000). "BMP2-induced apoptosis is mediated by activation of the TAK1-p38 kinase pathway that is negatively regulated by Smad6." J Biol Chem **275**(23): 17647-52.

Kinder, S. J., T. E. Tsang, et al. (2001). "The organizer of the mouse gastrula is composed of a dynamic population of progenitor cells for the axial mesoderm." Development **128**(18): 3623-34.

King, J. A., P. C. Marker, et al. (1994). "BMP5 and the molecular, skeletal, and soft-tissue alterations in short ear mice." Dev Biol **166**(1): 112-22.

Kinzler, K. W., J. M. Ruppert, et al. (1988). "The GLI gene is a member of the Kruppel family of zinc finger proteins." Nature **332**(6162): 371-4.

Kishigami, S. and Y. Mishina (2005). "BMP signaling and early embryonic patterning." Cytokine Growth Factor Rev **16**(3): 265-78.

Kluth, D. and H. Fiegel (2003). "The embryology of the foregut." Semin Pediatr Surg **12**(1): 3-9.

Kluth, D., G. Steding, et al. (1987). "The embryology of foregut malformations." J Pediatr Surg **22**(5): 389-93.

Knoepfler, P. S., P. F. Cheng, et al. (2002). "N-myc is essential during neurogenesis for the rapid expansion of progenitor cell populations and the inhibition of neuronal differentiation." Genes Dev **16**(20): 2699-712.

Komatsu, Y., H. Shibuya, et al. (2002). "Targeted disruption of the Tab1 gene causes embryonic lethality and defects in cardiovascular and lung morphogenesis." Mech Dev **119**(2): 239-49.

Kowanetz, M., U. Valcourt, et al. (2004). "Id2 and Id3 define the potency of cell proliferation and differentiation responses to transforming growth factor beta and bone morphogenetic protein." Mol Cell Biol **24**(10): 4241-54.

Krakow, D., K. Reinker, et al. (1998). "Localization of a multiple synostoses-syndrome disease gene to chromosome 17q21-22." Am J Hum Genet **63**(1): 120-4.

Kubo, F., M. Takeichi, et al. (2003). "Wnt2b controls retinal cell differentiation at the ciliary marginal zone." Development **130**(3): 587-98.

Kulessa, H. and B. L. Hogan (2002). "Generation of a loxP flanked bmp4loxP-lacZ allele marked by conditional lacZ expression." Genesis **32**(2): 66-8.

Kumar, M., N. Jordan, et al. (2003). "Signals from lateral plate mesoderm instruct endoderm toward a pancreatic fate." Dev Biol **259**(1): 109-22.

Kutiyanawala, M., R. K. Wyse, et al. (1992). "CHARGE and esophageal atresia." J Pediatr Surg **27**(5): 558-60.

Lamers, W. H., W. G. Spliet, et al. (1987). "The lining of the gut in the developing rat embryo. Its relation to the hypoblast (primary endoderm) and the notochord." Anat Embryol (Berl) **176**(2): 259-65.

Lammer, E. J. and J. F. Cordero (1986). "Exogenous sex hormone exposure and the risk for major malformations." Jama **255**(22): 3128-32.

Lander, T. A., G. Schauer, et al. (2004). "Tracheal agenesis in newborns." Laryngoscope **114**(9): 1633-6.

Langenfeld, E. M., Y. Kong, et al. (2006). "Bone morphogenetic protein 2 stimulation of tumor growth involves the activation of Smad-1/5." Oncogene **25**(5): 685-92.

Larrain, J., D. Bachiller, et al. (2000). "BMP-binding modules in chordin: a model for signalling regulation in the extracellular space." Development **127**(4): 821-30.

Larrain, J., M. Oelgeschlager, et al. (2001). "Proteolytic cleavage of Chordin as a switch for the dual activities of Twisted gastrulation in BMP signaling." Development **128**(22): 4439-47.

Lasorella, A., T. Uo, et al. (2001). "Id proteins at the cross-road of development and cancer." Oncogene **20**(58): 8326-33.

Lawson, A. and G. C. Schoenwolf (2003). "Epiblast and primitive-streak origins of the endoderm in the gastrulating chick embryo." Development **130**(15): 3491-501.

Lawson, K. A., N. R. Dunn, et al. (1999). "Bmp4 is required for the generation of primordial germ cells in the mouse embryo." Genes Dev **13**(4): 424-36.

Levak-Svajger, B. and A. Svajger (1974). "Investigation on the origin of the definitive endoderm in the rat embryo." J Embryol Exp Morphol **32**(2): 445-59.

Levay-Young, B. K. and M. Navre (1992). "Growth and developmental regulation of wnt-2 (irp) gene in mesenchymal cells of fetal lung." Am J Physiol **262**(6 Pt 1): L672-83.

Li, C., J. Xiao, et al. (2002). "Wnt5a participates in distal lung morphogenesis." Dev Biol **248**(1): 68-81.

Li, Q., Z. Liu, et al. (2002). "Integrated platform for detection of DNA sequence variants using capillary array electrophoresis." Electrophoresis **23**(10): 1499-511.

Li, X., Y. Luo, et al. (2005). "Polycystin-1 and polycystin-2 regulate the cell cycle through the helix-loop-helix inhibitor Id2." Nat Cell Biol **7**(12): 1102-12.

Li, Y., H. Zhang, et al. (2004). "Sonic hedgehog signaling regulates Gli3 processing, mesenchymal proliferation, and differentiation during mouse lung organogenesis." Dev Biol **270**(1): 214-31.

Li, Y., H. Zhang, et al. (2006). "Cholesterol modification restricts the spread of Shh gradient in the limb bud." Proc Natl Acad Sci U S A.

Lim, L., V. V. Kalinichenko, et al. (2002). "Fusion of lung lobes and vessels in mouse embryos heterozygous for the forkhead box f1 targeted allele." Am J Physiol Lung Cell Mol Physiol **282**(5): L1012-22.

Lin, Y., A. Liu, et al. (2001). "Induction of ureter branching as a response to Wnt-2b signaling during early kidney organogenesis." Dev Dyn **222**(1): 26-39.

Litingtung, Y. and C. Chiang (2000). "Specification of ventral neuron types is mediated by an antagonistic interaction between Shh and Gli3." Nat Neurosci **3**(10): 979-85.

Litingtung, Y., R. D. Dahn, et al. (2002). "Shh and Gli3 are dispensable for limb skeleton formation but regulate digit number and identity." Nature **418**(6901): 979-83.

Litingtung, Y., L. Lei, et al. (1998). "Sonic hedgehog is essential to foregut development." Nat Genet **20**(1): 58-61.

Liu, J., S. Wilson, et al. (2003). "BMP receptor 1b is required for axon guidance and cell survival in the developing retina." Dev Biol **256**(1): 34-48.

Long, F., X. M. Zhang, et al. (2001). "Genetic manipulation of hedgehog signaling in the endochondral skeleton reveals a direct role in the regulation of chondrocyte proliferation." Development **128**(24): 5099-108.

Luo, G., C. Hofmann, et al. (1995). "BMP-7 is an inducer of nephrogenesis, and is also required for eye development and skeletal patterning." Genes Dev **9**(22): 2808-20.

Lyden, D., A. Z. Young, et al. (1999). "Id1 and Id3 are required for neurogenesis, angiogenesis and vascularization of tumour xenografts." Nature **401**(6754): 670-7.

Lyons, K. M., B. L. Hogan, et al. (1995). "Colocalization of BMP 7 and BMP 2 RNAs suggests that these factors cooperatively mediate tissue interactions during murine development." Mech Dev **50**(1): 71-83.

Mahlapuu, M., S. Enerback, et al. (2001). "Haploinsufficiency of the forkhead gene Foxf1, a target for sonic hedgehog signaling, causes lung and foregut malformations." Development **128**(12): 2397-406.

Mahlapuu, M., M. Ormestad, et al. (2001). "The forkhead transcription factor Foxf1 is required for differentiation of extra-embryonic and lateral plate mesoderm." Development **128**(2): 155-66.

Mahlapuu, M., M. Pelto-Huikko, et al. (1998). "FREAC-1 contains a cell-type-specific transcriptional activation domain and is expressed in epithelial-mesenchymal interfaces." Dev Biol **202**(2): 183-95.

Manschot, H. J., J. N. van den Anker, et al. (1994). "Tracheal agenesis." Anaesthesia **49**(9): 788-90.

Marcelle, C., M. R. Stark, et al. (1997). "Coordinate actions of BMPs, Wnts, Shh and noggin mediate patterning of the dorsal somite." Development **124**(20): 3955-63.

Marsh, A. J., D. Wellesley, et al. (2000). "Interstitial deletion of chromosome 17 (del(17)(q22q23.3)) confirms a link with oesophageal atresia." J Med Genet **37**(9): 701-4.

Massague, J. (2000). "How cells read TGF-beta signals." Nat Rev Mol Cell Biol **1**(3): 169-78.

Massague, J. and Y. G. Chen (2000). "Controlling TGF-beta signaling." Genes Dev **14**(6): 627-44.

Massague, J. and D. Wotton (2000). "Transcriptional control by the TGF-beta/Smad signaling system." Embo J **19**(8): 1745-54.

McMahon, J. A., S. Takada, et al. (1998). "Noggin-mediated antagonism of BMP signaling is required for growth and patterning of the neural tube and somite." Genes Dev **12**(10): 1438-52.

McMullen, K. P., P. S. Karnes, et al. (1996). "Familial recurrence of tracheoesophageal fistula and associated malformations." Am J Med Genet **63**(4): 525-8.

Mendelsohn, C., D. Lohnes, et al. (1994). "Function of the retinoic acid receptors (RARs) during development (II). Multiple abnormalities at various stages of

organogenesis in RAR double mutants." Development **120**(10): 2749-71.

Merei, J. M., P. Farmer, et al. (1997). "Timing and embryology of esophageal atresia and tracheo-esophageal fistula." Anat Rec **249**(2): 240-8.

Merei, J. M. and J. M. Hutson (2002). "Embryogenesis of tracheo esophageal anomalies: a review." Pediatr Surg Int **18**(5-6): 319-26.

Mill, P., R. Mo, et al. (2003). "Sonic hedgehog-dependent activation of Gli2 is essential for embryonic hair follicle development." Genes Dev **17**(2): 282-94.

Miller, J. R. and R. T. Moon (1996). "Signal transduction through beta-catenin and specification of cell fate during embryogenesis." Genes Dev **10**(20): 2527-39.

Miller, M. E. and F. R. Cross (2001). "Cyclin specificity: how many wheels do you need on a unicycle?" J Cell Sci **114**(Pt 10): 1811-20.

Min, H., D. M. Danilenko, et al. (1998). "Fgf-10 is required for both limb and lung development and exhibits striking functional similarity to Drosophila branchless." Genes Dev **12**(20): 3156-61.

Ming, J. E., E. Roessler, et al. (1998). "Human developmental disorders and the Sonic hedgehog pathway." Mol Med Today **4**(8): 343-9.

Minoo, P., G. Su, et al. (1999). "Defects in tracheoesophageal and lung morphogenesis in Nkx2.1(-/-) mouse embryos." Dev Biol **209**(1): 60-71.

Mishina, Y. (2003). "Function of bone morphogenetic protein signaling during mouse development." Front Biosci **8**: d855-69.

Mishina, Y., R. Crombie, et al. (1999). "Multiple roles for activin-like kinase-2 signaling during mouse embryogenesis." Dev Biol **213**(2): 314-26.

Mishina, Y., M. C. Hanks, et al. (2002). "Generation of Bmpr/Alk3 conditional knockout mice." Genesis **32**(2): 69-72.

Mishina, Y., A. Suzuki, et al. (1995). "Bmpr encodes a type I bone morphogenetic protein receptor that is essential for gastrulation during mouse embryogenesis." Genes Dev **9**(24): 3027-37.

Miyazono, K. (1999). "Signal transduction by bone morphogenetic protein receptors: functional roles of Smad proteins." Bone **25**(1): 91-3.

Miyazono, K., S. Maeda, et al. (2005). "BMP receptor signaling: transcriptional targets, regulation of signals, and signaling cross-talk." Cytokine Growth Factor Rev **16**(3): 251-63.

Miyazono, K. and K. Miyazawa (2002). "Id: a target of BMP signaling." Sci STKE **2002**(151): PE40.

Moon, R. T., B. Bowerman, et al. (2002). "The promise and perils of Wnt signaling through beta-catenin." Science **296**(5573): 1644-6.

Moon, R. T., J. D. Brown, et al. (1997). "Structurally related receptors and antagonists compete for secreted Wnt ligands." Cell **88**(6): 725-8.

Mori, S., S. I. Nishikawa, et al. (2000). "Lactation defect in mice lacking the helix-loop-helix inhibitor Id2." Embo J **19**(21): 5772-81.

Morin, P. J. (1999). "beta-catenin signaling and cancer." Bioessays **21**(12): 1021-30.

Morin, P. J., A. B. Sparks, et al. (1997). "Activation of beta-catenin-Tcf signaling in colon cancer by mutations in beta-catenin or APC." Science **275**(5307): 1787-90.

Mortell, A., A. M. O'Donnell, et al. (2004). "Adriamycin induces notochord hypertrophy with conservation of sonic hedgehog expression in abnormal ectopic notochord in the adriamycin rat model." J Pediatr Surg **39**(6): 859-63.

Motoyama, J., J. Liu, et al. (1998). "Essential function of Gli2 and Gli3 in the formation of lung, trachea and oesophagus." Nat Genet **20**(1): 54-7.

Moustakas, A. and C. H. Heldin (2005). "Non-Smad TGF-beta signals." J Cell Sci **118**(Pt 16): 3573-84.

Moyson, F. (1970). "[Congenital esophageal stenosis and cervical tracheo-esophageal fistula]." Ann Chir Infant **11**(3): 179-83.

Mucenski, M. L., S. E. Wert, et al. (2003). "beta-Catenin is required for specification of proximal/distal cell fate during lung morphogenesis." J Biol Chem **278**(41): 40231-8.

Muller, F. and R. O'Rahilly (2003). "The prechordal plate, the rostral end of the notochord and nearby median features in staged human embryos." Cells Tissues Organs **173**(1): 1-20.

Muller, I., A. Jenner, et al. (1997). "Effect of concentration on the cytotoxic mechanism of doxorubicin--apoptosis and oxidative DNA damage." Biochem Biophys Res Commun **230**(2): 254-7.

Mullor, J. L., N. Dahmane, et al. (2001). "Wnt signals are targets and mediators of Gli function." Curr Biol **11**(10): 769-73.

Myers, N. A. (1974). "Oesophageal atresia: the epitome of modern surgery." Ann R Coll Surg Engl **54**(6): 277-87.

Neubuser, A., H. Koseki, et al. (1995). "Characterization and developmental expression of Pax9, a paired-box-containing gene related to Pax1." Dev Biol **170**(2): 701-16.

Nezarati, M. M. and D. R. McLeod (1999). "VACTERL manifestations in two generations of a family." Am J Med Genet **82**(1): 40-2.

Ng, Y. S., R. Rohan, et al. (2001). "Differential expression of VEGF isoforms in mouse during development and in the adult." Dev Dyn **220**(2): 112-21.

Nishanian, T. G., J. S. Kim, et al. (2004). "Suppression of tumorigenesis and activation of Wnt signaling by bone morphogenetic protein 4 in human cancer cells." Cancer Biol Ther **3**(7): 667-75.

Nogawa, H., K. Morita, et al. (1998). "Bud formation precedes the appearance of differential cell proliferation during branching morphogenesis of mouse lung epithelium in vitro." Dev Dyn **213**(2): 228-35.

Nohe, A., E. Keating, et al. (2004). "Signal transduction of bone morphogenetic protein receptors." Cell Signal **16**(3): 291-9.

Nora, J. J., A. H. Nora, et al. (1978). "Exogenous progestogen and estrogen implicated in birth defects." Jama **240**(9): 837-43.

Nurse, P. (1994). "Ordering S phase and M phase in the cell cycle." Cell **79**(4): 547-50.

O'Rahilly, R. and F. Muller (1984). "Chevalier Jackson lecture. Respiratory and alimentary relations in staged human embryos. New embryological data and congenital anomalies." Ann Otol Rhinol Laryngol **93**(5 Pt 1): 421-9.

Okubo, T. and B. L. Hogan (2004). "Hyperactive Wnt signaling changes the developmental potential of embryonic lung endoderm." J Biol **3**(3): 11.

Onichtchouk, D., Y. G. Chen, et al. (1999). "Silencing of TGF-beta signalling by the pseudoreceptor BAMBI." Nature **401**(6752): 480-5.

Orford, J., M. Glasson, et al. (2000). "Oesophageal atresia in twins." Pediatr Surg Int **16**(8): 541-5.

Orford, J., P. Manglick, et al. (2001). "Mechanisms for the development of esophageal atresia." J Pediatr Surg **36**(7): 985-94.

Ovchinnikov, D. A., J. Selever, et al. (2006). "BMP receptor type IA in limb bud mesenchyme regulates distal outgrowth and patterning." Dev Biol **295**(1): 103-15.

Papaioannou, V. E. (2001). "T-box genes in development: from hydra to humans." Int Rev Cytol **207**: 1-70.

Park, H. L., C. Bai, et al. (2000). "Mouse Gli1 mutants are viable but have defects in

SHH signaling in combination with a Gli2 mutation." Development **127**(8): 1593-605.

Park, J. P., J. B. Moeschler, et al. (1992). "A unique de novo interstitial deletion del(17)(q21.3q23) in a phenotypically abnormal infant." Clin Genet **41**(1): 54-6.

Pearce, J. J., G. Penny, et al. (1999). "A mouse cerberus/Dan-related gene family." Dev Biol **209**(1): 98-110.

Pelc, P., T. Prigogine, et al. (2001). "Tracheoesophageal fistula: case report and review of literature." Acta Otorhinolaryngol Belg **55**(4): 273-8.

Pepicelli, C. V., P. M. Lewis, et al. (1998). "Sonic hedgehog regulates branching morphogenesis in the mammalian lung." Curr Biol **8**(19): 1083-6.

Perez-Roger, I., S. H. Kim, et al. (1999). "Cyclins D1 and D2 mediate myc-induced proliferation via sequestration of p27(Kip1) and p21(Cip1)." Embo J **18**(19): 5310-20.

Perl, A. K. and J. A. Whitsett (1999). "Molecular mechanisms controlling lung morphogenesis." Clin Genet **56**(1): 14-27.

Persson, M., D. Stamataki, et al. (2002). "Dorsal-ventral patterning of the spinal cord requires Gli3 transcriptional repressor activity." Genes Dev **16**(22): 2865-78.

Peterson, R. S., L. Lim, et al. (1997). "The winged helix transcriptional activator HFH-8 is expressed in the mesoderm of the primitive streak stage of mouse embryos and its cellular derivatives." Mech Dev **69**(1-2): 53-69.

Peverali, F. A., T. Ramqvist, et al. (1994). "Regulation of G1 progression by E2A and Id helix-loop-helix proteins." Embo J **13**(18): 4291-301.

Piccolo, S., E. Agius, et al. (1999). "The head inducer Cerberus is a multifunctional antagonist of Nodal, BMP and Wnt signals." Nature **397**(6721): 707-10.

Piccolo, S., Y. Sasai, et al. (1996). "Dorsoventral patterning in Xenopus: inhibition of ventral signals by direct binding of chordin to BMP-4." Cell **86**(4): 589-98.

Pierrou, S., M. Hellqvist, et al. (1994). "Cloning and characterization of seven human forkhead proteins: binding site specificity and DNA bending." Embo J **13**(20): 5002-12.

Pineda-Salgado, L., E. J. Craig, et al. (2005). "Expression of Panza, an alpha2-macroglobulin, in a restricted dorsal domain of the primitive gut in Xenopus laevis." Gene Expr Patterns **6**(1): 3-10.

Pogue, R. and K. Lyons (2006). "BMP signaling in the cartilage growth plate." Current Topics in Developmental Biology **76**: 1-48.

Possoegel, A. K., J. A. Diez-Pardo, et al. (1999). "Notochord involvement in experimental esophageal atresia." Pediatr Surg Int **15**(3-4): 201-5.

Possogel, A. K., J. A. Diez-Pardo, et al. (1998). "Embryology of esophageal atresia in the adriamycin rat model." J Pediatr Surg **33**(4): 606-12.

Price, M. A. and D. Kalderon (2002). "Proteolysis of the Hedgehog signaling effector Cubitus interruptus requires phosphorylation by Glycogen Synthase Kinase 3 and Casein Kinase 1." Cell **108**(6): 823-35.

Qi, B. Q. and S. W. Beasley (1999). "Communicating bronchopulmonary foregut malformations in the adriamycin-induced rat model of oesophageal atresia." Aust N Z J Surg **69**(1): 56-9.

Qi, B. Q. and S. W. Beasley (1999). "Relationship of the notochord to foregut development in the fetal rat model of esophageal atresia." J Pediatr Surg **34**(11): 1593-8.

Qi, B. Q. and S. W. Beasley (2000). "Stages of normal tracheo-bronchial development in rat embryos: resolution of a controversy." Dev Growth Differ **42**(2): 145-53.

Qi, B. Q., S. W. Beasley, et al. (2001). "Evidence of a common pathogenesis for foregut

duplications and esophageal atresia with tracheo-esophageal fistula." Anat Rec **264**(1): 93-100.

Que, J., M. Choi, et al. (2006). "Morphogenesis of the trachea and esophagus: current players and new roles for noggin and Bmps." Differentiation **74**(7): 422-37.

Quelle, D. E., R. A. Ashmun, et al. (1993). "Overexpression of mouse D-type cyclins accelerates G1 phase in rodent fibroblasts." Genes Dev **7**(8): 1559-71.

Reed, M. F. and D. J. Mathisen (2003). "Tracheoesophageal fistula." Chest Surg Clin N Am **13**(2): 271-89.

Rosenzweig, B. L., T. Imamura, et al. (1995). "Cloning and characterization of a human type II receptor for bone morphogenetic proteins." Proc Natl Acad Sci U S A **92**(17): 7632-6.

Rossi, J. M., N. R. Dunn, et al. (2001). "Distinct mesodermal signals, including BMPs from the septum transversum mesenchyme, are required in combination for hepatogenesis from the endoderm." Genes Dev **15**(15): 1998-2009.

Ruiz, I. A. A. (1999). "The works of GLI and the power of hedgehog." Nat Cell Biol **1**(6): E147-8.

Ruppert, J. M., K. W. Kinzler, et al. (1988). "The GLI-Kruppel family of human genes." Mol Cell Biol **8**(8): 3104-13.

Ruzinova, M. B. and R. Benezra (2003). "Id proteins in development, cell cycle and cancer." Trends Cell Biol **13**(8): 410-8.

Sakiyama, J., A. Yamagishi, et al. (2003). "Tbx4-Fgf10 system controls lung bud formation during chicken embryonic development." Development **130**(7): 1225-34.

Saleeby, M. G., M. Vustar, et al. (2003). "Tracheal agenesis: a rare disease with unique airway considerations." Anesth Analg **97**(1): 50-2, table of contents.

Sanudo, J. R. and J. M. Domenech-Mateu (1990). "The laryngeal primordium and epithelial lamina. A new interpretation." J Anat **171**: 207-22.

Sasaki, H., Y. Nishizaki, et al. (1999). "Regulation of Gli2 and Gli3 activities by an amino-terminal repression domain: implication of Gli2 and Gli3 as primary mediators of Shh signaling." Development **126**(17): 3915-24.

Sasaki, T., T. Kusafuka, et al. (2001). "Analysis of the development of normal foregut and tracheoesophageal fistula in an adriamycin rat model using three-dimensional image reconstruction." Surg Today **31**(2): 133-9.

Sausedo, R. A. and G. C. Schoenwolf (1994). "Quantitative analyses of cell behaviors underlying notochord formation and extension in mouse embryos." Anat Rec **239**(1): 103-12.

Schachtner, S. K., Y. Wang, et al. (2000). "Qualitative and quantitative analysis of embryonic pulmonary vessel formation." Am J Respir Cell Mol Biol **22**(2): 157-65.

Scheufler, C., W. Sebald, et al. (1999). "Crystal structure of human bone morphogenetic protein-2 at 2.7 A resolution." Journal of Molecular Biology **287**(1): 103-15.

Schmid, P., W. A. Schulz, et al. (1989). "Dynamic expression pattern of the myc protooncogene in midgestation mouse embryos." Science **243**(4888): 226-9.

Schmidt, M., M. Tanaka, et al. (2000). "Expression of (beta)-catenin in the developing chick myotome is regulated by myogenic signals." Development **127**(19): 4105-13.

Sekine, K., H. Ohuchi, et al. (1999). "Fgf10 is essential for limb and lung formation." Nat Genet **21**(1): 138-41.

Serra, R. and H. L. Moses (1995). "pRb is necessary for inhibition of N-myc expression by TGF-beta 1 in embryonic lung organ cultures." Development **121**(9): 3057-66.

Serra, R., R. W. Pelton, et al. (1994). "TGF beta 1 inhibits branching morphogenesis and

N-myc expression in lung bud organ cultures." Development **120**(8): 2153-61.

Shalaby, F., J. Ho, et al. (1997). "A requirement for Flk1 in primitive and definitive hematopoiesis and vasculogenesis." Cell **89**(6): 981-90.

Shalaby, F., J. Rossant, et al. (1995). "Failure of blood-island formation and vasculogenesis in Flk-1-deficient mice." Nature **376**(6535): 62-6.

Shapiro, R. N., W. Eddy, et al. (1958). "The incidence of congenital anomalies discovered in the neonatal period." Am J Surg **96**(3): 396-400.

Sharma, A. K., N. S. Shekhawat, et al. (2000). "Esophageal atresia and tracheoesophageal fistula: a review of 25 years' experience." Pediatr Surg Int **16**(7): 478-82.

Shaw-Smith, C. (2006). "Oesophageal atresia, tracheo-oesophageal fistula, and the VACTERL association: review of genetics and epidemiology." J Med Genet **43**(7): 545-54.

Sherr, C. J. (1993). "Mammalian G1 cyclins." Cell **73**(6): 1059-65.

Sherr, C. J. and J. M. Roberts (1999). "CDK inhibitors: positive and negative regulators of G1-phase progression." Genes Dev **13**(12): 1501-12.

Shi, Y. and J. Massague (2003). "Mechanisms of TGF-beta signaling from cell membrane to the nucleus." Cell **113**(6): 685-700.

Shtutman, M., J. Zhurinsky, et al. (1999). "The cyclin D1 gene is a target of the beta-catenin/LEF-1 pathway." Proc Natl Acad Sci U S A **96**(10): 5522-7.

Shu, W., S. Guttentag, et al. (2005). "Wnt/beta-catenin signaling acts upstream of N-myc, BMP4, and FGF signaling to regulate proximal-distal patterning in the lung." Dev Biol **283**(1): 226-39.

Shu, W., Y. Q. Jiang, et al. (2002). "Wnt7b regulates mesenchymal proliferation and vascular development in the lung." Development **129**(20): 4831-42.

Sikder, H. A., M. K. Devlin, et al. (2003). "Id proteins in cell growth and tumorigenesis." Cancer Cell **3**(6): 525-30.

Skandalakis, J. E., Gray, S.W. & Ricketts, R. (1994). Embryology for Surgeons. Baltimore, Williams and Wilkins.

Smith, W. C. and R. M. Harland (1992). "Expression cloning of noggin, a new dorsalizing factor localized to the Spemann organizer in Xenopus embryos." Cell **70**(5): 829-40.

Sparey, C., G. Jawaheer, et al. (2000). "Esophageal atresia in the Northern Region Congenital Anomaly Survey, 1985-1997: prenatal diagnosis and outcome." Am J Obstet Gynecol **182**(2): 427-31.

Stemple, D. L. (2005). "Structure and function of the notochord: an essential organ for chordate development." Development **132**(11): 2503-12.

Stolt, C. C., P. Lommes, et al. (2003). "The Sox9 transcription factor determines glial fate choice in the developing spinal cord." Genes Dev **17**(13): 1677-89.

Sulik, K., D. B. Dehart, et al. (1994). "Morphogenesis of the murine node and notochordal plate." Dev Dyn **201**(3): 260-78.

Sutliff, K. S. and G. M. Hutchins (1994). "Septation of the respiratory and digestive tracts in human embryos: crucial role of the tracheoesophageal sulcus." Anat Rec **238**(2): 237-47.

te Welscher, P., A. Zuniga, et al. (2002). "Progression of vertebrate limb development through SHH-mediated counteraction of GLI3." Science **298**(5594): 827-30.

Tebar, M., O. Destree, et al. (2001). "Expression of Tcf/Lef and sFrp and localization of beta-catenin in the developing mouse lung." Mech Dev **109**(2): 437-40.

Tellier, A. L., V. Cormier-Daire, et al. (1998). "CHARGE syndrome: report of 47 cases and review." Am J Med Genet **76**(5): 402-9.

ten Dijke, P., O. Korchynskyi, et al. (2003). "Controlling cell fate by bone morphogenetic protein receptors." Mol Cell Endocrinol **211**(1-2): 105-13.

Tetsu, O. and F. McCormick (1999). "Beta-catenin regulates expression of cyclin D1 in colon carcinoma cells." Nature **398**(6726): 422-6.

Tewey, K. M., T. C. Rowe, et al. (1984). "Adriamycin-induced DNA damage mediated by mammalian DNA topoisomerase II." Science **226**(4673): 466-8.

Thomas, P. and R. Beddington (1996). "Anterior primitive endoderm may be responsible for patterning the anterior neural plate in the mouse embryo." Curr Biol **6**(11): 1487-96.

Thompson, D. J., J. A. Molello, et al. (1978). "Teratogenicity of adriamycin and daunomycin in the rat and rabbit." Teratology **17**(2): 151-7.

Torfs, C. P., C. J. Curry, et al. (1995). "Population-based study of tracheoesophageal fistula and esophageal atresia." Teratology **52**(4): 220-32.

Unger, S., I. Copland, et al. (2003). "Down-regulation of sonic hedgehog expression in pulmonary hypoplasia is associated with congenital diaphragmatic hernia." Am J Pathol **162**(2): 547-55.

Urist, M. R. (1965). "Bone: formation by autoinduction." Science **150**(698): 893-9.

Urist, M. R., A. Mikulski, et al. (1975). "Reversible extinction of the morphogen in bone matrix by reduction and oxidation of disulfide bonds." Calcif Tissue Res **19**(1): 73-83.

Urist, M. R., H. Nogami, et al. (1976). "A bone morphogenetic polypeptide." Calcif Tissue Res **21 Suppl**: 81-7.

van Bokhoven, H., J. Celli, et al. (2005). "MYCN haploinsufficiency is associated with reduced brain size and intestinal atresias in Feingold syndrome." Nat Genet **37**(5): 465-7.

van Es, J. H., N. Barker, et al. (2003). "You Wnt some, you lose some: oncogenes in the Wnt signaling pathway." Curr Opin Genet Dev **13**(1): 28-33.

van Tuyl, M. and M. Post (2000). "From fruitflies to mammals: mechanisms of signalling via the Sonic hedgehog pathway in lung development." Respir Res **1**(1): 30-5.

van Veenendaal, M. B., K. D. Liem, et al. (2000). "Congenital absence of the trachea." European Journal of Pediatrics **159**(1-2): 8-13.

Villavicencio, E. H., D. O. Walterhouse, et al. (2000). "The sonic hedgehog-patched-gli pathway in human development and disease." Am J Hum Genet **67**(5): 1047-54.

Vortkamp, A., T. Franz, et al. (1992). "Deletion of GLI3 supports the homology of the human Greig cephalopolysyndactyly syndrome (GCPS) and the mouse mutant extra toes (Xt)." Mamm Genome **3**(8): 461-3.

Vortkamp, A., M. Gessler, et al. (1991). "GLI3 zinc-finger gene interrupted by translocations in Greig syndrome families." Nature **352**(6335): 539-40.

Wang, B., J. F. Fallon, et al. (2000). "Hedgehog-regulated processing of Gli3 produces an anterior/posterior repressor gradient in the developing vertebrate limb." Cell **100**(4): 423-34.

Wang, Y., J. P. Macke, et al. (1996). "A large family of putative transmembrane receptors homologous to the product of the Drosophila tissue polarity gene frizzled." J Biol Chem **271**(8): 4468-76.

Warburton, D., M. Schwarz, et al. (2000). "The molecular basis of lung morphogenesis." Mech Dev **92**(1): 55-81.

Watkins, D. N., D. M. Berman, et al. (2003). "Hedgehog signalling within airway epithelial progenitors and in small-cell lung cancer." Nature **422**(6929): 313-7.

Weaver, M., L. Batts, et al. (2003). "Tissue interactions pattern the mesenchyme of the embryonic mouse lung." Dev Biol **258**(1): 169-84.

Weaver, M., N. R. Dunn, et al. (2000). "Bmp4 and Fgf10 play opposing roles during lung bud morphogenesis." Development **127**(12): 2695-704.

Weaver, M., J. M. Yingling, et al. (1999). "Bmp signaling regulates proximal-distal differentiation of endoderm in mouse lung development." Development **126**(18): 4005-15.

Wells, J. M. and D. A. Melton (1999). "Vertebrate endoderm development." Annu Rev Cell Dev Biol **15**: 393-410.

Wetmore, C. (2003). "Sonic hedgehog in normal and neoplastic proliferation: insight gained from human tumors and animal models." Curr Opin Genet Dev **13**(1): 34-42.

Wharton, K. A., Jr. (2003). "Runnin' with the Dvl: proteins that associate with Dsh/Dvl and their significance to Wnt signal transduction." Dev Biol **253**(1): 1-17.

Whitsett, J. (1998). "A lungful of transcription factors." Nat Genet **20**(1): 7-8.

Wijgerde, M., J. A. McMahon, et al. (2002). "A direct requirement for Hedgehog signaling for normal specification of all ventral progenitor domains in the presumptive mammalian spinal cord." Genes Dev **16**(22): 2849-64.

Wild, A., M. Kalff-Suske, et al. (1997). "Point mutations in human GLI3 cause Greig syndrome." Hum Mol Genet **6**(11): 1979-84.

Williams, A. K., B. Q. Qi, et al. (2000). "Temporospatial aberrations of apoptosis in the rat embryo developing esophageal atresia." J Pediatr Surg **35**(11): 1617-20.

Williams, A. K., B. Q. Qi, et al. (2001). "Demonstration of abnormal notochord development by three-dimensional reconstructive imaging in the rat model of esophageal atresia." Pediatr Surg Int **17**(1): 21-4.

Williams, A. K., Q. B. Quan, et al. (2003). "Three-dimensional imaging clarifies the process of tracheoesophageal separation in the rat." J Pediatr Surg **38**(2): 173-7.

Wozney, J. M. (1992). "The bone morphogenetic protein family and osteogenesis." Mol Reprod Dev **32**(2): 160-7.

Wozney, J. M. (1998). "The bone morphogenetic protein family: multifunctional cellular regulators in the embryo and adult." Eur J Oral Sci **106 Suppl 1**: 160-6.

Wozney, J. M., V. Rosen, et al. (1988). "Novel regulators of bone formation: molecular clones and activities." Science **242**(4885): 1528-34.

Yamada, M., J. P. Revelli, et al. (2000). "Expression of chick Tbx-2, Tbx-3, and Tbx-5 genes during early heart development: evidence for BMP2 induction of Tbx2." Dev Biol **228**(1): 95-105.

Yamagishi, H., J. Maeda, et al. (2003). "Tbx1 is regulated by tissue-specific forkhead proteins through a common Sonic hedgehog-responsive enhancer." Genes Dev **17**(2): 269-81.

Yang-Snyder, J., J. R. Miller, et al. (1996). "A frizzled homolog functions in a vertebrate Wnt signaling pathway." Curr Biol **6**(10): 1302-6.

Yang, L., K. Yamasaki, et al. (2006). "Bone morphogenetic protein-2 modulates Wnt and frizzled expression and enhances the canonical pathway of Wnt signaling in normal keratinocytes." J Dermatol Sci **42**(2): 111-9.

Yang, Y., K. C. Palmer, et al. (1998). "Role of laminin polymerization at the epithelial mesenchymal interface in bronchial myogenesis." Development **125**(14): 2621-9.

Yang, Y., N. K. Relan, et al. (1999). "Embryonic mesenchymal cells share the potential for smooth muscle differentiation: myogenesis is controlled by the cell's shape." Development **126**(13): 3027-33.

Yasui, K., H. Sasaki, et al. (1997). "Distribution pattern of HNF-3beta proteins in developing embryos of two mammalian species, the house shrew and the mouse." Dev Growth Differ **39**(6): 667-76.

Ying, Q. L., J. Nichols, et al. (2003). "BMP induction of Id proteins suppresses

differentiation and sustains embryonic stem cell self-renewal in collaboration with STAT3." Cell **115**(3): 281-92.

Yokota, N., S. Nishizawa, et al. (2002). "Role of Wnt pathway in medulloblastoma oncogenesis." Int J Cancer **101**(2): 198-201.

Yoon, J. W., Y. Kita, et al. (2002). "Gene expression profiling leads to identification of GLI1-binding elements in target genes and a role for multiple downstream pathways in GLI1-induced cell transformation." J Biol Chem **277**(7): 5548-55.

Yoshikawa, S. I., S. Aota, et al. (2000). "The ActR-I activin receptor protein is expressed in notochord, lens placode and pituitary primordium cells in the mouse embryo." Mech Dev **91**(1-2): 439-44.

Young, R. C., R. F. Ozols, et al. (1981). "The anthracycline antineoplastic drugs." N Engl J Med **305**(3): 139-53.

Yu, C., C. J. Mazerolle, et al. (2006). "Direct and indirect effects of hedgehog pathway activation in the mammalian retina." Mol Cell Neurosci **32**(3): 274-82.

Zakin, L. D., S. Mazan, et al. (1998). "Structure and expression of Wnt13, a novel mouse Wnt2 related gene." Mech Dev **73**(1): 107-16.

Zaret, K. S. (2000). "Liver specification and early morphogenesis." Mech Dev **92**(1): 83-8.

Zaret, K. S. (2001). "Hepatocyte differentiation: from the endoderm and beyond." Curr Opin Genet Dev **11**(5): 568-74.

Zaret, K. S. (2002). "Regulatory phases of early liver development: paradigms of organogenesis." Nat Rev Genet **3**(7): 499-512.

Zaw-Tun, H. A. (1982). "The tracheo-esophageal septum--fact or fantasy? Origin and development of the respiratory primordium and esophagus." Acta Anat (Basel) **114**(1): 1-21.

Zeng, X., M. Gray, et al. (2001). "TGF-beta1 perturbs vascular development and inhibits epithelial differentiation in fetal lung in vivo." Dev Dyn **221**(3): 289-301.

Zeng, X., S. E. Wert, et al. (1998). "VEGF enhances pulmonary vasculogenesis and disrupts lung morphogenesis in vivo." Dev Dyn **211**(3): 215-27.

Zhang, L., S. E. Zgleszewski, et al. (1998). "Differential display of genes in normal and hypoplastic fetal murine lungs." J Surg Res **75**(1): 66-73.

Zhang, Y., C. Chang, et al. (2001). "Regulation of Smad degradation and activity by Smurf2, an E3 ubiquitin ligase." Proc Natl Acad Sci U S A **98**(3): 974-9.

Zhang, Y., Z. Zhang, et al. (2000). "A new function of BMP4: dual role for BMP4 in regulation of Sonic hedgehog expression in the mouse tooth germ." Development **127**(7): 1431-43.

Zhang, Z., Y. Song, et al. (2002). "Rescue of cleft palate in Msx1-deficient mice by transgenic Bmp4 reveals a network of BMP and Shh signaling in the regulation of mammalian palatogenesis." Development **129**(17): 4135-46.

Zhao, G. Q. (2003). "Consequences of knocking out BMP signaling in the mouse." Genesis **35**(1): 43-56.

Zhao, J., R. Pestell, et al. (2001). "Transcriptional activation of cyclin D1 promoter by FAK contributes to cell cycle progression." Mol Biol Cell **12**(12): 4066-77.

Zhou, B., J. M. Hutson, et al. (1999). "Apoptosis in tracheoesophageal embryogenesis in rat embryos with or without adriamycin treatment." J Pediatr Surg **34**(5): 872-5; discussion 876.

Zhu, H., P. Kavsak, et al. (1999). "A SMAD ubiquitin ligase targets the BMP pathway and affects embryonic pattern formation." Nature **400**(6745): 687-93.

Zimmerman, L. B., J. M. De Jesus-Escobar, et al. (1996). "The Spemann organizer signal noggin binds and inactivates bone morphogenetic protein 4." Cell **86**(4): 599-606.

Zuniga, A., A. P. Haramis, et al. (1999). "Signal relay by BMP antagonism controls the SHH/FGF4 feedback loop in vertebrate limb buds." Nature **401**(6753): 598-602.